INFORMATION TO USERS

This manuscript has been reproduced from the microfilm master. UMI films the text directly from the original or copy submitted. Thus, some thesis and dissertation copies are in typewriter face, while others may be from any type of computer printer.

The quality of this reproduction is dependent upon the quality of the copy submitted. Broken or indistinct print, colored or poor quality illustrations and photographs, print bleedthrough, substandard margins, and improper alignment can adversely affect reproduction.

In the unlikely event that the author did not send UMI a complete manuscript and there are missing pages, these will be noted. Also, if unauthorized copyright material had to be removed, a note will indicate the deletion.

Oversize materials (e.g., maps, drawings, charts) are reproduced by sectioning the original, beginning at the upper left-hand corner and continuing from left to right in equal sections with small overlaps. Each original is also photographed in one exposure and is included in reduced form at the back of the book.

Photographs included in the original manuscript have been reproduced xerographically in this copy. Higher quality 6" x 9" black and white photographic prints are available for any photographs or illustrations appearing in this copy for an additional charge. Contact UMI directly to order.

U·M·I

University Microfilms International
A Bell & Howell Information Company
300 North Zeeb Road. Ann Arbor, MI 48106-1346 USA
313/761-4700 800/521-0600

Order Number 9409288

A new dual-stage multicomponent thermosetting polymer system

Brouns, Richard Allan, Ph.D.

University of Washington, 1993

U·M·I

300 N. Zeeb Rd.
Ann Arbor, MI 48106

A New Dual-Stage Multicomponent Thermosetting Polymer System

by

Richard Allan Brouns

A dissertation submitted in partial fulfillment
of the requirements for the degree of

Doctor of Philosophy

University of Washington

1993

Approved by G. Graham Allan

Professor G. Graham Allan
(Chairperson of Supervisory Committee)

Program Authorized
to Offer Degree Department of Chemical Engineering

Date August 6, 1993

© Copyright 1993

Richard Allan Brouns

In presenting this dissertation in partial fulfillment of the requirements for the Doctoral degree at the University of Washington, I agree that the Library shall make its copies freely available for inspection. I further agree that extensive copying of this dissertation is allowable only for scholarly purposes, consistent with the "fair use" as prescribed in the U.S. Copyright Law. Requests for copying or reproduction of this dissertation may be referred to University Microfilms, 1490 Eisenhower Place, P.O. Box 975, Ann Arbor, MI 48106, to whom the author has granted "the right to reproduce and sell (a) copies of the manuscript in microform and/or (b) printed copies of the manuscript made from microform."

Signature Richard Allan Brown

Date August 6, 1993

University of Washington

Abstract

A New Dual-Stage Multicomponent Thermosetting Polymer System

by Richard Allan Brouns

Chairperson of Supervisory Committee: Professor G. Graham Allan,

Department of Chemical Engineering

A new polymer combining the processing advantages of epoxy resins with the superior thermal performance of the dicyanate resins was developed for use in bonding aramid honeycomb core composites. Dual-stage curing to meet the unique requirements of the honeycomb manufacturing process was achieved with a tricomponent mixture of epoxy and dicyanate monomers and a carboxylic acid anhydride hardener. In the first stage of curing the anhydride hardener advances the resin mixture to the appropriate tack condition. Heat-activated latent curing reactions complete the polymer crosslinking at a later manufacturing stage. The effect of variations in the levels of cyanate and anhydride on the bonding strength to the aramid paper and the time to reach tack-free conditions were studied.

Characterization of the polymers chemical network development through kinetic investigations, thermal analysis and FT-IR spectroscopy was also undertaken. The reaction between cyanate ester groups and anhydride rings produced linear polyimidocarbamates that were identifiable by their FT-IR spectrum as one of the principal polymerization pathways. In the presence of an epoxy resin and tertiary amine catalysts, these imidocarbamates further reacted to form polyimides with possible organic carbonate branching. The resulting polymers showed good thermal stability with a single glass transition temperature that indicates the formation of an interconnecting polymer with significant crosslinking. Little if any polycyanurate was detected in the final product.

Polymerization kinetics were studied using dynamic differential scanning calorimetry (DSC). The imidocarbamate forming reaction was found to be of the same order as the competing epoxy/acid anhydride esterification reaction and significantly faster than the

dicyanate/epoxy or dicyanate cyclotrimerization reactions. Autocatalytic kinetic behavior was observed for the imidocarbamate reaction. When all three components were reacted in a combined system, the extent of epoxy esterification appeared to be largely over predicted by the isolated DSC results. The overall reactive system appears to be more complex than can be modeled by a simple combination of the individual reactions.

TABLE OF CONTENTS

LIST OF FIGURES

Number Page

LIST OF TABLES

Number Page

ACKNOWLEDGEMENTS

I wish to thank Professor G. Graham Allan for his direction and support, and most importantly his insights on the countless topics we discussed during the course of this research project. I must also acknowledge Battelle Northwest Laboratory for the financial support that made graduate school possible and Northwest Composites for helping define the problem, providing samples and supplemental research support.

Acknowledgement is also needed for the other members of my supervisory committee:

Barbara B. Krieger-Brockett,
James C. Seferis,
Buddy D. Ratner,
Christopher Viney.

I especially want to thank Professor Ratner for the generous access to his FTIR spectrometer and Professor Barbara Krieger-Brockett for her friendship and interest in my work.

Most importantly, a very special thanks to my wife and family for their love and endless patience.

1 INTRODUCTION

Aramid fiber structures are widely used in advanced composites for demanding aerospace applications. The high specific strength and stiffness of the constituent fibers combined with a superior thermal and chemical stability compared to most other polymers make these fibers well suited for reinforcing the composite matrix. The less demanding applications in the floors and internal compartments of aircraft employ a honeycomb type composite made from a nonwoven aramid paper containing a mixture of aramid fiber and fibrids. These lightweight composites find extensive use because of their high strength-to-weight ratio, low flammability and good insulating properties.

The core of the honeycomb panel is formed from many sheets of Nomex® aramid paper that are glued together in a unique pattern of connecting hexagonal cells. Costly failures that result in the rejection of large amounts of product can occur at several stages in the manufacturing process. These can frequently be attributed to the adhesive used in gluing the individual sheets.

The gluing operation is complicated by the use of a volatile organic solvent-based adhesive with a high molecular weight thermoplastic as one of the major components. This thermoplastic instills toughness in the cured glue and ensures quick gelling once the glue line is printed. Premature gelling and inadequate dissolution of raw materials during glue preparation however, forces the use of cumbersome filtering steps. The rapid gelling tendency of this adhesive also leads to occasional difficulties with plugging the small orifices that control the critical thickness and width of the glue lines during application. Shutdown for cleaning and disassembly of the glue printing equipment is generally required when plugging occurs. While these problems have largely been dealt with by equipment redesign and administrative controls, they continue to effect plant productivity.

Studies were initiated at the University of Washington in the second half of 1989 to address the problems associated with the manufacturing of Nomex honeycomb core. The initial task targeted selection of an alternative adhesive formulation with a design goal of

---

® poly(*m*-phenyleneisophthalamide), trademarked Nomex, E. I. du Pont de Nemours & Co., Inc., Wilmington, DE.

reducing product failures and the workers exposure to organic solvents. The research project was conducted in two phases. Phase I involved screening candidate adhesives to identify an alternative Nomex glue with improved processing characteristics and thermal stability. The results of this work are presented in Chapter 3 and have been published elsewhere (Allan and Brouns, 1991). Following development of this new adhesive the phase II task of characterizing the polymers network development through kinetic investigations, thermal analysis and FT-IR spectroscopy was undertaken. The phase II studies are the subject of Chapter 4.

2 BACKGROUND

Nomex core is produced by a multiple stage process involving node-line glue printing, sheet stacking or layup, and curing at elevated temperature and pressure to form a single block [12,13]. The node lines are staggered in a special pattern that allows the block to be mechanically expanded and form the system of contiguous hexagonal cells. The expanded block is subsequently impregnated with various resins in a multistage dip and cure process to reach the desired core density and rigidity. A typical finished honeycomb panel consists of core material laminated with solid sheets of plastic.

The node-line glue must rapidly dry, gel or partially cure to reach a tack-free condition shortly after being printed as a precursor to cutting and stacking the paper. Drying times on the order of one or two minutes are needed for efficient production. The solidified glue must retain its meltability at this stage so adequate wetting and bonding to the adjacent sheet will occur during the final curing step. Thermosetting, partially-advanced prepolymers (B-staged) are well suited in this application because additional curing produces crosslinking that greatly reduces their tendency to creep during the subsequent high temperature resin impregnation steps.

Aramid fibers are inherently difficult to bond with because of their chemical inertness. Interfacial adhesion in aramid-fiber/epoxy-matrix composites has been studied by several researchers in an effort to improve the performance of these structures through a variety of fiber surface modification techniques [2-11]. Allred *et al.* [6] report that in the absence of surface treatments which produce direct chemical bonding between the fiber and adhesive, failures in aramid-epoxy composites typically occur at less than half the load of their glass or graphite fiber-reinforced counterparts by a mechanism indicative of weak interfacial adhesion. These findings are based on a specific type of high modulus aramid fiber, namely poly(*p*-phenyleneterephthalamide), PPTP, which is characterized by an unusually high degree of orientation and crystallinity. They may not, therefore, be generally applicable to Nomex, but serve to underscore the potential difficulty in bonding aramids, and logically focused our initial screening of adhesive materials on the results of bonding tests.

A preliminary review and screening of selected thermosetting polymer systems was undertaken after a review of the literature failed to produce any nonproprietary

information to guide the adhesive selection [12,13,14]. A simple screening test was designed to compare the features of the various candidates. The adhesive strength was qualitatively examined by peeling cured samples of selected polymers from a sheet of the aramid paper and observing the degree to which fibers were removed from the surface. The leading candidates from this preliminary evaluation were the pure dicyanate resins and the epoxy-dicyanate, epoxy-polyamide and phenolic-polyamide mixtures. Handling and processing ease were also subjectively assessed during the preparation and curing of these samples. The epoxy/cyanate formulations emerge as the preferred option for reasons that included cost, handling ease and because:

1) Both resins are available in a sufficiently wide range of molecular weights and room-temperature viscosity's ranging from light oils to solids. Thus, sufficient flexibility in the rheological properties of the glue can be attained without the use of solvents.
2) Their polymerization reactions are additive in nature and so do not result in the generation of volatile byproducts, entrapped gases or much shrinkage during curing.
3) Both monomers and their resins exhibit relatively low toxicity.
4) Epoxy resins are well recognized for their excellent adhesive properties with numerous substrates and are already widely used in composites.
5) The dicyanate/epoxy copolymerization reactions have been investigated [5,6].
6) Dicyanate resins can be blended readily with various high temperature thermoplastics to improve toughness and tack properties while maintaining reasonably high thermal stability [7-20]. Likewise, epoxy resins can be blended with reactive rubbers for similar results.
7) Both resins can form stable B-stage prepolymers (partially advanced intermediates) that are later crosslinkable with additional heating. This feature allows either or both resins to be advanced shortly after printing to achieve the solid tack-free condition that is needed for stacking the sheets.
8) The dicyanate resins are converted into high temperature polycyanurate thermosetting plastics with glass transition temperatures (Tg) approaching 290°C [17,21]. When co-reacted with epoxies the dicyanate resins also tend to produce more thermally stable polymers [15,22].

3 ADHESIVE DEVELOPMENT -- Phase I

The principal goal at this phase in the project was to develop an alternative adhesive with reduced tendency to plug the glue preparation and applicator equipment. Plugging had been attributed to the high tendency of the Nomex glue to quickly form a gel as the solvent evaporated. The high gelling tendency and volatile nature of the solvent were desirable characteristics, designed to ensure the glue reached tack-free conditions quickly after printing. Precipitation of adhesive however, also occurred at all air-liquid interfaces in the equipment. The decision to abandon the conventional method of controlling glue viscosity and tack with solvents and to develop a solvent-free system was driven by a desire to offer a significantly different approach with reduced worker exposure to hazardous materials. This decision required the adhesive to be applied as a molten polymer or as a room temperature liquid (monomer or oligomer) with subsequent advancing. The latter approach was adopted. The methodology and experimental results used in developing a workable solvent-free composition are described in this chapter.

3.1 Processing Considerations

Chapter 2 summarized the general criteria that led to selection of an epoxy-dicyanate resin-based mixture for the adhesive. Further refinement of these criteria was needed to define a workable composition that met all the unique performance requirements including good adhesive strength, reasonable viscosity and pot life for ease of printing, an ability to reach the intermediate tack-free condition and be processed within the temperature limits of the Nomex sheet. The refined set of criteria are shown in Table 1.

Table 1. Performance criteria for adhesive comparisons

Adhesive Property	Acceptable Performance
Viscosity	$< \sim 200$ poise @ room temp.
Pot life	> 2 days
Cure temperature	$< 250°C$
Tack-free time	< 100 s @ 350°F
Pre-cure adhesion	The tack-free solid must withstand reasonable handling during sheet layup.
Post-cure adhesion	T-peel strength > 1.5 lb_f/in of adhesive width

The criteria on viscosity and pot life were selected based on engineering judgment alone. Nomex paper, which has a continuous use rating of 220°C (10 yr UL rating), can withstand short term exposures to temperatures above 250°C for up to a several hours with little or no damage and greater than about 370°C is needed before it degrades rapidly to a friable char [23]. Thus, the temperature limit for processing adhesives was conservatively established at 250°C.

The tack-free times were suggested by the honeycomb core manufacturer for efficient production. This initial advancement from liquid to a tack-free stage must be controlled to ensure the polymer is advanced only to an intermediate prepolymer (B-stage) resin and remains sufficiently below its gel point for good melting and penetration into the adjacent sheet during final curing. As a further complexity, the final curing step may not occur until several days after the sheets have been printed. Thus, the curing also needs to be effectively stopped once tack-free conditions are reached.

The precure adhesion criteria is obvious, while the postcure value comes from peel testing good adhesives and establishing a level when much of the failure is observed in the Nomex sheet rather than the glue itself or at the interface.

3.2 Review of Curing Reactions.

Dicyanate resins will co-react with epoxies [15,16, 24-32]. During screening tests both the dicyanate homopolymerization and epoxy/dicyanate co-reaction gave good adhesive properties but reacted much too slowly to be useful as the initial tack-free forming step even when catalysts were used. This co-reaction seemed however, to be ideally suited for the final post cure crosslinking step. The search for a primary curing agent (resin hardener) that provided faster tack-free forming reactions began with a review of epoxy and cyanate curing reactions.

Polymerization of epoxy resins can occur *via* the epoxide groups and the functional hydroxyl groups along the backbone of the chain through the action of curing agents which serve as co-reactant hardeners or catalysts. Common curing agents and their reactions are well documented in introductory texts [33-37].

Tertiary amines and quaternary ammonium salts are common examples of catalytic agents. The most common co-reactive hardeners are the amines and polyamides [34]. Alcohols, phenols, thiols and carboxylic acids or acid anhydrides are also used but much less frequently for a variety of reasons including handling convenience and cure rate. Formaldehyde-based resins, e.g. phenol-formaldehyde polymers, have been used for curing high molecular weight epoxy resins through the secondary hydroxyl groups. Because the latter curing agents are condensation reactions which liberate water and/or formaldehyde they were excluded from consideration.

Primary amines are generally very reactive with terminal epoxy groups. The reaction produces a secondary amine, which in turn can further react with other epoxies to form a tertiary amine. Both reactions result in the generation of pendant hydroxyl groups that may enter into additional curing reactions under the right conditions.

The mechanism of epoxy curing with polyamides is not completely clear. Gorton [38] showed that epoxy resins reacted with the amide hydrogens of aliphatic polyamides, but it is generally recognized that the secondary amine and terminal amino groups are much more reactive [39, 40].

The mechanism in uncatalyzed carboxylic acid anhydride hardening of epoxies is believed to primarily involve the opening of the anhydride ring by secondary hydroxyl groups along the epoxy backbone or by traces of moisture in the mix. This ring opening is followed by reaction of the resultant carboxylic group with the epoxide to form ester linkages. A competing epoxy etherification reaction can also occur with the new hydroxyl groups formed when the epoxy ring opens. The tertiary amine catalyzed system is very fast and produces high molecular weight polyesters while suppressing the formation of secondary hydroxyl groups [41, 42]. The polar ester linkages produced in this reaction might bond well with the amide groups in the aramid polymer. A high degree of crosslinking is possible with the use of dianhydride hardener.

Dicyanate resins are also polymerized with active hydrogen compounds including alcohols, phenols, thiols, amines and amides [43]. Some of these reactions produce thermally reversible adducts which can serve as intermediates in the cyclotrimerization curing of dicyanate resins. The adducts decompose to a cyanate derivative with the release of a phenol by the general scheme of Fig. 1. Shimp *et al.* [17] suggests that this

reversal occurs above about 150°C. Thus, a dicyanate could be reacted with an aromatic diol as shown in Fig. 1 to produce a large linear polymer that would later thermally reverse and further polymerize to a heavily crosslinked thermoset. The initial attempts at testing this reaction scheme using either hydroquinone or bisphenol A failed to produce acceptable adhesion to the aramid paper however, and so no further development was undertaken.

The reaction between a primary amine and a cyanate ester forms stable bis(imidocarbonate)imide compounds. Fig. 1 suggests that the primary monofunctional amine should afford a stable linear polymer while the employment of a primary diamine would yield a branched structure.

The reaction between cyclic carboxylic acid anhydrides and aryl cyanate esters has been studied by Grigat [44] and Pandratov *et al.* [45]. In the presence of a tertiary amine a linear imidocarbamate can form (Fig. 2).

3.3 Experimental

The three leading candidate hardeners identified from the literature review were:

- primary amines
- polyamides, and
- carboxylic acid anhydrides

Adhesive testing was done prior to selecting one o these hardeners for more detailed investigations of tack-free times and thermal stability.

3.3.1 Test materials.

Nominal 2 mil thick Nomex® Type 412 nonwoven paper (E. I. du Pont de Nemours & Co., Inc., Wilmington, DE) was used in this study. The paper sheet is 100% poly(*m*-phenyleneisophthalamide).

The selected epoxy resin was a low molecular weight diglycidyl ether of bisphenol-A (DGEBA) type liquid resin (Epon®Resin 828, Shell Chemical Co., Houston TX.). Although the bisphenol-A type epoxies are generally less chemically and thermally stable than the novolac type, their lower viscosity was judged to be a more important consideration in light of our solvent-free goal.

The recently introduced liquid dicyanate monomer (AroCy®L10 bisphenol-E dicyanate, Rhône-Poulenc Inc., Louisville, KY, formerly Hi-Tek Polymers, Inc.) was chosen for its low viscosity and ease of blending with epoxy resins [46].

The amine and anhydride hardeners were aromatic types that offered latent curing behavior and good thermal stability. Both hardeners were technical grade. The polyamide was a commercial epoxy curing agent.

3.3.2 Sample preparation and test procedures.

All resin mixtures were prepared and spread on the aramid paper at room temperature. Shortly thereafter they were cured at 177°C (350° F) for 2 h in a heated press . In many cases the mixtures required mild heating to aid blending, which may have caused slight resin advancement. Adhesion samples were prepared by gluing the two faces of a folded 12 inch square sheet of 2.0 mil aramid paper together as shown in Fig. 3. Because of the anisotropic paper properties the samples were prepared with the peel direction in line with the papermaking machine direction. After curing at a pressure of 70 psig, the samples were cut into 2.54 cm (1 in.) wide strips with a precision sample cutter. The adhesive strength was then assessed using the T-peel procedure specified in ASTM-D 1876. The force required to separate the inch-wide sample and the peel length were measured in a conventional tensile tester from which the average force was calculated (total work output/peel length). Since it was not possible to maintain the ASTM specified peel rate of 10 in./min (25.4 cm/min)without premature failure of the sample, a rate of only 1 cm/min was used. Even at this low rate the typical peel length to failure was only 3-5 cm .

The times for the adhesives to become tack-free were measured by removing test samples from a 177°C hot plate at regular intervals and quenching them quickly on an ice-cooled plate to stop the polymerization. The samples consisted of a small sheet of aramid paper containing 1 drop of the test adhesive. The tack condition was determined by the degree to which the glue stuck to the clean portion of the aramid paper after cooling to room temperature, when the sample was folded back onto itself. If the two sections of paper could be separated easily without transferring any of the glue to the initially clean side of the paper it was judged to be adequately tack-free.

The glass transition temperature was measured by differential scanning calorimetry (DSC) at a heating rate of 10°C/min under a nitrogen cover gas. The temperature at the onset of the transition region in the DSC scan was taken as the Tg value.

3.4 Results and Discussion

3.4.1 Hardener testing.

The aromatic amine and polyamide hardeners were found to react more rapidly with the dicyanate resin than the epoxy. The third hardener, a carboxylic acid anhydride reacted quickly with both the epoxy and the dicyanate in the presence of tertiary amine catalysts, but only with the epoxy when the catalyst was removed.

The important characteristics for the various resin and hardener combinations are summarized in Table 2. The aromatic amine, *m*-phenylenediamine (MPDA), shows latent curing behavior and good thermal performance. With some trial and error a level of addition was identified that produced a partially advanced prepolymer from the liquid resin mixture and still gave reasonable adhesion after post cure. At a level of 14 phr (parts per hundred parts of resin) MPDA cured epoxies and produced good adhesion, although tack-free times tended to be slower than desired.

With the addition of 25 wt. % dicyanate monomer and a lower amine level (5 phr) good adhesion was maintained while appreciably faster resin advancement was secured; presumably from the reaction between primary amines and dicyanates (see Fig 1). If the dicyanate level was increased to 50 wt. % the adhesion became poor.

A polyamide curing agent (Table 2; samples G, R and S) also produced reasonable adhesion and fast tack-free times. The polyamide reacted very quickly with the mixtures containing dicyanate resin and separated into two distinct phases during blending at room temperature. The precipitated solid phase, which was presumably the product of a reaction between the polyamide and the dicyanate, could be dispersed in the remaining epoxy phase if the concentration of dicyanate was sufficiently high. Sample S represents this latter situation. However, when the dicyanate level was increased to 50 wt. % a decrease in the adhesive strength was observed.

Pyromellitic dianhydride (PMDA) was selected because of its compact aromatic structure and multifunctionality towards epoxy resins which creates polymers with a high degree of crosslinking [36]. Since the PMDA is both solid and insoluble in the resin mix at room temperature, it poses some handling problems. Good adhesion and fast tack-free times were measured for both pure epoxy systems and epoxy/dicyanate blends with PMDA hardener. Small amounts of the tertiary amine catalyst *N,N*-dimethyl-*p*-toluidine (DMPT) were used in these tests after it was shown to noticeably accelerate the curing.

The measured peel strength data from the T-peel tests are presented in Fig. 4. All formulations with good adhesion approach the same peel strength value of roughly 2 lb_f/inch of width. The failure mechanism was always by fiber pullout from the aramid paper substrate rather than at the interface or within the adhesive layer itself even though the adhesive did not appear to penetrate the paper. In other words, the adhesive joint is limited by the strength of the aramid paper and not the bond itself. Instead of the poor interfacial bonding often seen between epoxy adhesives and aramid surfaces, in this particular application the aramid fiber/fibrid interface is the weak link. This finding suggests that measurements of physical strength properties for the adhesive itself are not relevant in this application.

Of the five samples that adhered well to the aramid paper, formulations G, N, and F showed the best overall performance. All other formulations rated poorly in two or more of the selection criteria. The anhydride-cured systems (formulations N and F) are expected to have the best thermal stability and pot life.

A comparison of formulations N and F shows the effects of adding a small amount of dicyanate resin to the adhesive. The improvement in viscosity is canceled by the decrease in pre-cure adhesion which suggests that the best compromise may fall in the region between these two compositions.

3.4.2 Final formulation.

The effect of variations in the epoxy, dicyanate and pyromellitic dianhydride (PMDA) levels on the adhesive quality are presented in Fig. 5. The ordinate axis represents a measure of adhesive quality based on the average force required to peel one inch wide samples over a distance of one to two inches. Five peel tests were typically made on each adhesive. The only significant procedural change initiated at this stage of development

was to introduce a tack-free forming step followed by a 7 day hold. This was done prior to final curing in order to better simulate the actual manufacturing conditions. The anhydride was initially assumed to react primarily with the epoxy and so all anhydride levels reported in this section are based on the weight of the epoxy resin only except where specifically noted.

In most cases the adhesive bonded well enough so that the aramid fiber/fibrid matrix failed before the glue. However, the adhesive did not spread uniformly in all cases due to inadequate melting of the partially cured, tack-free resin. As a result, some of the mixtures never sufficiently wet the adjacent sheet and so the quality of the adhesion varied considerably; even within the same sample. This behavior was reflected by lower average peel force values with large variability.

While these same adhesive blends might show excellent adhesion if cured shortly after application, the practical processing requirements dictate that the adhesive be partially advanced before the two aramid faces are brought together. In other words, though the thermodynamics may be favorable, poor practical adhesion is observed due to fluid dynamic effects or wetting kinetics.

As seen in Fig. 5, the adhesive quality of epoxy resins is improved initially by increasing either the dicyanate or anhydride concentration. An adhesive maximum is also noted at all levels of anhydride around a dicyanate/epoxy ratio of between 0.2 and 0.4. The lower adhesion observed at higher levels of dicyanate are also accompanied by a failure to reach tack-free conditions in a reasonable time as shown in Fig. 6, although the two phenomena should not be related.

At low anhydride levels or high dicyanate levels tack-free conditions could not be reached in a reasonable time. The other extreme of high anhydride or low dicyanate levels caused premature gelling during the tack-free stage and the adhesive would not melt sufficiently for the final cure. For the case where no dicyanate was used, it was observed that the lowest PMDA level (10 phr) produced an inadequately cured resin with very poor adhesion while the next higher PMDA level (20 phr) produced poor adhesion due to rapid gelling of the mixtures. Furthermore, 20 phr is still well below that recommended level [36] and is expected to have both poor thermal resistance and elevated temperature

strength. With the addition of dicyanate as a reactive diluent, the gelling was prevented and better control of the tack-free step was achieved.

The observed decrease in peel strength at higher dicyanate/epoxy ratios for a fixed hardener concentration and the improved adhesion observed with the increasing anhydride level (up to about 20 phr) at all dicyanate/epoxy ratios implies that the polycyanurates reduce the adhesion. At higher dicyanate levels the polymer structure may become too rigid for good bonding.

Measurements of the glass transition temperature (Tg) were used to assess whether the selected formulations would retain sufficient strength during curing of the impregnating resin to avoid separation of the node lines. Near the Tg, the mechanical strength of the adhesive is expected to decrease rapidly. For this reason it is common to find the usable temperature limits for epoxy polymers based on some percentage of their Tg value (e.g. 80-90%). Since neither the mechanical strength of the adhesive nor the interfacial adhesion were found to be limiting at room temperature in this application, it was assumed that the useful temperature of the adhesive would be its Tg value. It was also assumed that the acceptable Tg value would be greater than or equal to the curing temperature of the impregnating resin, which is typically in the range of 150° to 180°C.

Resin samples were cured for 1 h at 125°C followed by 2 h at 177°C. The samples were then crushed and ground before the final post-curing at 250°C to help ensure a uniform thermal history. The effectiveness of the post-curing time was assessed by measuring the Tg for a single sample following additional post-curing. At the end of each DSC thermal scan the sample was held at 250°C for 1 h of additional curing before being rapidly cooled. The procedure was repeated for a total of 4 h post-curing, but as shown in Fig. 7, a period of 2 h appears to be adequate. The effect of additional curing was also observable by the shape of the thermal scan including the disappearance of an exotherm around 250°C. The heatup time for the sample was ignored because the DSC scans showed no distinct evidence of reactions much before 250°C. The fact that only one distinct Tg was detected in thermal scans to 300°C is evidence of a single phase polymer structure rather than an interpenetrating network of the two polymerized resins.

The polymer network that develops with this tertiary system is expected to form in two stages. Competing anhydride reactions with both the epoxy and dicyanate should occur

relatively quickly during the initial tack-free forming step compared to the much slower cyanate homopolymerization and epoxy cyanate coreation. DSC scans of the uncured resin at a heating rate of 10°C per minute showed two distinct exothermic peaks indicative of this two stage curing. The tack-free forming reactions with the anhydride hardener were centered around 125 - 140°C while the epoxy and dicyanate post-curing reactions were centered above about 200°C. Only the single peak above 200°C was detected without the anhydride.

The effect of the epoxy/dicyanate ratio and anhydride concentration on Tg values are presented in Fig. 8. The improvement in Tg which is observed for the higher dicyanate concentration is attributed to more complete curing from both the increased total hardener level and the delayed gelling that occurs with dicyanate addition. Since the dianhydride PMDA has a higher functionality (f=4) towards the epoxy than does the *s*-triazine ring (f=3), higher Tg values were also expected for greater PMDA levels due to an increase in crosslinking densities within the network. The data does not however support this hypothesis. For the 20/80 wt. % dicyanate-epoxy mixture the Tg value only increases as the PMDA levels go from 0 to 10 phr and then fall off again. By itself 20 wt. % dicyanate is insufficient hardener to produce acceptable polymers as evidenced by both the low Tg shown in Fig. 8 and the poor adhesion noted in Fig. 5. Consequently, a significant enhancement in the Tg is observed with the addition of more hardener, as either dicyanate or anhydride. In fact, it would appear that the dicyanate is actually the more efficient hardener since it produces the larger increase in Tg for roughly an equivalent change in level. Only when the amount of PMDA was further augmented did the resin gel very quickly, before the dicyanate curing reactions could occur.

The lack of any significant Tg dependence on the anhydride level for the 30 wt. % dicyanate case indicates that this level provides a reasonable hardener concentration. Premature gelling was still observed for the highest PMDA level (35 phr), but this time it had little effect if any on the glass transition temperature; an anomaly that requires further study. Nonetheless, the data clearly indicates a substantial increase in the Tg correlated with the increase in dicyanate concentration as well as a lesser sensitivity to the amount of the PMDA hardener added.

Additional curing of the 30 wt. % dicyanate samples for 1 h at 300°C resulted in a further increase in the Tg for the 35 phr sample only, and a slight decrease in all others as seen in

Fig. 8. This improvement, which results from either further crosslinking reactions or the decomposition and volatilization of residual monomers/oligomers, supports the assumption that incomplete curing occurred in the samples which gelled prematurely.

3.5 Phase I Summary and Conclusions

An acceptable adhesive formulation for use with aramid honeycomb has been developed. The required dual-stage curing was achieved with a three-component heat activated mixture. In the first stage of curing, pyromellitic dianhydride (PMDA) is reacted at elevated temperatures with an epoxy and a cyanate resin in competing reactions. The residual cyanate homopolymerization and co-reaction with the epoxy resin occurs at a much slower rate and therefore, serves as a delayed, second-stage curing step. Both stages have sufficiently low reaction rates at room temperature to ensure good pot life and the required B-stage stability. Dynamic DSC showed the two distinct exothermic peaks that are indicative of the dual stage curing

The effects of the epoxy/dicyanate ratio and anhydride concentration on adhesive strength, tack-free times and glass transition temperature (Tg) were examined in some detail as part of the phase I development. In general, improved adhesion and glass transition temperatures correlated with increased levels of either cyanate ester or anhydride, but not linearly or continuously. For example, an adhesive maximum was observed at all tested levels of anhydride around a cyanate ester/epoxy ratio of 0.2 to 0.4 . The lower adhesion observed at higher levels of cyanate ester was also accompanied by a failure to reach tack-free conditions in a reasonable time. Likewise, excessive anhydride resulted in a loss of good adhesion. In this latter case the adhesive formulations gelled too quickly, presumably before the secondary cyanate curing reactions could occur. Consequently. the adhesive would no longer melt sufficiently to wet the adjacent sheet during secondary curing. Glass transition temperatures also fell.

Based largely on bonding strength and the need to reach tack-free conditions rapidly, a dicyanate level of 30 wt. % (cyanate/epoxy mol ratio of 0.55:1) and a PMDA hardener level around 20 phr (22 mol%) appears to meet the necessary adhesive requirements for honeycomb core manufacturing. This level produced an adhesive that was easily advanced to a tack-free solid shortly after printing and yet remained sufficiently meltable for good wetting and bonding to the adjacent sheet during final post-curing. The onset

temperature for the glass transition region of this mixture at roughly 160 °C is judged to be satisfactory.

The important key to improving the node line strength lies in improving the aramid paper rather than the adhesive itself. This may include modifying the paper to allow better glue penetration and subsequent bonding between fibers. Failures within the finished honeycomb core, which is a composite of the bonded aramid paper embedded in phenolic resin, may also be related to the same type of fiber pullout or delamination within the paper layer that was observed for the node-line glues. Thus, improved bonding between fibers may also be a key to improving the overall strength of finished aramid honeycomb composites.

Table 2. Performance summary for selected Adhesives

Sample #	Resin mix	Hardener * (phr)	Viscosity	Pot life	Tack-free time	Pre-cure adhesion	Post-cure adhesion
831P	Epon 828	MPDA (14)	medium	medium	medium	poor	fair
831H	E828/L10 (3:1)	MPDA (5)	medium	short	medium	poor	good
831Q	E828/L10 (1:1)	MPDA (6)	medium	short	fast	fair	poor
831G	Epon 828	polyamide (50) (Versamid 150)	medium	short	fast	good	good
831R	E828/L10 (3:1)	polyamide (9) (Versamid 150)	high	short	fast	fair	good
831S	E828/L10 (1:1)	polyamide (10) (Versamid 150)	medium	short	medium	fair	fair
831N	Epon 828	PMDA (20)	high	medium	fast	good	good
831F	E828/L10 (3:1)	PMDA (25)	medium	medium	medium	poor	good
831L	L828/L10 (1:1)	PMDA (25)	medium	medium	medium	poor	poor

* Based on total resin mix phr (parts per hundred parts resin).

E828: Epon 828 epoxy, Shell Chemical Co., Houston, TX.

L10: AroCy L10 dicyanate monomer, Rhône-Poulenc Inc., Louisville, KY.

Versamid 150: polyamide curing agent, Henkel Corporation, LaGrange, IL.

MPDA: *m*-phenylenediamine.
PMDA: pyromellitic dianhydride.

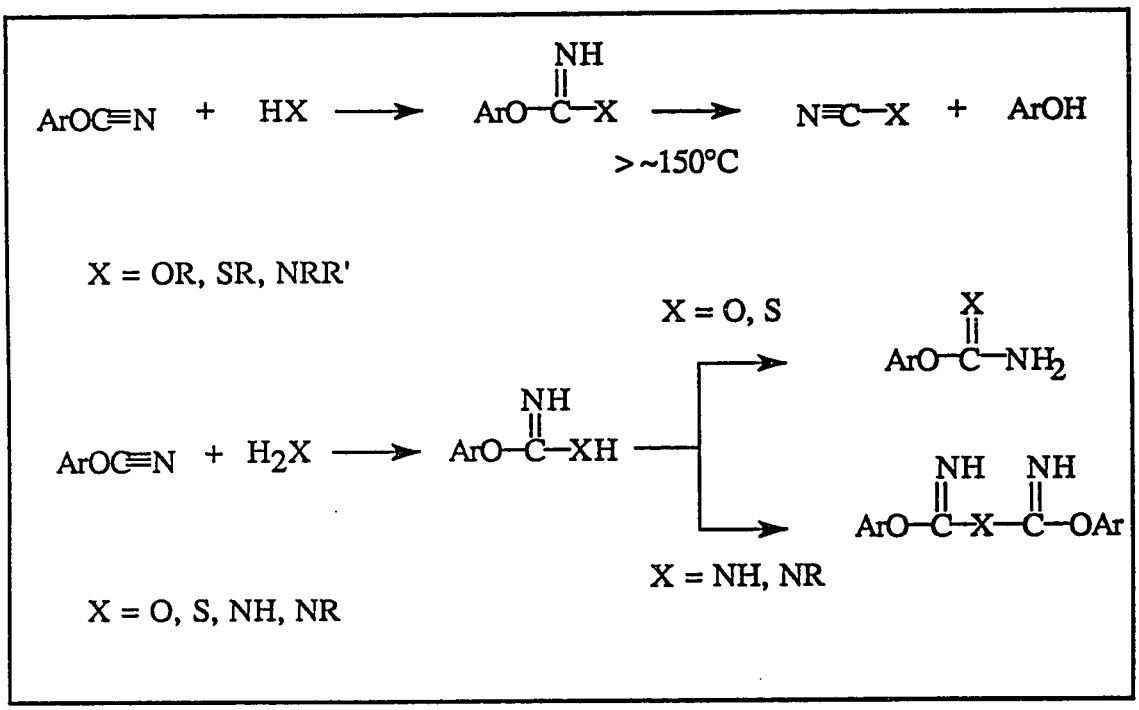

Figure 1. Reactions between aryl cyanate esters and active hydrogen compounds as formulated by Grigat and Pütter [43].

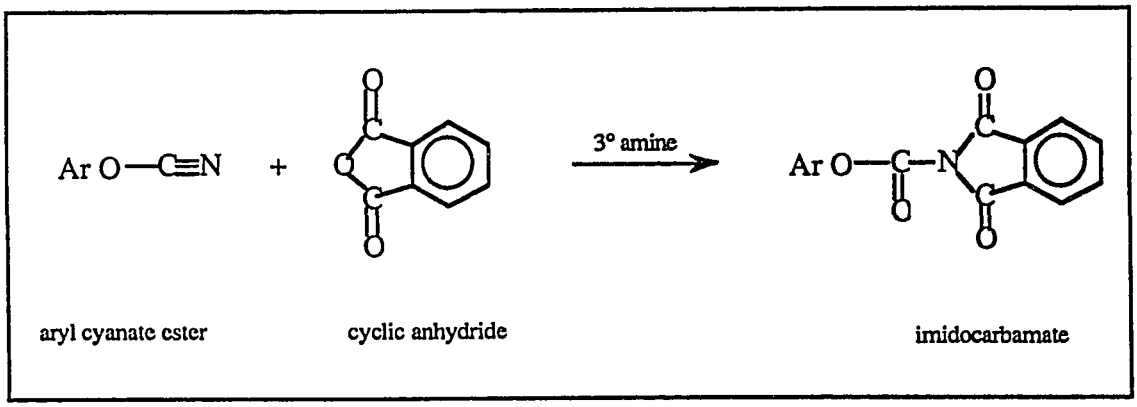

Figure 2. Imidocarbamate formation from the amine-catalyzed reaction of aryl cyanate esters with carboxylic acid anhydrides

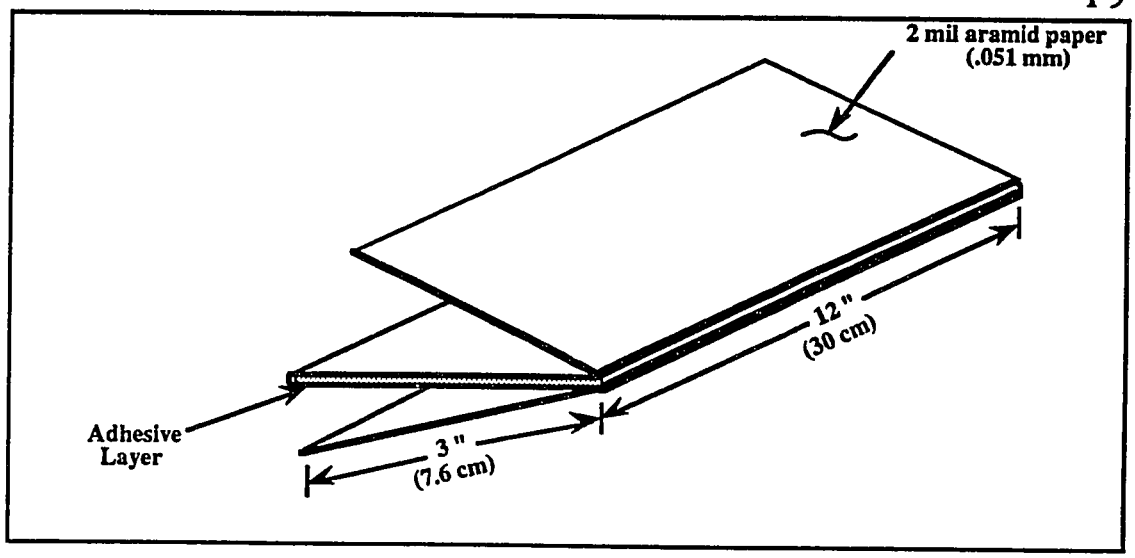

Figure 3. T-peel Test Panel

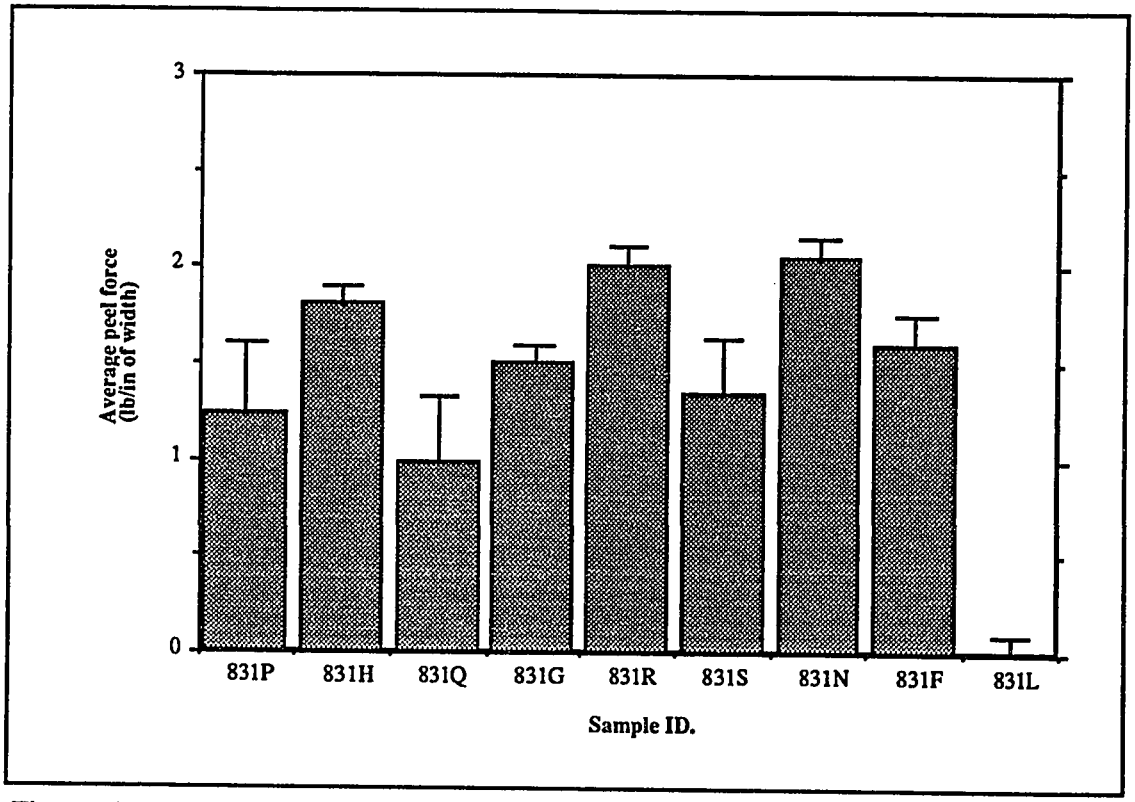

Figure 4. Average force required to separate the faces of bonded aramid paper @ 22°C and a peel rate of 0.4 in/min. Selected adhesive formulations are shown in Table 2

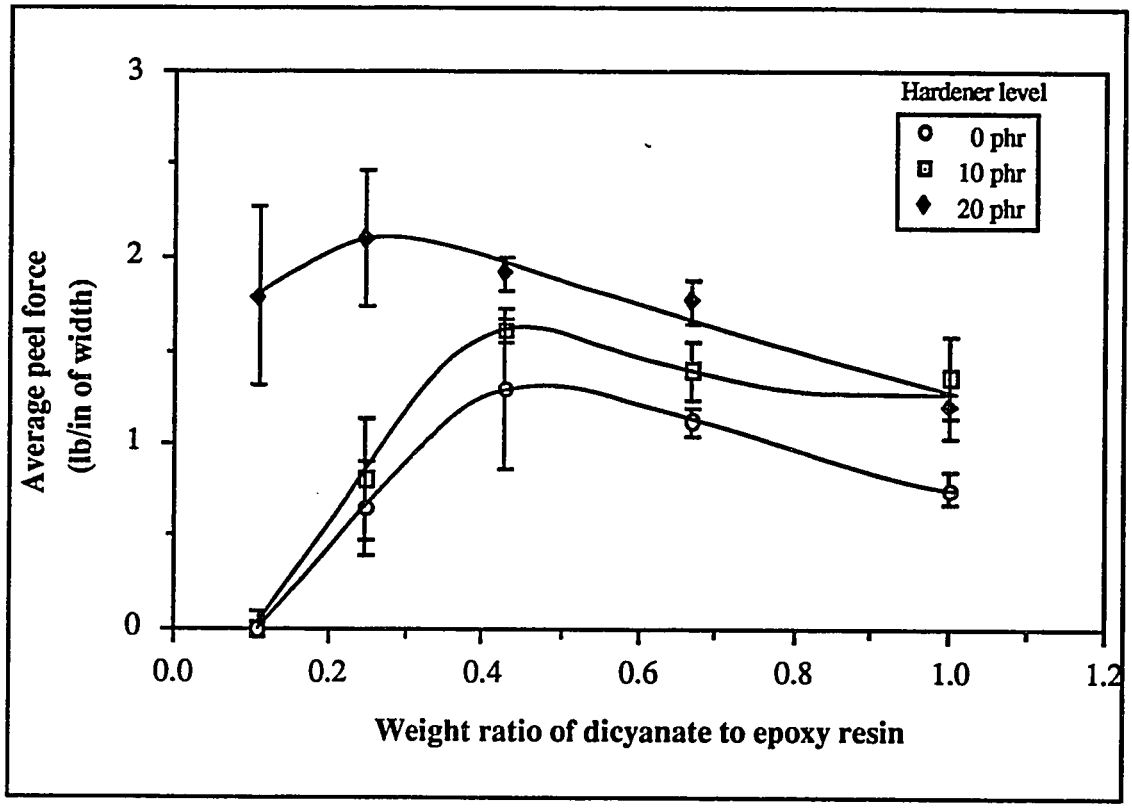

Figure 5. The variation in peel force as a function of the dicyanate/epoxy ratio and PMDA hardener level.

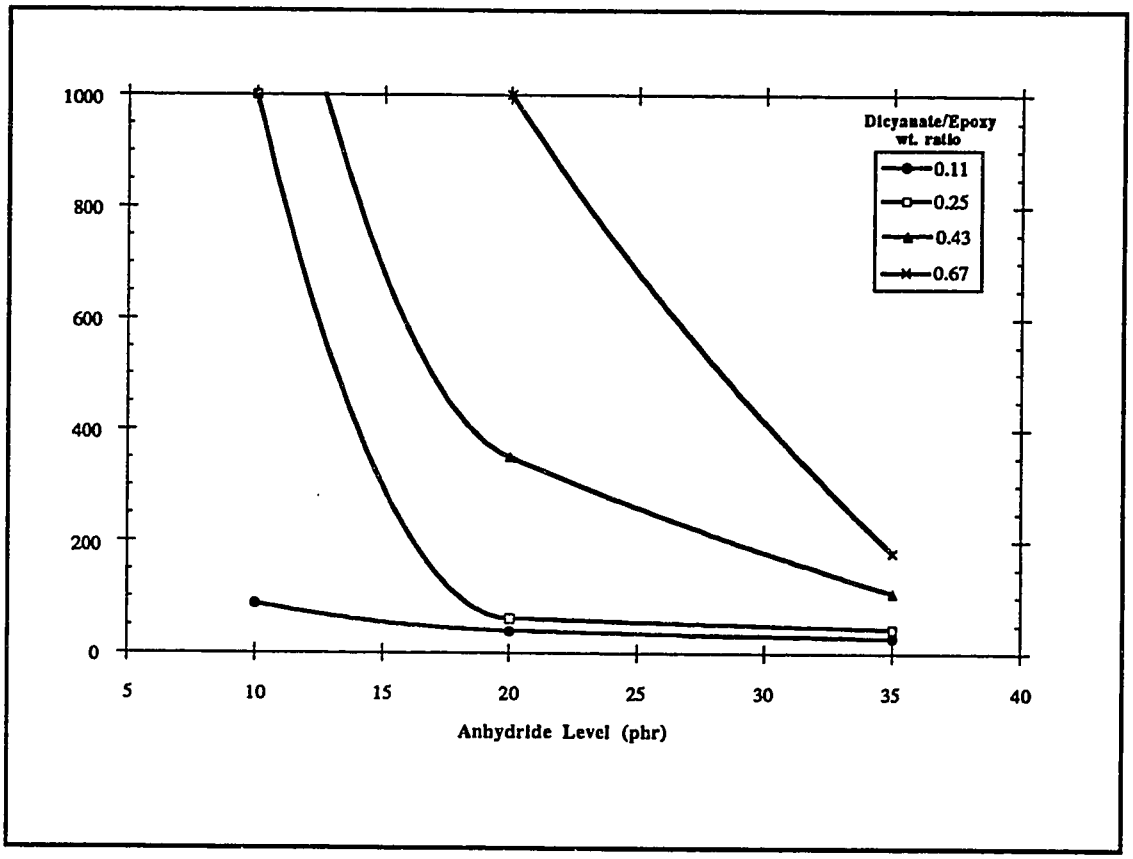

Figure 6. The time to reach room temperature tack-free conditions as a function of both the PMDA hardener level and the dicyanate-epoxy resin weight ratio.

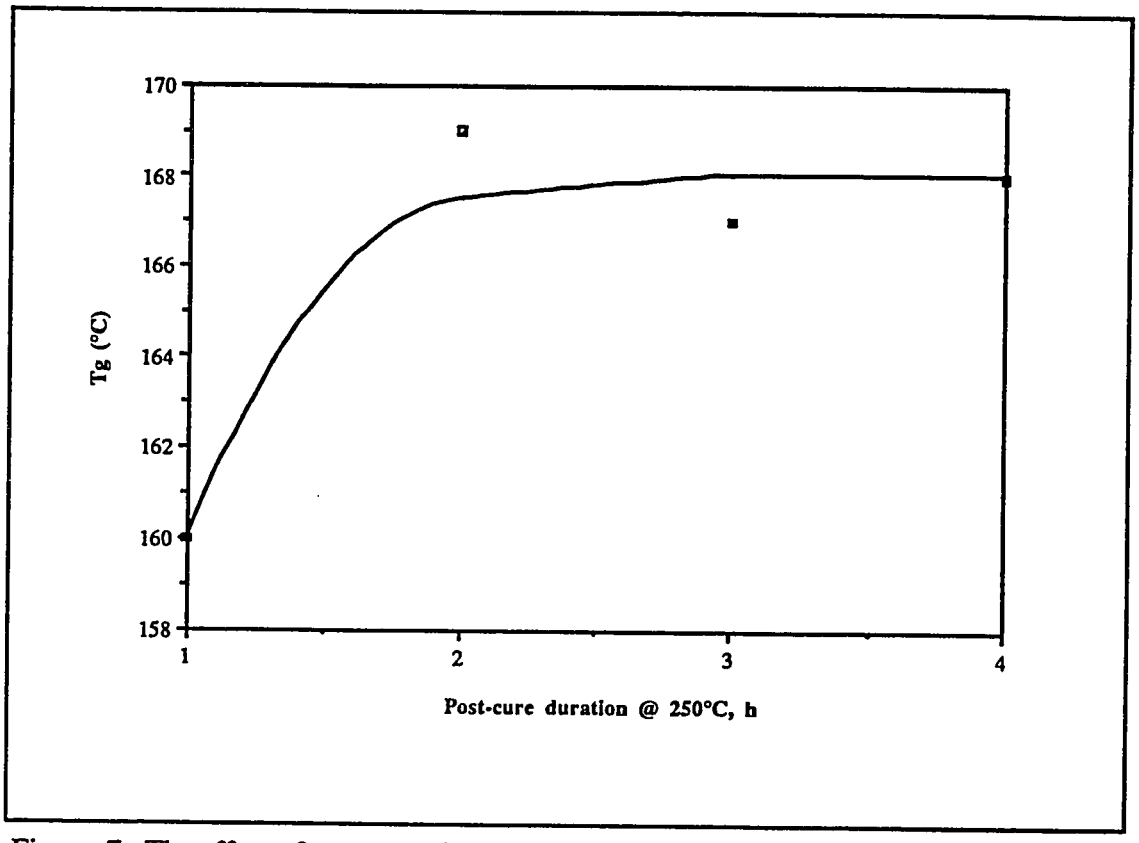

Figure 7. The effect of post-cure time on the final glass transition temperature.

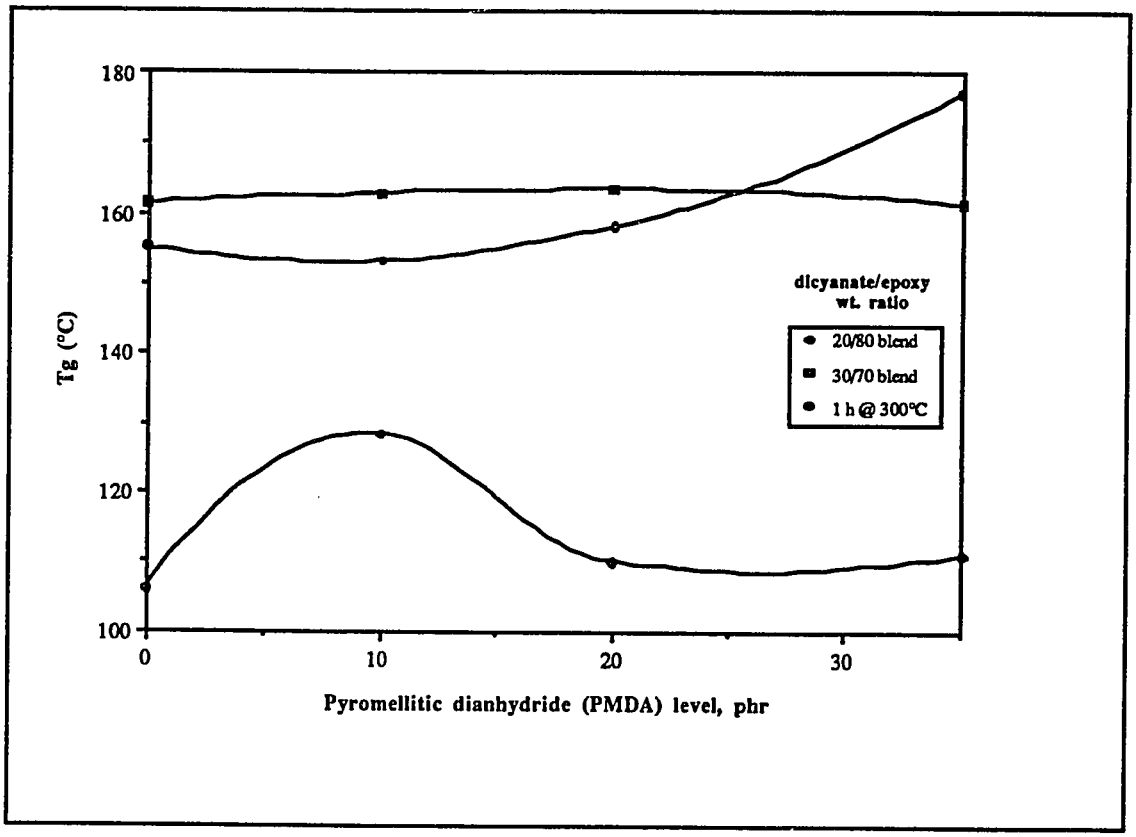

Figure 8. The variation in glass transition temperature as a function of PMDA hardener level for two dicyanate-epoxy resin blends. All samples post-cured for 4 h @ 250°C. Sample o = 30/70 blend after one hour of additional post-cured. Tg measured by DSC @ 10°C/min under a nitrogen blanket.

4 POLYMER CHARACTERIZATION -- Phase II

Empirical studies were used in the preceding chapter on adhesive development to define the compositional envelope for acceptable adhesive properties. A more fundamental understanding of the complex polymer network structure and chemical reactions of these materials is now sought as the means of furthering their development. It is expected that a knowledge of the primary reaction mechanisms and their interdependency will allow the important controllable parameters to be defined and perhaps manipulated for improved polymer performance. The scope for phase II of this research project includes model compound studies to identify the principal curing reactions and kinetic parameter measurements in independent calorimetry tests to support model development. Kinetic model simulations for the overall reaction are compared with experimental data to confirm the reaction behavior. Attempts to explain the observed differences in the thermal performance of selected compositions are made using the model predictions.

The dicyanate resins are the products of an esterification reaction between cyanic acid and a bisphenol derivative, although more typically they are produced from the cyanogen halides. These resins are often referred to in the literature as cyanate esters to help distinguish them from isocyanate compounds. The terms cyanate and cyanate ester are used interchangeably in the sections that follow.

4.1 Kinetic Modeling Methodology

Kinetic modeling by Bauer and Bauer [16] illustrates the complexity of the binary mixture of cyanate ester and epoxy resins. The tricomponent system involving acid anhydrides requires at least two additional competing reactions. Modeling for this complex tricomponent mixture was viewed as exceedingly difficult given the large number of competing reactions and corresponding degrees of freedom that could make a unique solution to any model parameter fitting impossible. In an attempt to avoid these difficulties an experimental approach was selected in which the major reactions were individually studied to determine the appropriate kinetic parameters. These parameters were then combined to build a model for the overall system, and the resulting system of differential equations solved numerically.

Six two-way interactions are possible with a tricomponent reactive system when all like-component pairs are included. Only the acid anhydride homopolymerization reaction was not considered credible; although at least one research group has observed some evidence that this reaction may occur under unique conditions [47]. The other five credible reactions are listed below. In the case of (5) the reaction proceeds via cyclotrimerization (reaction 1), followed by the epoxy resin coreacting with this *s*-triazine product instead of directly with the cyanate as implied. Early scoping studies identified reaction (6) as the only three-way interaction. The imidocarbamate product from (2) undergoes additional reactions when epoxy resins are added. Figure 9 illustrates this overall reaction scheme.

(1) cyanate homopolymerization
(2) cyanate + anhydride
(3) epoxy + anhydride
(4) epoxy homopolymerization
(5) cyanate + epoxy, and
(6) (cyanate + anhydride) + epoxy

Reactions (1), (3) and (4) are well documented in the literature. The reaction mechanisms and kinetics remain an area of continuing research, but reasonably good agreement exists among the investigators regarding the overall stoichiometry and reaction products of these three, as described more fully in the next section. The remaining three reactions require additional clarification. For example, recent studies of reaction (5) have reported significantly different results [27, 48]. In the case of reaction (2), very little information was found in the literature and no applicable studies were uncovered for reaction (6).

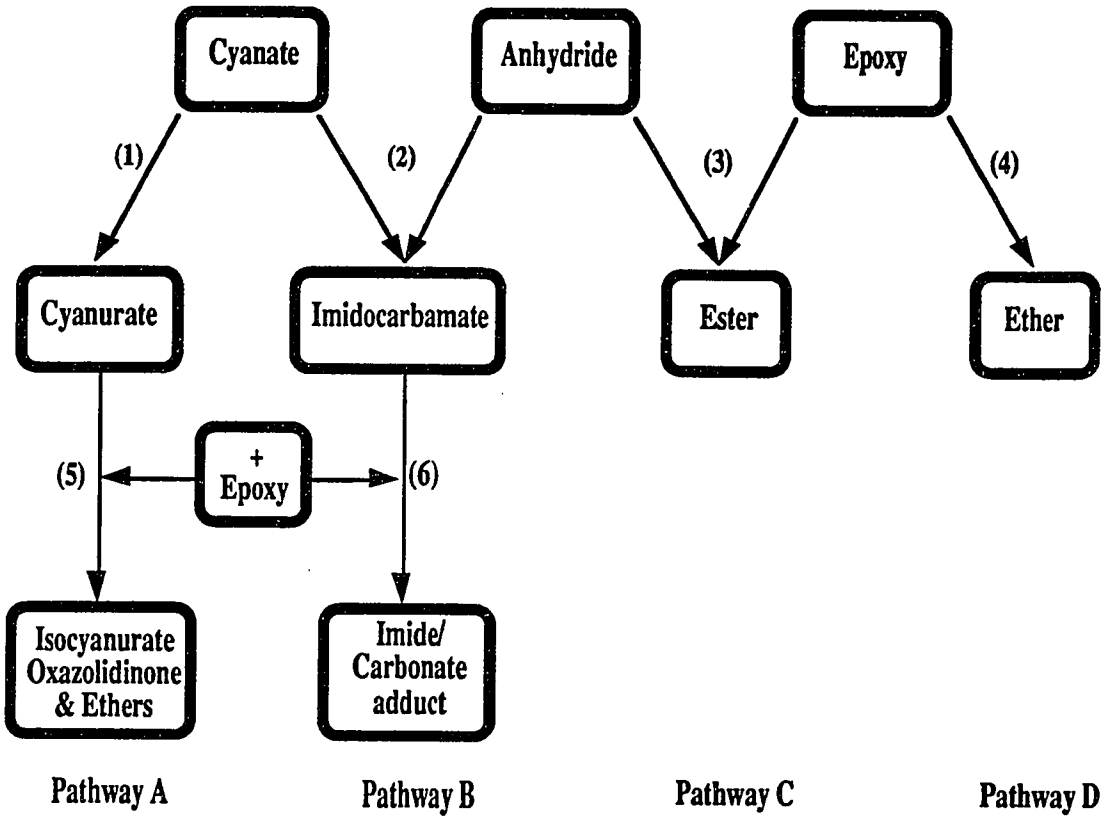

Figure 9. Hypothesized reaction scheme for the tricomponent mixture of a cyanate and epoxy resins with carboxylic acid anhydride hardeners.

4.2 Literature Review

This review of the reaction studies for the selected polymer system is presented in terms of the two independent reactions, cyclotrimerization and polyetherification, and the three competing binary reactions, epoxy/acid anhydride esterification, cyanate ester/epoxy copolymerization, and the cyanate ester/acid anhydride reaction with imidocarbamate formation. This separation is convenient for discussion purposes, but some important synergistic effects may have been ignored. For example, the catalytic role that triazine is believed to play in both the epoxy polyetherification reaction and the epoxy/cyanate ester co-reaction [48] may be important.

Penczek and Kaminska [49] recently published a review that provides a good summary of the known reactions for polymer systems containing cyanate esters. Since their

commercialization in the mid 1970's these resins have been growing steadily in their applications as a matrix for composite fibers and as a modifier to bismaleimide and epoxy thermosets [20, 29, 50-55]. The literature on cure kinetics and reaction mechanisms has grown significantly, but in comparison to most polymer systems the published data remains quite scarce and is limited for the most part to a handful of researchers. The reactions between epoxies and cyanate resins are not yet fully understood, or at least agreed upon, as indicated by the different mechanisms being reported in recent articles [16, 25, 29, 48].

4.2.1 Cyanate ester Cyclotrimerization. Grigat and Pütter [43] described the catalytic role of active hydrogen compounds, e.g. alcohols, phenols, thiols, amines and amides, in the polymerization of cyanate esters. The general reaction scheme presented in Fig. 10 was suggested by Shimp *et al.* [17].

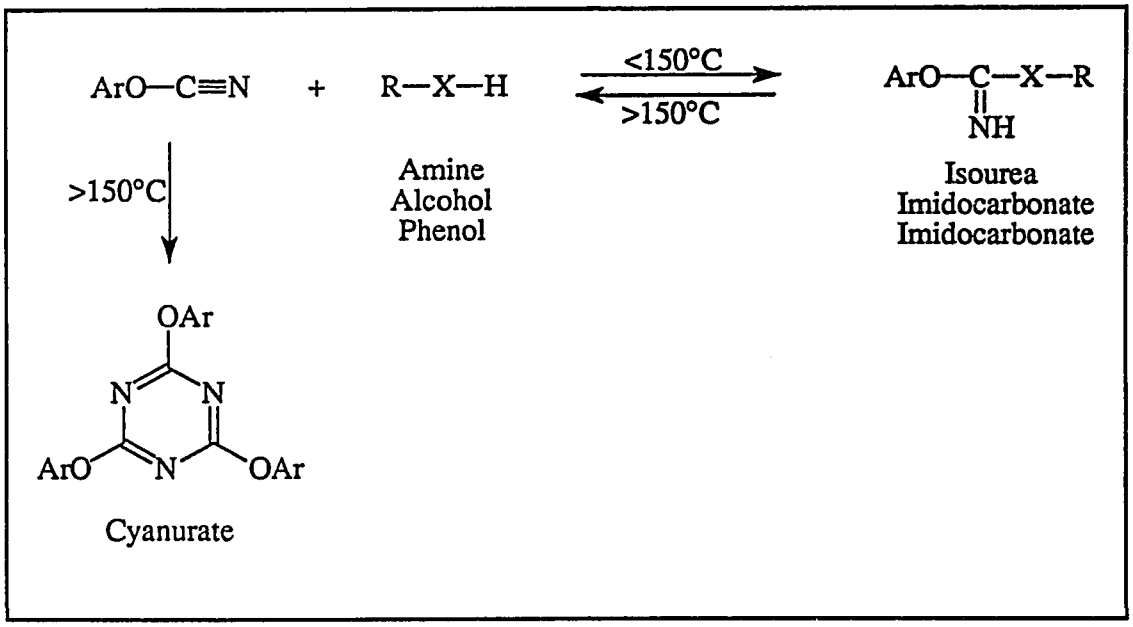

Figure 10. Aryl cyanate ester trimerization *via* reversible reaction intermediate formation from active hydrogen compounds(Shimp *et al.* [17]).

The infrared vibrational spectra provides an easily identifiable method of monitoring the cyclotrimerization reaction. The disappearance of the cyanate ester lines near 2280 and 2240 cm^{-1} and the appearance of the two triazine bands near 1580 and 1380 cm^{-1} has

been successfully applied by several researchers for the quantitative determination of rate parameters [56-60]. In most cases, differential scanning calorimetry has also been used in combination with FT-IR studies to help determine kinetic parameters and/or validate the models.

The cyanate ester homopolymerization reaction is generally thought to be free of secondary reactions, although Cozzens *et al.* [60] reported the appearance of two new weak FT-IR bands at 2220 and 1640 cm^{-1} during their studies with bisphenol A dicyanate. Neither band had been detected in their model compound studies and so they were assigned to unknown side reaction products. These secondary reactions have either not been detected or assumed negligible in all other mechanistic studies. The need to further consider these reactions in this current work has not been established.

Several kinetic models are described in the literature. In the absence of additional trimerization catalyst the cyanate ester homopolymerization is thought to be initiated by trace phenol and water impurities which catalyze the formation of a small amount a triazine [56]. The reaction is further propagated by a triazine catalyzed reaction between the trace phenol co-catalyst and a cyanate ester to buildup an imidocarbonate; which further reacts with additional cyanates to form the polycyanurate network shown in Fig. 11. The phenol catalyst is regenerated in this final step. This scheme is generally consistent with the reactions described by Grigat and Pütter [43].

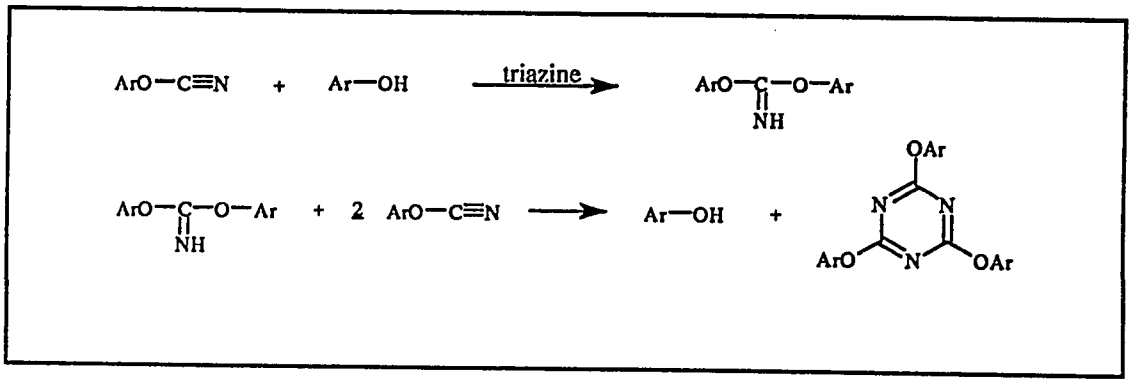

Figure 11. The cyclotrimerization mechanism proposed by Bauer *et al.* [56].

The authors modeled this reaction scheme as autocatalytic assuming first order dependence for each reacting functional group including the phenol and triazine catalysts. They then solved the resulting system of two ordinary differential equations using a

numerical procedure. Excellent agreement with data from differential scanning calorimetry (DSC) up to about 60% conversion was observed. The lack of good agreement beyond the 60% point was attributed to the onset of a diffusion controlled mechanism, as is common with thermosetting resins. In a separate analysis, using on-line FT-IR, these same authors also showed the overall reaction could be adequately modeled using only a simple first order kinetic equation with dependence on the cyanate ester concentration [C], alone (Eq. 1). However, this latter modeling approach ignored the initial induction period.

$$- d[C]/dt = k[C] \tag{1}$$

The uncatalyzed cyclotrimerization reaction studied by Simon and Gillham [57] using FT-IR analysis was modeled as two simultaneous reactions in which one is autocatalytic (Eq. 2). Both reactions were found to be second order in the fractional conversion x (where, $x = 1 - [C]/[C_o]$). The initiating reaction is catalyzed by trace amounts of hydroxyl groups while the second reaction is auto catalyzed with a first order dependency. The hydroxyl group is assumed to remain at a constant concentration and therefore, can be included in the rate constant k_1 rather than appear independently in the expression. After substituting for the fractional conversion x, and collecting the constants, the overall rate equation can be written in the following form:

$$- d[C]/dt = k_1[C]^2 + k_2[C]^2[T] \tag{2}$$

where; [T] = *s*-triazine concentration, and
[C] = cyanate ester concentration.

Subsequent comparisons between the degree of curing predicted by the model and the measured glass transition temperature from DSC data provided additional model validation.

The cure kinetics of two different cyanate resins investigated by Zeng *et al.* [58] were also shown to follow the autocatalytic behavior of Eq. 2, but with first order dependence on the cyanate concentration in both terms. The authors did not clarify whether the initially high level of triazine in their particular resins was accounted for in the parameter estimation.

Bonetskaya *et al.* [59] proposed a mechanism for cyanate ester homopolymerization reactions in the presence of a specific chelated metal (Cr^{3+} acetylacetonate) trimerization catalyst. The activated catalyst reacts with the nitrogen of a cyanate ester group to produce an intermediate with reduced charge density around the carbon. The trimerization reaction then proceeds by the reactive intermediate attacking the nucleophilic nitrogen of two more cyanate esters in a stepwise addition. After various simplifications to the system of coupled differential equations describing their mechanism, the authors proposed the following overall rate equation for the consumption of cyanate ester monomer [C]:

$$d[C]/dt = - [C] (k_b + k_c t) \qquad (3)$$

The overall rate constants k_b and k_c are functions only of the individual rate constants for the various reaction steps.

This form of rate equation also accounts for the observed autocatalytic behavior of the trimerization reaction through the t = time term on the right hand side (RHS), but is not conducive to analysis when competing reactions exist. However, it could be modified for more general use by substituting the t with an appropriate expression for the triazine concentration.

Two component trimerization catalyst systems containing nonylphenol and either a transition metal carboxylate or acetylacetonate are often advocated [17,61,62]. Kinetic modeling has not been done for these systems however.

4.2.2 Epoxy Etherification. Polyether formation occurs with hydroxyl containing hardeners such as alcohols, phenols or carboxylic acids. They are also the product of amine- and phenol-catalyzed epoxy homopolymerization reactions involving the secondary alcohols along the backbone of the epoxy chain. In both cases the hydroxyl group is transferred to the next polymer chain segment so its concentration remains constant. Tertiary amines are present in our system as catalysts for the epoxy-anhydride and cyanate-anhydride reactions and additional phenols may be generated as a secondary product of the cyanate-epoxy coreaction. The phenols are known to react directly with the epoxide ring as well as catalyze homopolymerization reactions with the epoxies.

Fedtke [63] and coworkers studied the tertiary amine-catalyzed epoxide homopolymerization using model compounds and actual epoxy resins. These authors identified several polyether products which they attribute to three main reaction mechanisms. In the absence of proton donors and at temperatures above 80°C, products from all three proposed mechanisms were observed. The dominant pathway at low temperatures (< 80°C) produced unsaturated carbon-carbon bonds in the final product.

DSC kinetic studies with diglycidyl ether of bisphenol A (DGEBA) and benzyldimethylamine catalyst were completed by Vazquez *et al.* [64]. These authors suggest that after some initial induction period the consumption of epoxy could be modeled with a simple first-order dependence on both the tertiary amine and epoxide concentration [E]. They also found the rate constant to be essentially independent of temperature above about 120°C, and only mildly dependent in the range of 80° to 120°C. When the amine concentration remains a constant, the rate expression is written:

$$d[E]/dt = - k [E] \qquad (4)$$

where; [E] = epoxy concentration

In the presence of phthalic anhydride Fedtke *et al.* [63,65] found that the amine-induced homopolymerization reactions were effectively suppressed. This finding is well established in the literature for carboxylic acids and their anhydrides [34-37,66], and presumably applies to proton donors in general. For example, phenols are observed to serve as both co-reactants and homopolymerization catalysts for epoxy resins. The latter competing reaction can be effectively suppressed however, with the selection of an appropriate catalyst such as an inorganic base (e.g. KOH), a tertiary amine or a quaternary ammonium salt [36]. The catalyzed reaction is commonly used to produce high molecular weight epoxy resins from bisphenol A.

The preceding review suggests that the uncatalyzed reaction between an epoxy and a phenol will include the epoxy homopolymerization reaction. However, the addition of the tertiary amine might effectively eliminate the homopolymerization term from this reaction by making the phenol-epoxy reaction much more dominant.

4.2.3 Epoxy/Acid Anhydride Reactions. The mechanism for uncatalyzed anhydride hardening of epoxies was previously described in Chapter 3. The reactions in the presence tertiary amines are outlined in Fig. 12. The specific mechanism involved in these base-catalyzed reactions is not fully understood as evidenced by the partially conflicting theories in the literature. One of the points of departure between the proposed mechanisms relates to whether the reaction is initiated by the catalyst acting on the anhydride ring as first suggested by Fisher [41], or on the epoxide ring as suggested by Tanaka and Kakiuchi [67] and in the more recent theory of Matejka *et al.* [42]. Even within the more recent theories we find the experimental results continue to differ greatly.

Tanaka and Kakiuchi proposed an initiating mechanism involving the catalyzed isomerization of the epoxy resin to an unsaturated alcohol based on experimental observations. Matejka *et al.* however, found no evidence of the double bond formation reported by these authors and suggested a completely different mechanism wherein the tertiary amine becomes irreversibly bound to the epoxide as an accelerator rather than a catalyst. Fedtke and Domaratius [65] proposed a modified mechanism by which the tertiary amine was released from the epoxide with the formation of a double bond at the end of the polymer chain in the same manner they hypothesized for catalyzed epoxy homopolymerization reactions [63]. In a recent investigation Steinmann [47] found no good evidence to support either of the double bond formation theories in references [67] and [65], nor could the author fully support the mechanism proposed by Matejka *et al.*. in which the amine became irreversibly bound.

Likewise, the results of kinetic modeling for this reaction are largely variable. Some investigators are reporting induction periods with sigmoidal shaped monomer consumption curves [42,47,67,68] while others continue to report simple n'th order kinetics [69-72]. References [69,71] provide good summaries of reported kinetic parameters from a number studies which suggest a reaction order anywhere from zero to four.

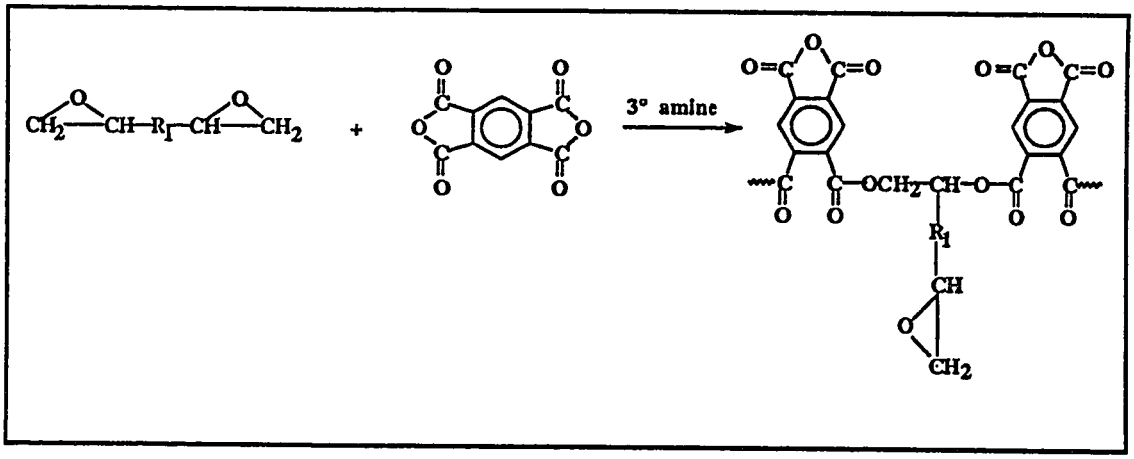

Figure 12. Polymerization reaction between epoxy resins and carboxylic acid anhydrides in the presence of a tertiary amine catalyst.

4.2.4 Cyanate ester/Epoxy Copolymerization. The co-reaction between cyanate esters and epoxy resins was investigated by Kubens *et al.* in the late 1960's [24]. Shimp *et al.* [15,48] have since studied this system with model compounds and identified the three principal reactions indicated in Fig. 13. The co-reaction product identified by these researchers is the five membered oxazoline ring. The products of this reaction were separated by liquid chromatography techniques and identified via their FT-IR spectra. According to these authors cyclotrimerization of the cyanate ester is initially the predominant reaction. The cyanurate (*s*-triazine) rings that form are believed to function as a nucleophilic catalyst for both the dicyanate/epoxy co-reaction and the epoxide homopolymerization (polyetherification) reactions that follow. Other researchers have also reported the formation of oxazoline (or isoxazoline) structures when epoxy and cyanate esters are reacted [22,28-32].

Shimp *et al.* found the cured-state mechanical, thermal and moisture resistance properties for equimolar epoxy/cyanate ester mixtures to be independent of the degree to which the starting cyanate ester was pre-trimerized before blending with the epoxy (varied from 0% to 50% initial trimer). This supported their contention that the cyanurate ring was a catalyst for both the co-reaction and the epoxy homopolymerization. Further evidence was provided by an experiment in which a specific epoxy resin which itself is only weakly catalyzed by nucleophiles was also incompletely cured by the cyanate esters.

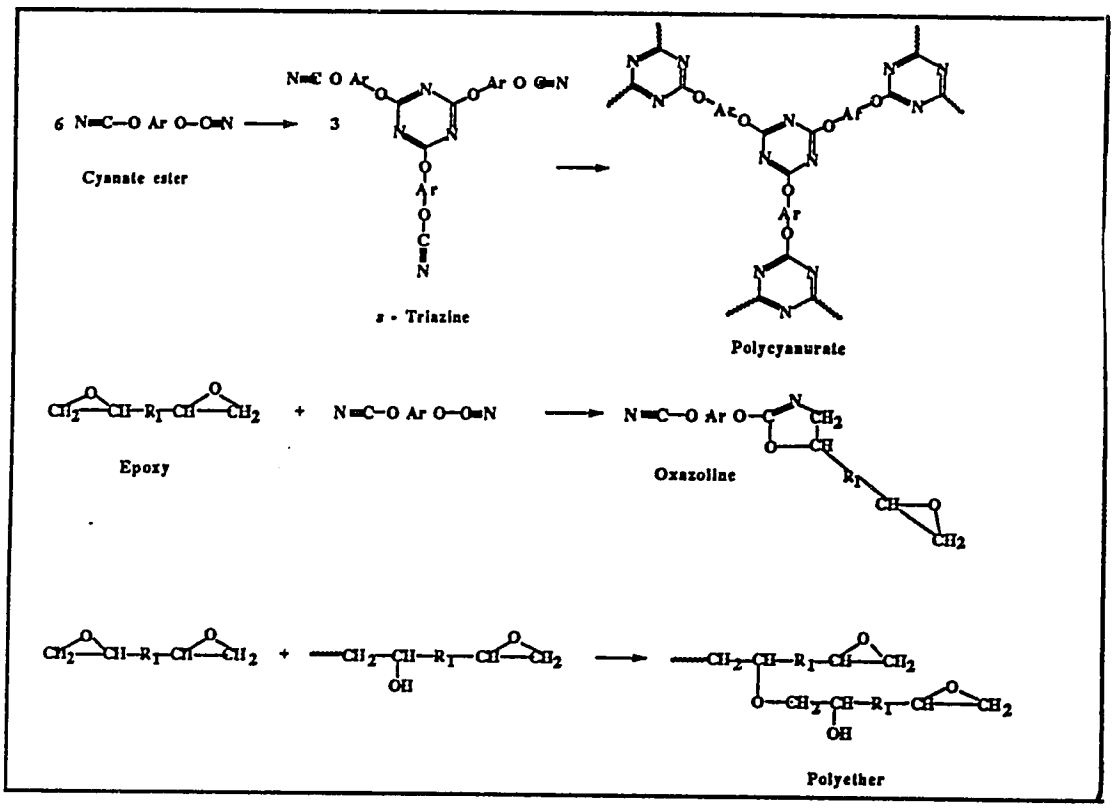

Figure 13. Scheme proposed by Shimp *et al.* [15,48] for the co-reaction of cyanate esters with epoxy resins.

The cured-state properties of equimolar epoxy/cyanate ester mixtures were also not significantly effected by whether or not a trimerization catalyst were used. However, the ratio of FT-IR absorbance spectra between the two wavenumbers Shimp assigned to the oxazoline ring noticeably varied with the type of catalyst and whether or not one was used. Shimp attributed this variation to the formation of different isomers which have little effect on the bulk polymer properties.

Bauer and Bauer [16,26,27,73,74] in a more extensive kinetic study have suggested a largely different reaction mechanism, Fig. 14. Here the cyanate ester trimerization is also the initial reaction (14a), but according to these authors the epoxy then reacts directly with

the triazine ring rather than with a cyanate ester group to form substituted cyanurates (14b). These substituted cyanurates are capable of undergoing isomerization reactions to isocyanurate (14c), which can further react with an epoxide to form the five membered cyclic oxazolidinone rings (14d). The alkyl substituted cyanurates and isocyanurates may also undergo a phenol abstraction which subsequently forms polyethers by reaction with the epoxy as shown in Fig. 14e and 14f.

The reactions were previously clarified by Korshak *et al.* [75] using the model compounds, phenyl glycidyl ether and triphenyl cyanurate. Infrared spectral identification confirmed the disappearance of the cyanurate bands and subsequent development of the C=O stretching bands near 1700 and 1460 cm^{-1} from an isocyanurate structure. A stoichiometric excess of epoxide or the substitution of isocyanurate for cyanurate produced oxazolidinones that were identified by a new IR band near 1750 cm^{-1} and a disappearance of the isocyanurate C=O stretching bands [75,76].

The Bauer and Bauer model appears consistent with the observations of Shimp *et al.* in that cyclotrimerization precedes the epoxy/cyanate ester co-reaction and the epoxy homopolymerization. Shimp's observation that cured state properties were not significantly effected by the initial trimer level of the cyanate reactant might be better explained if this trimer reacted with the available epoxy rather than with the cyanate. In other words, if a reaction mixture is started with 50% of the cyanate already as trimer (*s*-triazine) and both the trimerization reaction and the epoxy coreaction competed for the cyanate, than one would logically expect the level of polycyanurate in the finished product to be at least measurably higher than if the initial concentration of trimer were zero. Thus, with more of the cyanate converted to the cyanurate and the epoxy as polyethers instead of oxazoline, a significant decrease in mechanical properties should be observed. The fact that Shimp did not observe this provides a good indication the epoxy coreaction is not competing with trimerization.

Bauer and Bauer have assumed fundamental reaction equations for each of the steps in Fig. 14 and numerically solved the system of coupled ordinary differential equations. The five relative rate constants which remain as the adjustable parameters in their model were estimated by fitting the experimental data for various mixtures of bisphenol A dicyanate (BADCy) and diglycidyl ether of bisphenol A (DGEBA). The model appears to

effectively predict the complex chemical composition of the polymer network as a function of the cyanate ester fraction in the starting reaction mixture [26].

The reaction studies of Bauer and Bauer appear to have been done without the specific addition of trimerization catalysts. Shimp *et al.* [15] studied both the catalyzed and uncatalyzed systems and found the FT-IR spectra to be roughly the same in either case with only the relative heights of the two peaks in the 1700-1800 cm^{-1} region being different.

Table 3 summarizes the spectral assignments reported in the literature for cyanate ester reactions. In particular note that the 1760 and the 1695 peaks which Shimp *et al.* [15] associate with the oxazoline group are quite close to the 1750 (oxazolidinone) and 1700 (isocyanurate) peaks of Korshak *et al.* [75] or the 1740 and 1670 peak locations observed by Bauer *et al.* [26,73]. FT-IR spectral overlap, environmental effects or resolution difficulties could be the reason for the discrepancy between these groups.

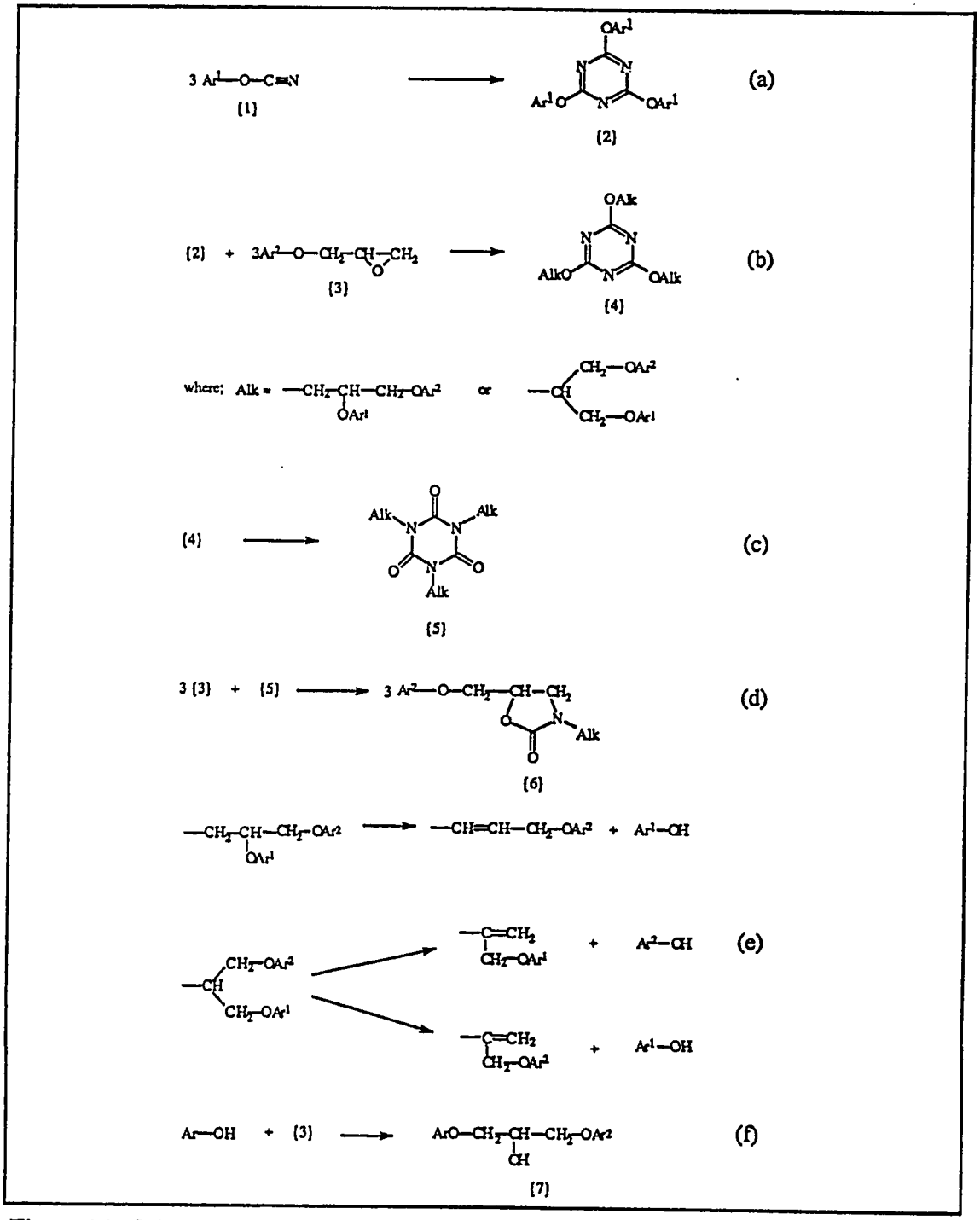

Figure 14. Scheme proposed by Bauer *et al.* [16] for the co-reaction of cyanate esters with epoxy resins. {1} cyanate ester; {2} *s*-triazine (cyanurate); {3} epoxy; {4} substituted triazine ; {5} isocyanurate; {6} oxazolidinone; {7} polyether. Ar^1 and Ar^2 are arbitrary aromatic groups.

Table 3. FT-IR spectral assignments used by various research groups

Wavenumber, cm-1	Bauer *et al.* [26,73]	Shimp *et al.* [15]	Korshak *et al.* [75]	Simon and Gillham [57]	Martin [77]	Feldman and Huang [51]	Gotro *et al.* [28,29]	Cozzens *et al.* [60]
2300-2200	cyanate -OCN	cyanate -OCN		cyanate -OCN	cyanate -OCN	cyanate -OCN	cyanate -OCN	cyanate -OCN
1760		C-O cyclic imidocarbonate						
1750			oxazolidinone C=O					
1740	oxazolidinone C=O							
1695 -1700		oxazoline C=N	isocyanurate C=O					
1670	isocyanurate C=O							
1640								unknown origin
1600-1608		oxazoline Ring					iso-oxazoline ring	
1560-1580	triazine ring	triazine ring	cyanurate ring 1580-1610	cyanurate -O-		triazine ring	triazine ring	triazine ring
1550-1600							oxazoline	
1500		benzene Ring						
1365-1380		cyanurate -O-	cyanurate ring 1380	triazine ring		triazine ring		triazine ring
1245		aromatic ether						
1190					phenyl ether			
915		epoxide ring					epoxide ring	

4.2.5 Cyanate ester/Acid Anhydride Reactions. Kinetic studies for this system were not found in the literature but the reaction is first described by Grigat [44]. Pandratov *et al.* [45] investigated the conditions under which the competing cyclotrimerization reaction could be effectively suppressed in order to produce linear polyimidocarbamates from pyromellitic dianhydride (PMDA) and bisphenol A dicyanate (Fig. 15). Reasonably high levels of triethylamine (~ 0.4 mole/mole PMDA) and reaction temperatures below 180°C produced polymers which lacked the 1575 and 1380 cm^{-1} IR spectral lines characteristic of the symmetrical *s*-triazine structure. Amine levels, more characteristic of what were used in these studies, produced polymers containing both triazine and imidocarbamate structures.

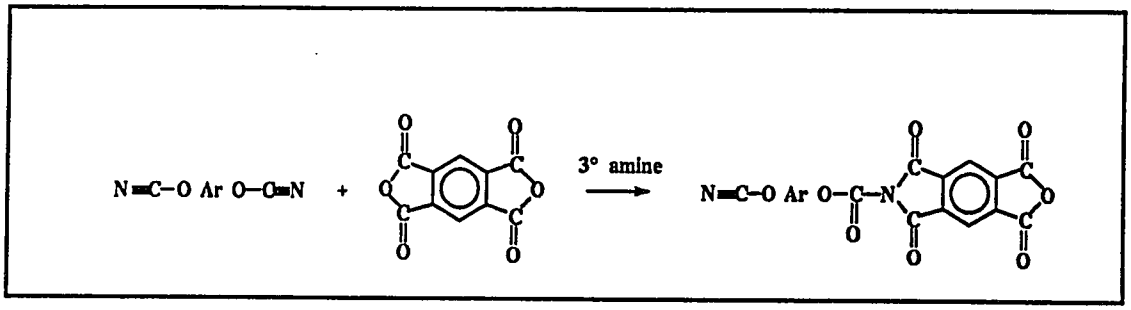

Figure 15: Imidocarbamate formation from the amine catalyzed reaction of aryl cyanate esters with carboxylic acid anhydrides [44].

The IR spectral features of the imidocarbamate structure were identified by the intense lines characteristic of an imide ring carbonyl at 1785 and 1735 cm^{-1}. The third intense line at 1825 cm^{-1} was attributed to the presence of three carbonyl groups instead of two around the nitrogen atom. The absorption line around 1320 cm^{-1} was assigned to the C-N vibrational band, which is typically observed at about 1370 cm^{-1} for true polyimide rings [45,78]. Polyimide structures also show a characteristic absorbance near 720 cm^{-1}, but there is no mention of this peak by the authors.

The 1780 and 720 cm^{-1} bands are commonly used to follow imidization reactions, but may be subject to interference from anhydride structures and thus, unreliable [78]. The C-N vibrational band located in this case, near 1320 cm^{-1}, is preferred. For normal imide structures this band occurs around 1370 cm^{-1} where it would overlap with the 1380 cm^{-1} cyanurate stretching band.

4.3 Experimental Description:

4.3.1 Analytical Methods.

Fourier Transform Infrared (FT-IR) Spectroscopy. Quantitative analysis with FT-IR transmission spectroscopy is governed by the Bouguer-Beer-Lambert law; more commonly referred to as simply *Beer's law*. For our purposes the most useful form is:

$$A(\nu) = \log\frac{1}{T(\nu)} = \log\frac{I_o(\nu)}{I(\nu)} = a(\nu)bc \qquad (5)$$

where: n = wavenumber,
A(n) = absorbance @ a specific wavenumber n,
T(n) = transmittance,
$I_o(n)$ = incident radiation intensity,
I(n) = transmitted radiation intensity,
a(n) = molar absorptivity (or extinction coefficient),
b = path length,
and c = concentration of the specific functional group(s).

Absorbance bands tend to be quite broad in many cases and so overlapping peaks are common. When more than one chemical species absorbs at or very near a specific wavenumber the total absorbance for the N species is given by:

$$A(\nu) = \sum_{1}^{N} a_i(\nu)bc_i \qquad (6)$$

Deviations from *Beer's law* are experienced for reasons that usually involve insufficient resolution, light scattering and various chemical effects such as hydrogen bonding or intermolecular association in general. For a given FT-IR instrument these deviations can often be minimized with adequate grinding of solids to less than about 2 μm in diameter and with proper sample dilution or thickness so that absorbance peaks are less than about 0.7 [79]. Sample dilution is controlled by dissolving the solid resin in a solvent, dispersing the ground resin solids in a KBr salt matrix, or using thin film casting techniques from a volatile solvent.

The molar absorptivity a(n) is specific to the molecular group and the type of interaction (e.g. bending, stretching, etc.). As shown in Eq. 5 and 6 it is only a function of the wavenumber for a specific chemical species, but in practice is also found to depend on the chemical environment due to intermolecular interactions. Consequently, not much effort has been expended in measuring and tabulating molar absorptivity values. An alternative and preferred approach for quantitative studies is to develop a calibration curve for the specific set of conditions. Calibration curves are generated through FT-IR measurements of the absorbing species under conditions of known concentration. When Beer's *law* is applicable, we only need a single non zero concentration to construct this curve and so the initial level could be used as the calibration point for the reactants. Multiple measurements throughout the concentration range of interest and as close to the same chemical environment as reasonable are generally used so that random errors are averaged out and systematic deviations from Beer's law are corrected for.

Direct measurement of the path length b is not required for our studies, nor does the sample's concentration need to be precisely known. Instead the normalized peak height is commonly used to extract the necessary information. The normalization factor is often an internal reference selected from one or more of the unchanging peaks within the spectrum. Dividing the peak height from a specific wavenumber by the height of a reference peak(s) corrects for minor differences in the samples dilution or thickness. Large differences in the concentration or sample thickness are best avoided to help ensure adherence to *Beer's law*.

Differential Scanning Calorimetry (DSC). Kinetic studies for thermosetting polymers are frequently done using DSC. Techniques and procedures for conducting these measurements are outlined in numerous texts; for example Prime (1981) [80]. The reaction rate dx/dt, of a single reaction is assumed to be directly proportional to the rate of heat generation, dH/dt, measured by the DSC. This assumption is only valid when the reaction can be isolated from competing side reactions and secondary thermal phenomena do not simultaneously occur. Reactant or product volatilization and melting are examples of secondary thermal phenomena.

The isothermal DSC technique is most often recommended, but in cases of very fast reactions this approach may be more inaccurate than dynamic measurements due to information that is lost during the initial heating phase before it reaches the isothermal

cure temperature. Attempts to minimize this heatup time include the use of rapid ramp rates (e.g. >150°C/min) [81], or preheating the DSC cell before inserting the sample [72]. When pressure DSC is required to reduce volatilization the preheating approach is no longer workable. Alternatively, the reaction can sometimes be run at lower temperatures to slow down the rate or reduce volatilization. The reaction rate constant (k), can be extrapolated to the desired cure temperature (T), if the k(T) relationship is known from the lower temperature curing. The latter approach does not work well however, if one of the reactants is insoluble at the reduced temperatures, as is the case for some acid anhydride hardeners. The low reaction temperatures may also significantly reduce total conversion and severely restrict mobility of the reacting species, thus lowering the onset of diffusion controlled reaction kinetics.

Dynamic DSC studies were selected to overcome some of the problems inherent in isothermal measurements. The dynamic tests are started at a low enough temperature to ensure that all of the reaction exotherm is captured in a single scan. Furthermore, the increasing reaction temperature helps to maintain a measurable rate in the face of the normal tendency for the reaction to fall off as the viscosity of the mixture increases with conversion and the concentration of reactants decreases. The major disadvantage of the dynamic DSC method is that it forces one to make an assumption about the temperature relationship of the rate constant. The Arrhenius form shown in Eq. 7 works well for many reactions. Deviations from this law often indicate diffusion controlled kinetics or an oversimplified model such as the use of a single rate constant when more than one rate controlling step exists.

$$k = A_0 e^{-E/RT} \tag{7}$$

where:
- k: rate constant
- T: temperature (°K),
- R: gas constant (kcal/kmol °K),
- E: activation energy (kcal/kmol), and
- A_0: frequency factor (or pre-exponential constant).

For the simple n'th order rate expression:

$$r = d[C]/dt = -k\,[C]^n \tag{8}$$

where: [C]: reactant concentration
$[C_o]$: initial concentration
n: reaction order.

we define the conversion: $$x = 1 - [C]/[C_o] \quad (9)$$

$$\text{or, } dx/dt = -1/[C_o] * d[C]/dt \quad (10)$$

substituting (10) into (8) gives:

$$dx/dt = k\,[C_o]^{n-1}(1 - x)^n \quad (11)$$

substituting (7) into (11) and applying some algebraic manipulations gives:

$$\ln\{(dx/dt)/(1 - x)^n\} = \ln\{A\,[C_o]^{n-1}\} - E/RT \quad (12)$$

The values for A and E are easily obtained by plotting the left hand side (LHS) of Eq. (12) vs. 1/T.
The reaction rate dx/dt and conversion x, are available from the DSC data using the relationships:

$$x = \Delta H(t)/\Delta H_{rxn} \text{ and,} \quad (13a)$$
$$dx/dt = dH/dt \,/\, \Delta H_{rxn} \quad (13b)$$

Where the heat of the reaction ΔH_{rxn} is the total area between the DSC peak trace and the baseline, $\Delta H(t)$ is the cumulative area to time t, and dH/dt is typically the ordinate in a DSC trace. For these studies the DSC ordinate is given in terms of a differential voltage signal V which must be corrected to dH/dt using the relationship:

$$dH/dt = \varepsilon V \quad (14)$$

Where ε is the calibration coefficient that must be measured independently using a standard of know thermal properties.

4.3.2 Test Materials. The diglycidyl ether of bisphenol A (DGEBA) epoxy resin has long been the industry standard for general purpose epoxy applications and one finds the literature full of curing and mechanical property studies for this material. Although the

DGEBA type resin is generally not used in the most chemically and thermally demanding environments required of advanced composite structures, its relatively low viscosity compared with the more stable novolac resin types makes it a good choice for the honeycomb adhesive application where ease of printing and lack of solvents were important considerations.

The specific DGEBA epoxy selected for this research project was DER 332®, the highest purity version available from Dow Chemical Company. Because of its high purity the resin tends to crystallize quickly at room temperature and form an almost waxy like solid. Mild heating however, easily returns the resin to the liquid form for ease of blending with the cyanate ester resin and anhydride. The chemical structures of the various monomers including the DGEBA resin are shown in Fig. 16. Pure DGEBA monomer with n=0 and a molecular weight of 340.42 has no secondary hydroxyl groups to promote side reactions with the cyanate ester or epoxy homopolymerization.

A high purity bisphenol E dicyanate monomer (AroCy® L10), was chosen for its ease of blending and similar chemical structure to the epoxy bisphenol A backbone [15,17,21,48]. The AroCy L10 is a room temperature liquid dicyanate monomer, and is miscible with DER-332 epoxy. The molecular weight of the monomer is 264.3.

Pyromellitic dianhydride (PMDA) was selected because of its high functionality towards epoxy resins and lack of secondary reactive groups which might enter into side reactions with both the cyanate ester and the epoxy resins. The difunctional behavior of PMDA towards cyanate esters allows for continuation of the polymer chain when imidocarbamate forming reactions occur (see Fig. 15). Furthermore, PMDA is known to produce cured epoxy polymers with high thermal stability, although its use has been limited by the high tendency to gel quickly before complete reaction [82]. The addition of the cyanate ester resin was expected to reduce the premature gelling and allow appreciably higher levels of anhydride hardener to be incorporated.

® DER332, Dow Chemical Co., Midland, Michigan.
® AroCy L10, Rhône-Poulenc Inc., Louisville, KY, formerly Hi-Tek Polymers, Inc.

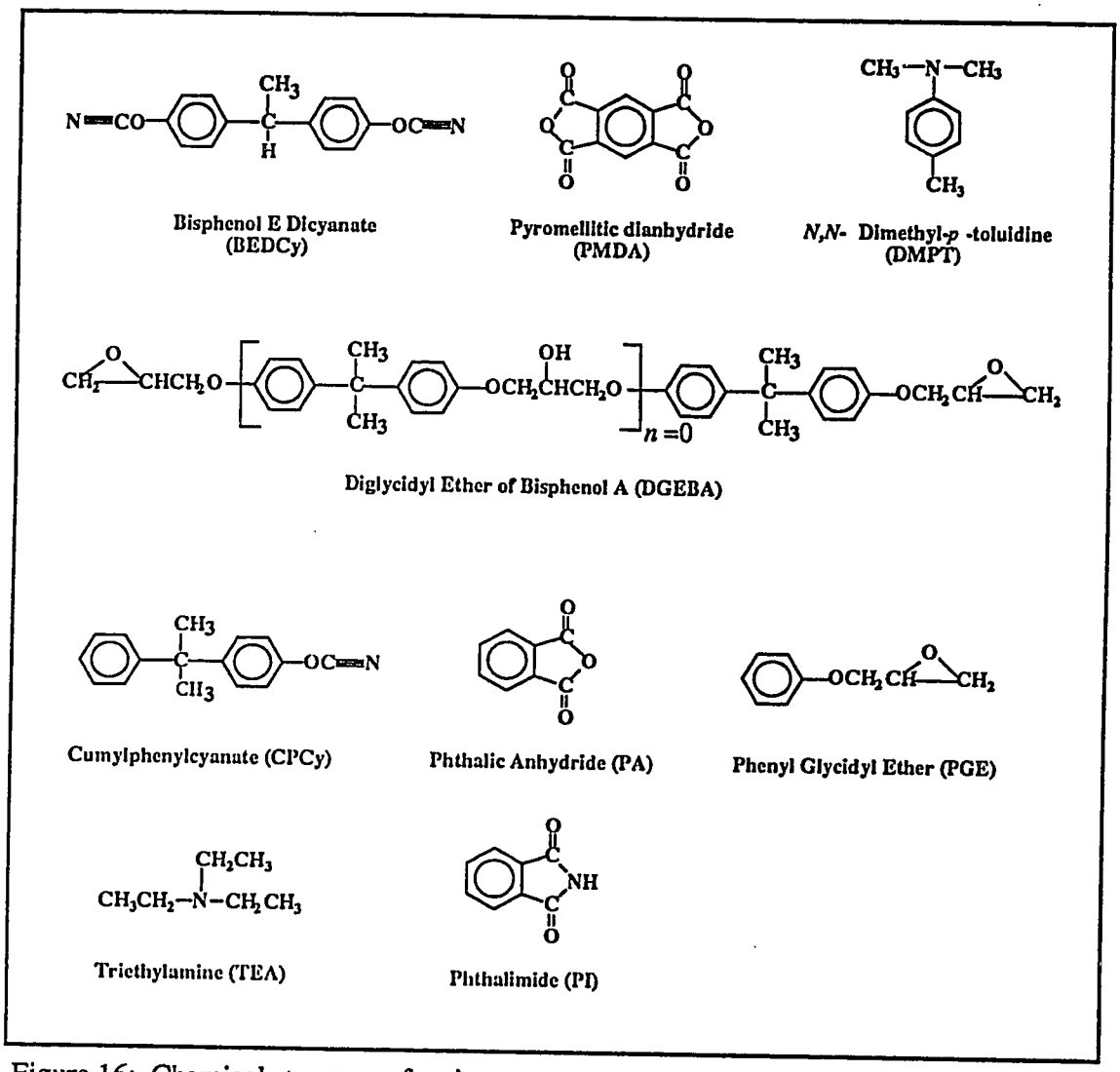

Figure 16: Chemical structure of resin monomers and model compounds used in experimental program.

Since the PMDA is both solid and insoluble in the resin mix at room temperature it poses some handling problems. Only at temperatures sufficiently high for the PMDA to react quickly was there noticeable dissolution observed in our laboratory. In fact, in one set of tests using an as-received 50 mesh PMDA, the solid particles took more than 30 min at 160°C to disappear.

This phenomena poses several major problems. It seems probable that the reaction rate will be controlled by the dissolution rate of the anhydride, which is particle size

dependent. With larger particles a viscous, diffusion-limiting reaction layer may form on the surface, further exacerbating the problem and producing a non homogeneous reaction system. The presence of large solid particles also complicates the FT-IR analysis due to scattering. To minimize these effects the PMDA has been ground to below about 10 μm size particles using a stainless steel ball mill. The grinding was done in a sealed container under wet conditions with chloroform as the solvent to prevent caking and to protect the finely divided anhydride from moisture. Traces of moisture and the ethanol preservative in the solvent were removed prior to use by passing the chloroform through a column of basic alumina [83]. The effectiveness of the grinding procedure was assessed by measuring the particle size distribution with a settling velocity approach.

Alternative approaches including the use of solvents to dissolve the PMDA instead of grinding were examined but later abandoned due to problems such as trace solvent residuals which complicated the interpretation of FT-IR spectra. Highly volatile solvents such as acetone evaporated too quickly leaving large crystals of precipitated anhydride before the reaction occurred. Dimethyl sulfoxide was also tested because of its tolerable IR spectra and high boiling point. A significant change in the reaction exotherm during DSC scanning was observed with DMSO, which raised questions about an altered reaction mechanism.

Tertiary amines are commonly added in concentrations of less than about 1 phr with anhydride hardeners. Triethylamine (TEA) was used in most of the initial model compound studies and dynamic DSC work. The isothermal reaction studies involved much longer curing schedules that may have allowed significant TEA volatilization before the reaction was complete so the catalyst was later switched to *N,N*-dimethyl-*p*-toluidine (DMPT) with its relatively low vapor pressure.

Cumylphenylcyanate (CPCy) and phenyl glycidyl ether (PGE) were selected as the appropriate model cyanate and epoxy compounds respectively. These monofunctional reactants were used in studies with phthalic anhydride and phthalimide to identify the main reaction pathways.

4.3.3 Sample Preparation and Test Procedures. Model compounds were synthesized in 20 mL Pyrex scintillation vials using a stirred oil bath. The vials contained a Teflon coated magnetic stirrer to ensure rapid mixing of the tertiary amine catalyst which was

usually added when the mixture reached its reaction temperature. In some tests, the tip of a thermocouple inserted directly into the reaction mixture monitored the reaction exotherms associated with catalyst addition.

The cyanate ester and epoxy resin mixtures used in kinetic studies were prepared at room temperature. The appropriate levels of catalyst and ground anhydride solution were then mixed with the resin using a combination of sonic agitation for a few minutes followed by about 30 min of vigorous blending on an automatic shaker. The solvent added with the anhydride solution was not removed until the mixing was complete.

Solvent evaporation caused the mixture to become increasingly viscous and difficult to remove the remaining solvent. Slowly rotating the sample jar while under vacuum minimized this problem and helped to prevent anhydride solids from settling in the early stages of evaporation when solution viscosities were low. Prepared resin samples were then placed in cold storage at 0°C until use.

Resin mixtures of nominal 0.5 gram size were cured in 8 mm ID glass test tubes for up to five days immersed in a stirred oil bath. The resin filled the tubes to a height of about 5 mm and were open to air at the top. At time zero the rack of sample filled test tubes were simultaneously transferred into the oil bath. At specified intervals a sample was pulled and quickly quenched in an ice bath. The small resin sample size was chosen to minimize the heating and cooling times for the reaction and to facilitate exothermic heat removal.

Calorimetry studies were performed on a DuPont Model 910® differential scanning calorimeter (DSC) with a Model R90® Thermal Analyzer using standard hermetically sealed aluminum sample pans for curing studies and the standard, non-hermetic DSC pans for glass transition measurements. Approximately 10 mg of uncured resin was used in these tests.

The isothermal curing studies were run at the specified temperature until the constant baseline was approached. After a rapid quench to ambient, the residual heat of reaction

---

® Model 910 DSC, DuPont Company, Analytical Instruments Division, Wilmington, DE.
® Model R90 Thermal Analyzer, DuPont Company, Scientific & Process Instruments Division, Wilmington, DE.

and the glass transition temperature were measured by subsequent dynamic scanning. The resin was assumed to be fully cured after this second high temperature scanning. A final isothermal scan was then used to establish the fully-cured baseline for use in exotherm integration. Dynamic tests were typically started at room temperature

4.3.4 Sample Analysis. FT-IR samples were prepared in one of two ways. Crystalline materials were ground with high purity KBr and pressed into a pellet. A blank KBr pellet prepared in the same way was used for the background spectrum. Bulk reaction mixtures as well as the room temperature liquid reactants were measured as neat films on 25mm KBr disks. The more viscous resin-like mixtures were first dissolved in chloroform, and subsequently cast as thin films on the KBr disks. Spin casting techniques were used to facilitate solvent removal and produce consistent film thickness. Samples that remained below their gel point were dissolved in chloroform for spin casting of films. Solution FT-IR was used with pure crystalline materials and other samples that tended to crystallize after solvent evaporation.

Samples which no longer could be dissolved in a suitable solvent were ground to a fine powder and pressed into KBr pellets. A Wig-L-Bug® dental amalgamator was used to grind the polymer and then blend it with the KBr powder. The stainless steel capsule containing several hundred milligrams of crushed polymer sample was cooled to liquid nitrogen temperatures before grinding. Grinding to a finely divided powder required 3 - 5 min with liquid nitrogen cooling after each minute. A few milligrams of this polymer powder was then blended with about 300 mg of dried FT-IR grade KBr to produce a 13 mm diameter pellet. The pellets were pressed in an evacuatable die. A small amount of baseline drift associated with light scattering was often observed but appeared to be tolerable, and otherwise good quality pellets were produced with this procedure. The sample closest to the gel point was analyzed both as a cast film and as a pressed pellet to ensure the spectra gave consistent results.

FT-IR spectra was collected at a resolution of 2 wavenumbers on a Bio-Rad® FTS-60A spectrometer with an MCT detector. Quantitative interpretation of the spectra was done

---

® Wig-L-Bug, Crescent Dental MFG. Co., Chicago, Ill.
® Bio-Rad FTS-60A, Bio-Rad Laboratories, Inc., Digilab Division, Cambridge, Massachusetts.

by the local baseline correction method with peak height normalization using selected reference peaks.

The glass transition temperature was measured for selected samples by differential scanning calorimetry (DSC) at a heating rate of 10°C/min. A nitrogen cover gas helped to minimize polymer decomposition by oxidation. The temperature at the onset of the transition region in the DSC scan was taken as the Tg value. The total and residual enthalpy of reaction referenced to some temperature (T_{ref}) was also measured with dynamic scanning for use in calculating the degree of conversion.

4.4 Results and Discussion

4.4.1 Model Compound Studies

The reaction studies with model compounds were used to help clarify three of the reactions (2, 5 & 6) defined at the beginning of chapter 4. These studies allowed the reaction products to be more easily isolated and purified for analysis.

High purity cumylphenylcyanate (CPCy) was provided by Rhône-Poulenc (REX-370) and used without further purification. The phenyl glycidyl ether (PGE) purchased from Aldrich Chemical Co., Inc., Milwaukee, Wis., required vacuum distillation in order to remove a broad OH stretching peak that appeared in the as received material. Both phthalic anhydride and pyromellitic dianhydride were purified by vacuum distillation shortly prior to use. The tertiary amine catalyst used in all of these tests was triethylamine. It was fractionally distilled using a 20 inch glass column. Phthalimide (Aldrich 98%) was recrystallized once from distilled water and then dried at 110°C for several hours.

Cyanate/epoxy coreaction. A 1:2 molar ratio of CPCy and PGE was reacted at 160°C to examine the reaction products with a tertiary amine present and to qualitatively compare these products with the predictions of Bauer and Bauer. Three drops of triethylamine were added for a concentration of roughly 2 mol%. After 15 min of stirring the mixture was cooled and sampled. The FT-IR spectrum of Fig. 17 shows the two carbonyl stretching peaks that are characteristic of the epoxy cyanate coreaction. The 1692 and 1754 wavenumber locations agree well with the isocyanurate and oxazolidinone

carbonyl groups respectively, that were described by Korshak et al. at 1700 cm^{-1} and 1750 cm^{-1}, but not as well with the 1670 cm^{-1} and 1740 cm^{-1} locations observed by Bauer and Bauer. Shimp also observed peaks at 1695 and 1760 wavenumbers but assigned them to an oxazoline structure. Korshak described a second isocyanurate peak at 1460 cm^{-1} that we were not able to confirm because of significant overlap with other reactant peaks. The 1760 cm^{-1} shoulder observed in this work may be one of the oxazolidinone isomers described by Bauer and Bauer [26,73].

Gotro *et al.* [28,29] and Shimp *et al.* [15] noted peaks between 1550 cm^{-1} and 1610 cm^{-1} that they assigned to oxazoline and isoxazoline structures. No significant spectral changes in this region were detected in the current study to support their findings. The absence of any peaks in this region may indicate the other two peaks Shimp *et al.* assigns to the oxazoline group are in fact, carbonyl stretchings associated with the oxazolidinone and isocyanurate structures rather than part of the oxazoline group observed near 1600 cm^{-1} where these structures are normally observed.

Homopolymerization of the CPCy to the *s*-triazine (cyanurate) structure produces the strong 1370 cm^{-1} and 1570 cm^{-1} absorbance bands shown in Fig. 18. These peaks should be easy to detected even in low concentrations. An equimolar cyanate/epoxy mixture produces these characteristic cyanurate peaks, which disappear with the addition of excess epoxy. Very little, if any, significant cyanurate product appears in the cured product for the 1:2 cyanate/epoxy mixture.

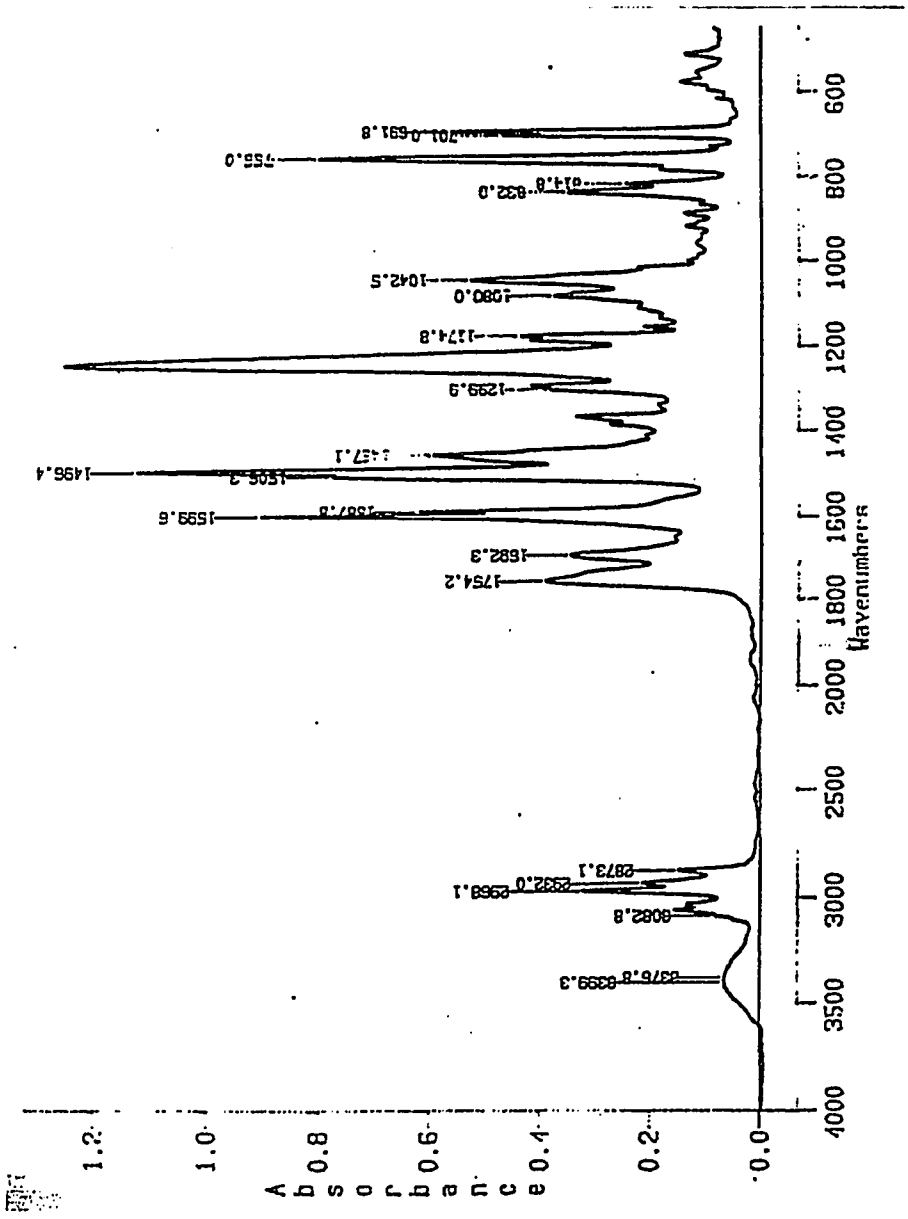

Figure 17: FT-IR spectra of the oxazolidinone and other products from the reaction between CPCy and PGE

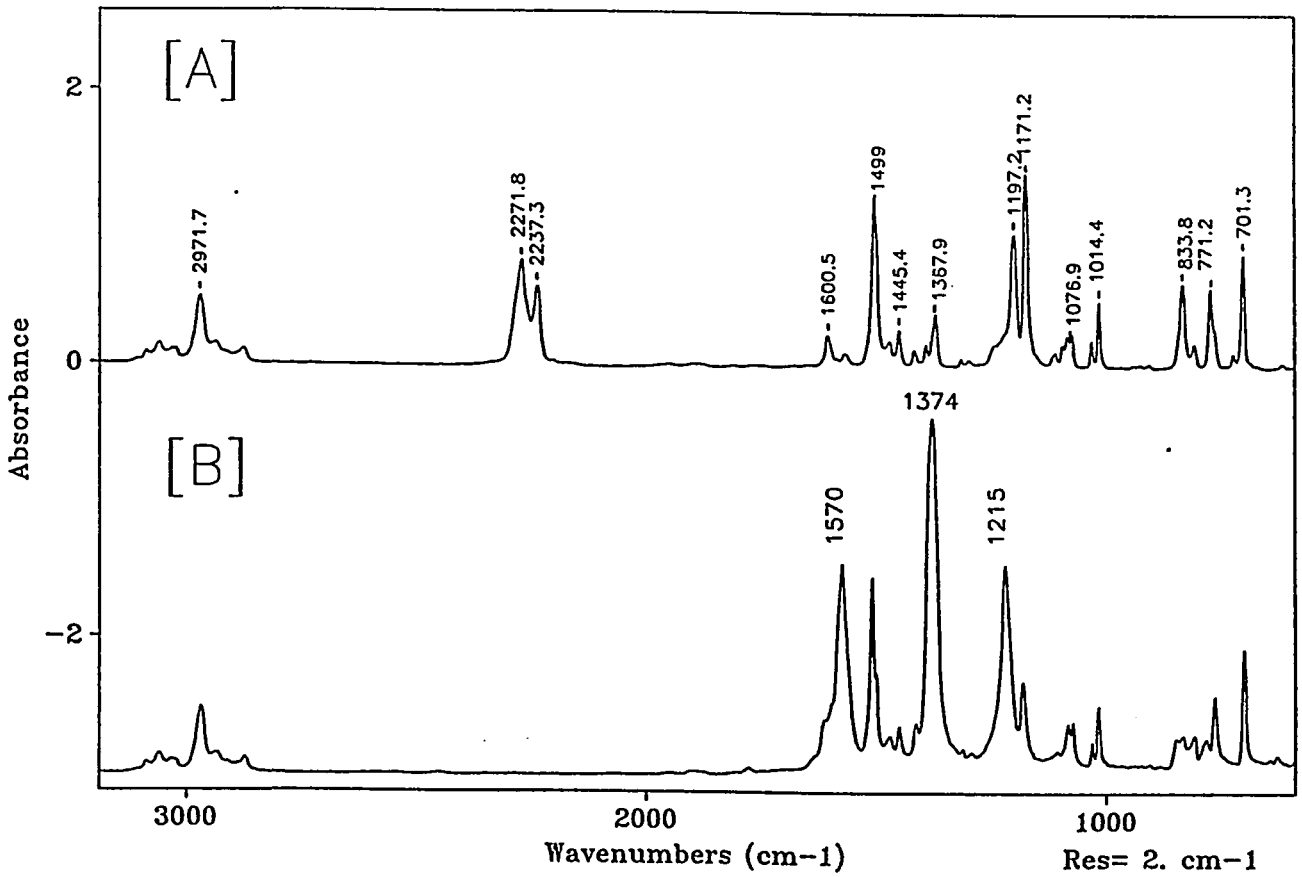

Figure 18: FT-IR spectra of the cyanurate product from the cyclotrimerization of CPCy. [A] monomer; [B] postcure product.

Cyanate/acid anhydride reaction. An equimolar mixture of 0.01 mol each CPCy and phthalic anhydride was heated to 180°C before adding 20 μL of triethylamine, (~ 0.7 mol%). Upon addition of the catalyst the reaction temperature quickly rose to around 195 °C. After 15 min the reaction was stopped. After recrystallizing the product 4 times from ethanol/5% water, a melting point of 156°C - 158°C as measured with a capillary melting point apparatus. The compound was also heated in air using a differential scanning calorimeter to estimate its boiling point. A decomposition exotherm was detected around 385°C before any boiling point was observed. The FT-IR spectra of the purified product, N-(4-cumylphenoxycarbonyl)phthalimide (MW = 385.42), is presented in Fig. 19. Note that the position of the third carbonyl peak depends upon whether the sample was in a solid KBr pellet or in solution with chloroform. The three carbonyl peaks and the strong absorption at 1320 are in good agreement with the literature. Comparison of the spectral features with a related compound (*N*-Carbethoxyphthalimide) from Aldrich is further confirmation of its structure. Proton NMR spectra were also collected and agree with the expected structure.

As an aside, the imidocarbamate is only moderately soluble in chloroform so further purification might be achieved with a change of solvents. Very little if any improvement in the boiling point was achieved between the 3'rd and 4'th recrystallization from ethanol/5% water.

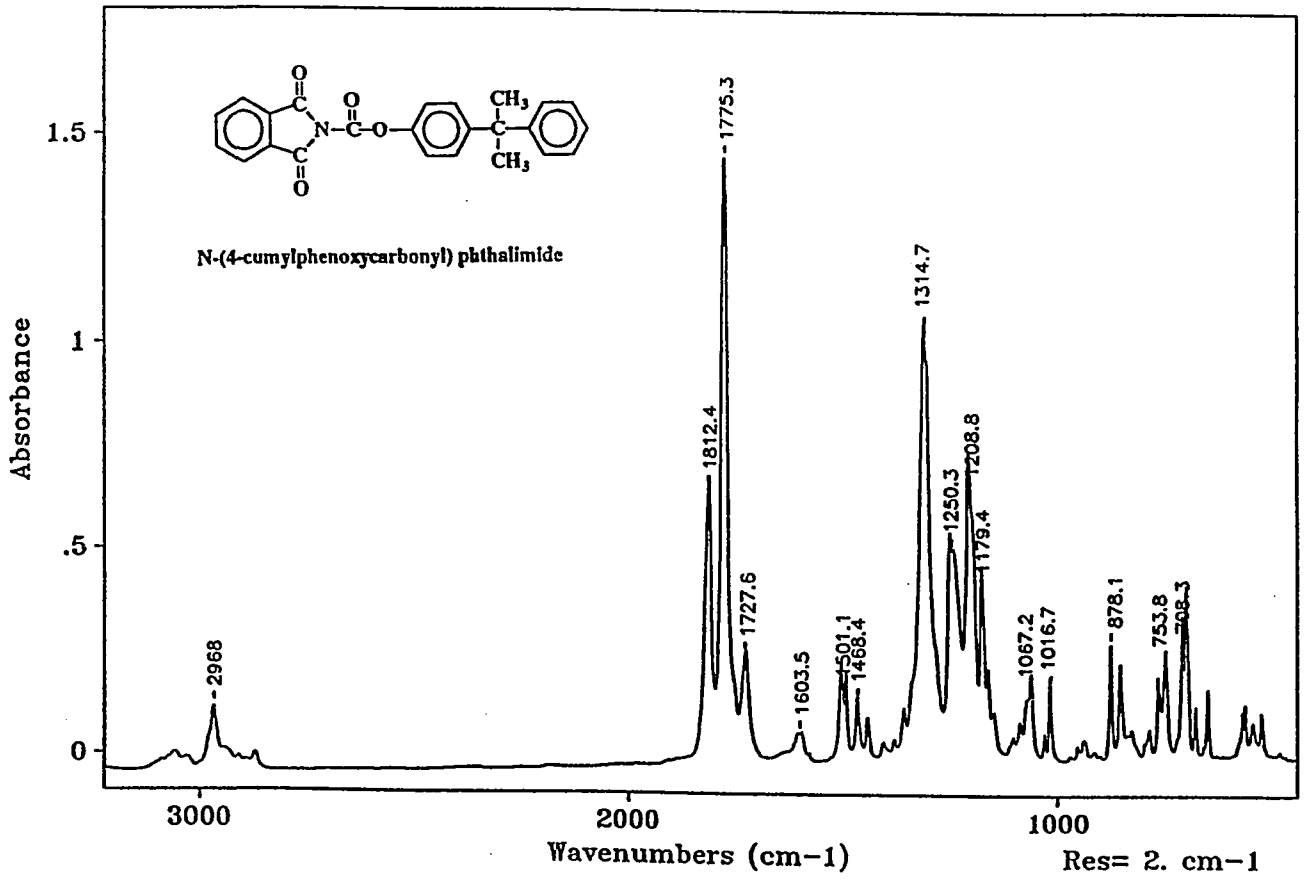

Figure 19: FT-IR spectra for the purified imidocarbamate product from the reaction of CPCy with phthalic anhydride.

Imidocarbamate/epoxy reaction. The imidocarbamate group was assumed to be a final reaction product but IR spectra showed evidence that further reactions occurred when the epoxy resin was added to the reaction mixture. An equimolar mixture of imidocarbamate from the preceding reaction and PGE was reacted at 180°C in the presence of a tertiary amine. The reaction temperature did not change noticeably with the addition of the catalyst. However, when either the epoxy or the tertiary amine were absent no reaction was detected. After 2 hours and again at 20 hours the mixture was sampled and an IR spectrum collected. As seen in Fig. 20 the characteristic imidocarbamate peaks disappear and are replaced by new peaks at 1770, 1710 and 1395 wavenumbers. The IR spectrum is characteristic of an imide formed by the hypothesized reaction Fig. 21.

Figure 20 also shows the spectrum for the model imide compound A. Compound A was synthesized from phthalimide and PGE in the presence of triethylamine catalyst. The product was initially recrystallized twice from methanol and then several more times from a isopropanol/water mixture until a sharp melting point was achieved (mp 113°C - 115°C). The proposed reaction is given in Fig. 22. Key spectral features from both the FT-IR and carbon13-NMR (Appendix) agree with similar compounds described by Bertran *et al.*[84].

The second carbonyl peak around 1770 appears to be composed of two overlapping peaks. Isolation of a second product was not achieved but the two peaks were better separated and the broad OH peak around 3500 was also reduced by repeated precipitation of a resin like material from solution as indicated in Fig. 23. Organic carbonates give rise to stretches in this same region which is consistent with the proposed structure.

In separate experiments where CPCy, PGE and phthalic anhydride were reacted simultaneously with a tertiary amine catalyst a very similar IR spectra was isolated after multiple separations steps. Also isolated as a precipitate in one case was a small amount of the compound presented in Fig. 24. For comparison the spectrum of a commercial bisphenol A polycarbonate (Lexan®) is overlaid to show the strong similarities. An insufficient quantity was recovered to undergo multiple purification steps so some of the differences noted could be simply impurities. Other differences are the result of

---

® Lexan, General Electric Company, GE Plastics Division, Pittsfield, MA.

expected differences in the structure of these two materials. For example, the mono-substituted benzene peak of the CPCy structure matches the absorbance near 700 that is absent in a bisphenol A structure. Not all features are so easily explained.

One explanation for these observations suggests that under certain conditions, for example with trace phenols present, the carbonate group is released during the imidocarbamate/epoxy reaction by combining with an available hydroxyl group to form the independent carbonate species outlined in Fig. 25. Under other conditions this group remains a branch of the newly formed imide as suggested in Fig 21. Alternatively, perhaps the carbonate precursor is released as an intermediate quaternary ammonium salt. This intermediate can subsequently react with trace alcohols/phenols, secondary OH groups of the newly formed imide, or directly with the epoxide ring to form a carbonate. In any case, there is compelling evidence that the imidocarbamate and epoxy react by a complicated mechanism to form a stable imide compound, the complete structure of which is not fully understood.

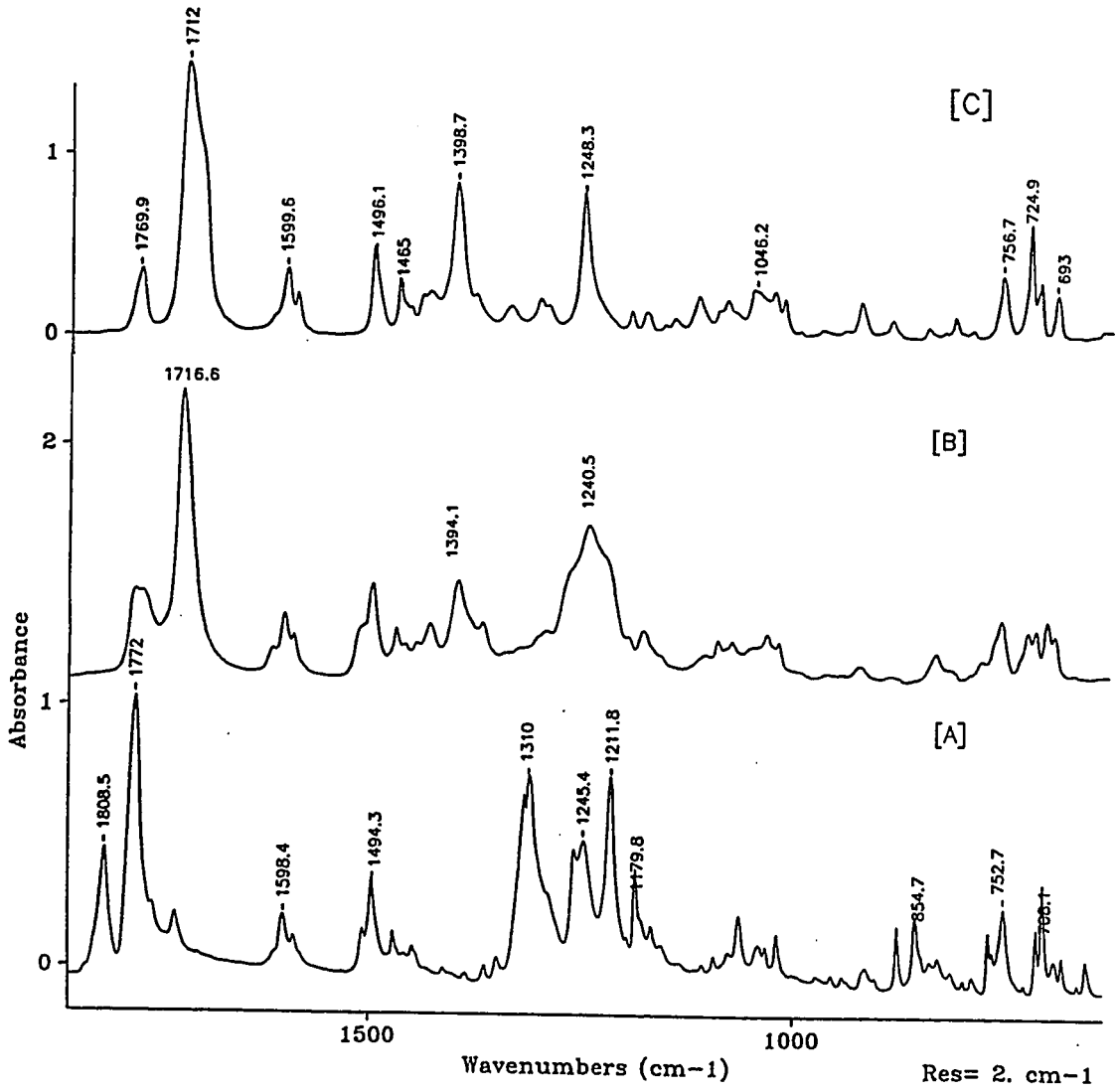

Figure 20: FT-IR spectrum changes that occur when PGE is reacted with an imidocarbamate in the presence of triethylamine. [A] Initial reactant mixture; [B] after 20 h at 180°C; [C] model compound A.

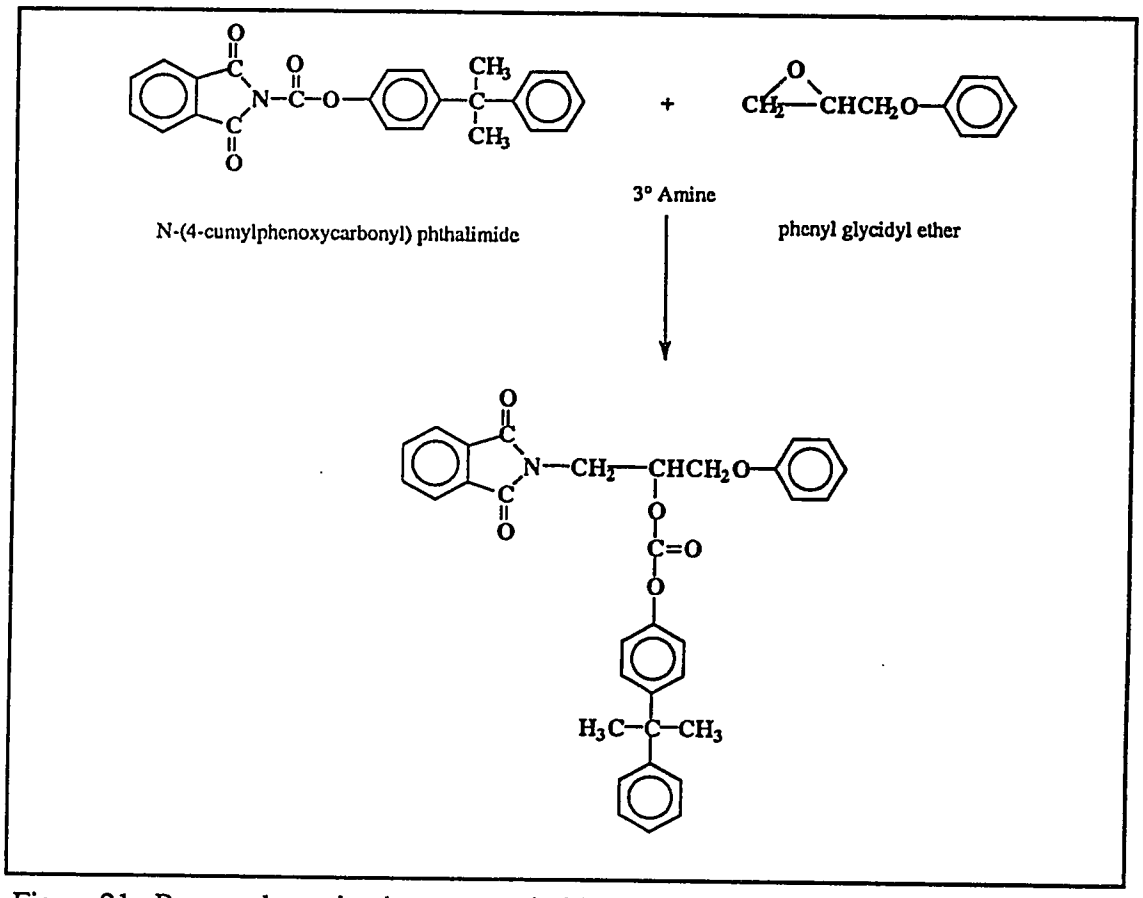

Figure 21: Proposed reaction between an imidocarbamate and an epoxy.

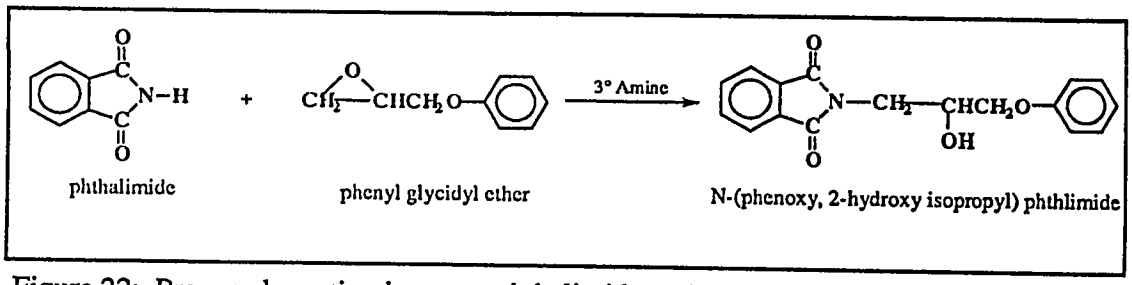

Figure 22: Proposed reaction between phthalimide and PGE.

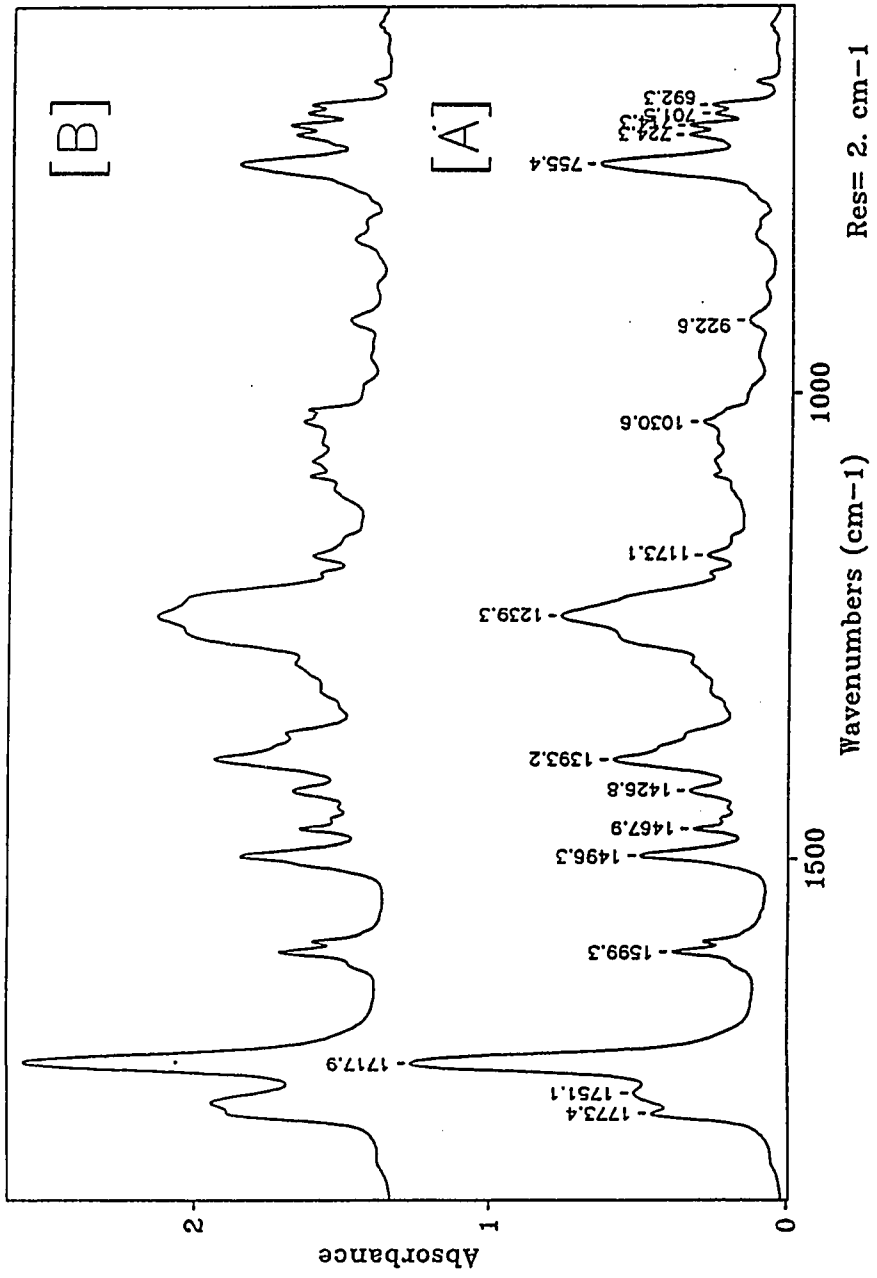

Figure 23: IR spectra after repeated precipitation of the resin like reaction mixture that forms when PGE is reacted with an imidocarbamate in the presence of triethylamine. [A] precipitated phase; [B] residual solvent phase.

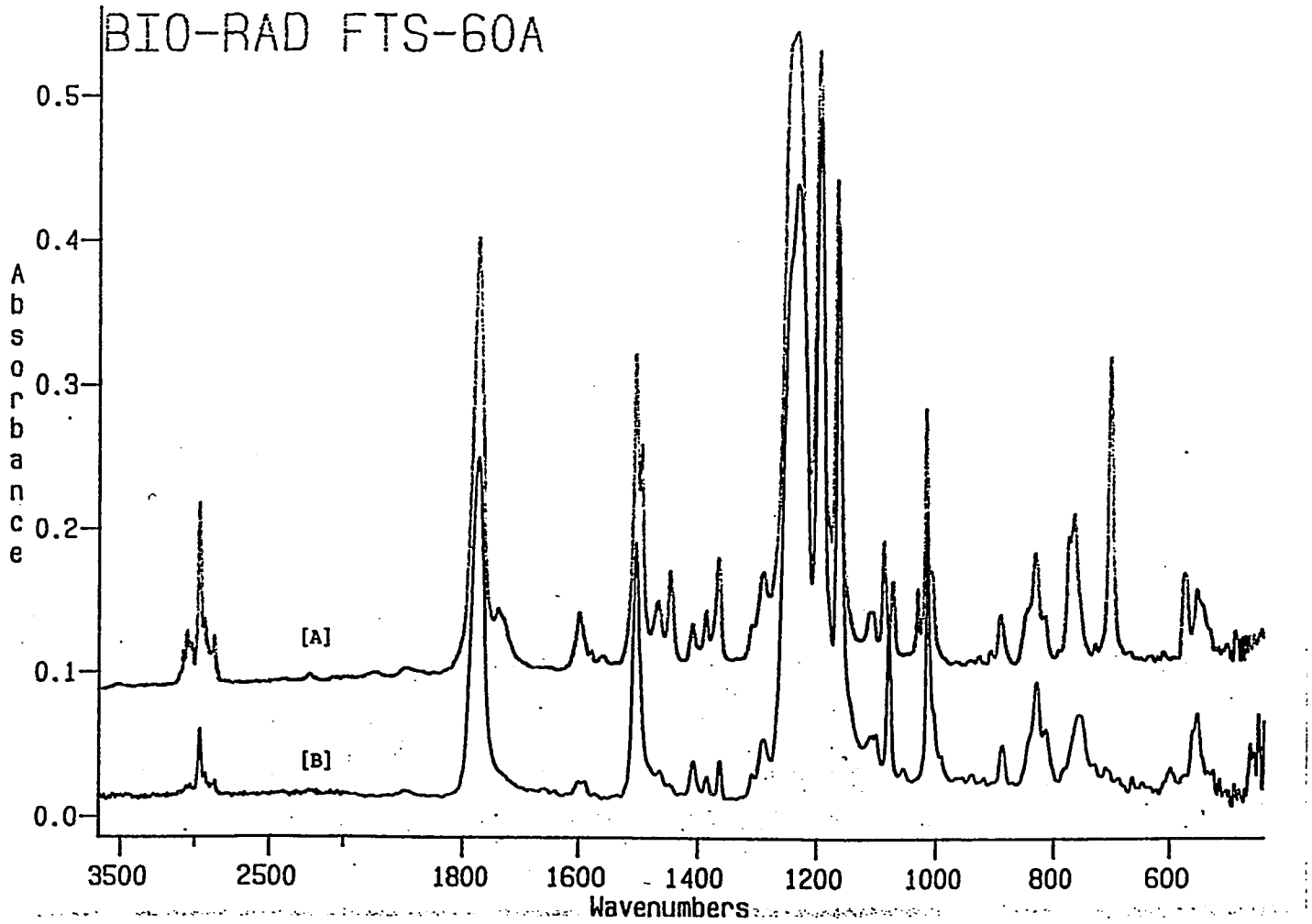

Figure 24: IR spectra of selected organic carbonate compounds. [A] precipitate of unknown structure from the coreaction of CPCy, PGE and phthalic anhydride; [B] Lexan film cast from $CHCl_3$]

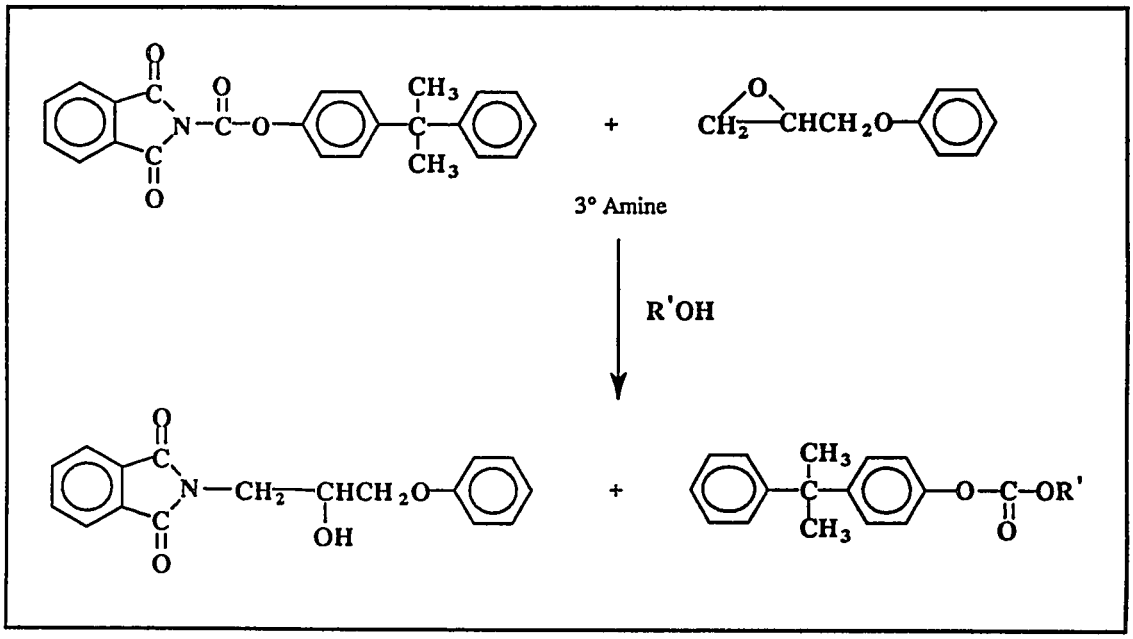

Figure 25: Alternative scheme for the reaction of imidocarbamates with an epoxy.

4.4.2 DSC Kinetic Studies of the Curing Reactions

Polymerization reactions are frequently studied using dynamic or isothermal differential scanning calorimetry [72,81,85-86]. Dynamic curing tests require some assumptions be made about the temperature relationship of the rate constant and so are generally less preferred. On the other hand, fewer tests are needed in order to obtain all the rate parameters and so more duplicate runs can easily be run. Furthermore, no information is lost during the initial heatup phase when very fast reactions are involved. The goal of this research phase was to validate the general form of the rate expression and to obtain an order of magnitude estimate of the kinetic parameters for preliminary modeling/analysis of the polymerization. Figure 26 provides a qualitative comparison of the four major reactions. We can readily see that the cyanate/anhydride and epoxy/anhydride reactions are roughly comparable in importance and both occur at relatively low temperatures. The trimerization reaction, while somewhat slower, can not be ignored either. The epoxy/cyanate coreaction is ultimately controlled by the trimerization rate and so it can't be any faster. The trimerization rate may even be slowed more by the loss of trimer catalyst when it reacts with the epoxy.

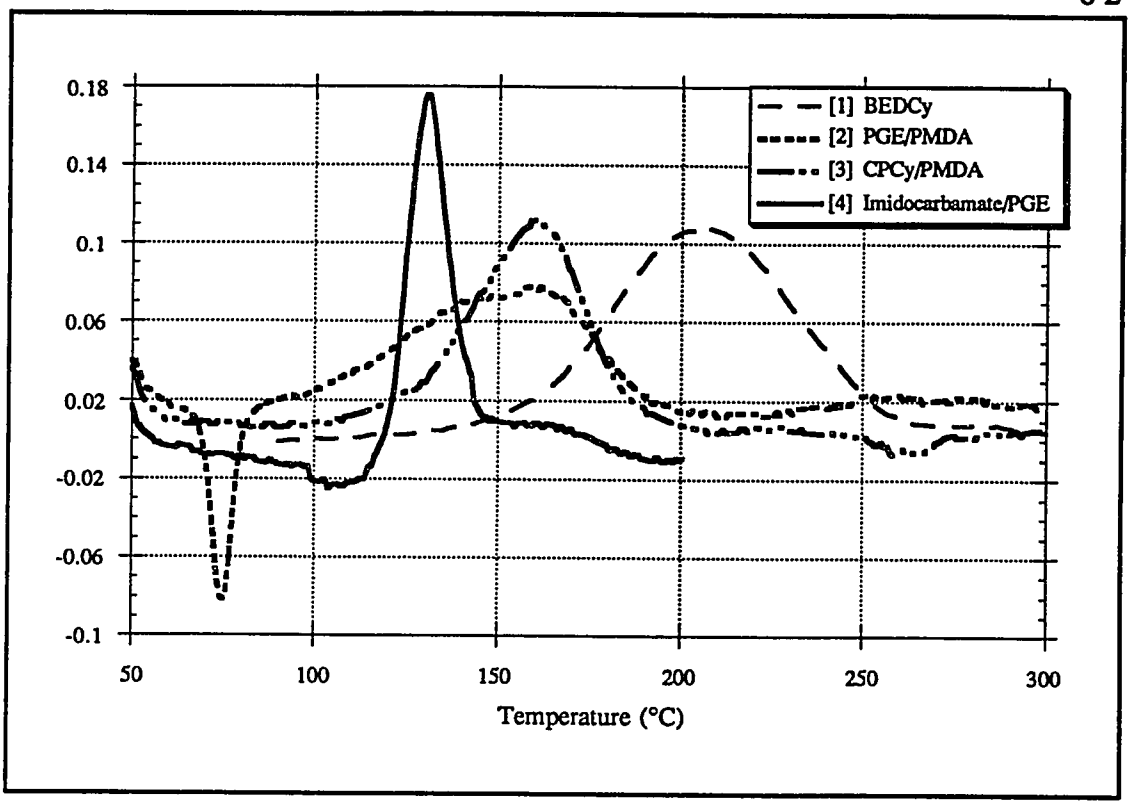

Figure 26: DSC scan at 10°C/min for the four major competing reactions. [1] cyanate cyclotrimerization; [2] epoxy/anhydride co-reaction; [3] cyanate/anhydride co-reaction [4] imidocarbamate/epoxy co-reaction.

Thermosetting polymers form heavily crosslinked networks which are often referred to as 3-dimensional polymers. The gel point in thermosets signifies the irreversible transition from a viscous liquid to a crosslinked polymer that will no longer flow or dissolve in any solvents. It is reached when the degree of crosslinking is sufficiently high that the polymer is effectively a continuous network. In reality, some amount of residual monomer and low molecular weight fragments will exist beyond the gel point, and so the degree of crosslinking is sometimes characterized by the fraction of soluble material. The polymers glass transition temperature (Tg) and its solvent swelling behavior are also frequently used as a measure of crosslinking or degree of cure. A secondary consequence of crosslinking and gelling is that the polymer chains are dramatically restricted in their mobility and so diffusional limitations begin to control the reaction rate in the late stages of curing. At this stage in the research the interest is in modeling the kinetics of the reaction in the absence of significant diffusional limitations and will

address diffusional effects at a later stage if necessary. In some cases it is possible to select monofunctional species for one of the reactants so that chain growth and crosslinking is precluded.

Cyanate homopolymerization. In recent studies the cyclotrimerization reaction was found to follow autocatalytic behavior both with and without the addition of a phenol catalyst of the form shown in Eq. 15.

$$dC/dt = -(k_1[C]^n + k_2[C]^n[T]) \quad (15)$$

One group of researchers found a first order dependence on cyanate concentration (i.e. n=1) while the other found second order [57,58]. Bauer and Bauer studied the effect of OH groups on the reaction kinetics. Their proposed mechanism in the presence of either trace or added OH groups included the formation of a thermally reversible carbamate intermediate as a precursor to the cyclotrimerization. A two step reaction model with the carbamate formation provided a good fit to the data but they also proposed the following simple kinetic model which fits the data reasonably well:

$$dC/dt = -k[C][H] \quad (16)$$

Dynamic DSC experiments were attempted with the monofunctional cyanate model compound CPCy to avoid gelling, but excessive volatilization was detected. After changing to the dicyanate monomer AroCy L10, the weight loss decreased to less than 1%.

The polymerization of cyanate resins in the presence of a tertiary amine were first examined. Comparison of dynamic DSC traces with and without 1 mol% triethylamine mixture showed a clear acceleration of the amine containing case. The triethylamine catalyst had been purified by fractional distillation shortly before its use but was not checked for purity level. A significantly modified exothermic peak shape was produced which was flatter, broader and shifted to a lower temperature by as much as 60°C compared with the uncatalyzed case. FT-IR analysis revealed the characteristic cyanurate peaks and disappearance of the cyanate bands. There were no peaks detected in the 1700 cm-1 region to indicate residual carbamate or imidocarbonate intermediates in the end product.

Dynamic scans were collected at 5, 10 and 20°C/min scan rates with the 1 mol% triethylamine mixture. Gelling is commonly observed around 60% conversion with dicyanates [17]. Above this level the reaction rate becomes diffusion rather than reactant limited. Similar results were apparent from our DSC data. A simple 2'nd order reaction kinetic model could be fit reasonably well below about 60% conversion level.

$$\ln[dx/dt/(1-x)^n] = \ln A - E/RT \qquad (17)$$

where; dx/dt is proportional to the DSC output in volts, and
x = conversion factor

A small improvement in the model fit is achieved with an autocatalytic second term added as follows:

$$dx/dt = k_1(1-x)[(1-x) + \beta x] \qquad (18)$$

where; x = fractional conversion
$k_1 = A_1 \exp(-E_1/RT)$, and
ß = proportionality constant (k_2/k_1)

Figures 27 & 28 present the LHS of Eq. 18 plotted on the left Y-axis for two different scan rates with an overlay of the DSC exothermic peak plotted on the right Y-axis. Both curves are plotted against inverse temperature in °K. The solid vertical lines represent the boundaries of the region from 5 to 60% conversion in which the linear curve fitting was done in order to determine lnA and E/R. This region has been expanded in the lower half of each figure for easier comparison of the linear fit. The Eq. 17 simple n'th order model with n = 2 is represented by the ß = 0 case in Figures 27 and 28.

For reasons of simplicity and limited experimental data this rate expression is a rough approximation that assumes only one independent rate constant; a reasonable assumption if the activation energies (E_1 & E_2) for the two rate constants were nearly equal, and therefore: $k_2/k_1 \approx A_2/A_1$. It is know from others research that $E_1 \neq E_2$, and so the model undoubtedly has a fairly narrow temperature range over which it can predict reasonable results. Zeng *et al.* [58] reports an activation energy for the auto-catalyzed term (E_2) that

is about 1.5 times smaller than the initiating reaction term (~52 vs. 78 kJ/mol). In a separate study with a different dicyanate resin the reverse was observed by Simmon *et al.* [57]; and this time the auto-catalytic rate constant was 3 times larger (134 vs. 44 kJ/mol). These latter researchers also measured an activation energy of 95 kJ/mol by assuming a single overall reaction with one rate constant. This value compares well with the 98 kJ/mol value that was measured for the simplified one rate constant model of Eq. 18.

Diffusion-controlled reactions kinetics were observed above about 60% conversion for the cyanate trimerization reaction. The decrease in the reaction rate that accompanied this onset was more pronounced at low heating rates and resulted in the development of a secondary reaction shoulder on the high temperature side of the exothermic DSC peak. This shoulder was not readily obvious in the 20°C/min scan rate case, but the experimental data still indicates a slightly slowed reaction rate near the end of the cure when compared with the model.

The quality of the fit can alternatively be viewed by plotting the predicted dynamic DSC trace against the actual (Fig 29). The proposed rate expression was solved numerically using the LSODAR [87-90] routine and a variable rate constant. The solid line representing the model fits quite well for much of the conversion. The enhanced reaction in the early part of the scan is assumed to be an initiating step or side reaction involving trace impurities (e.g. hydroxyl groups) that later volatilize or are consumed.

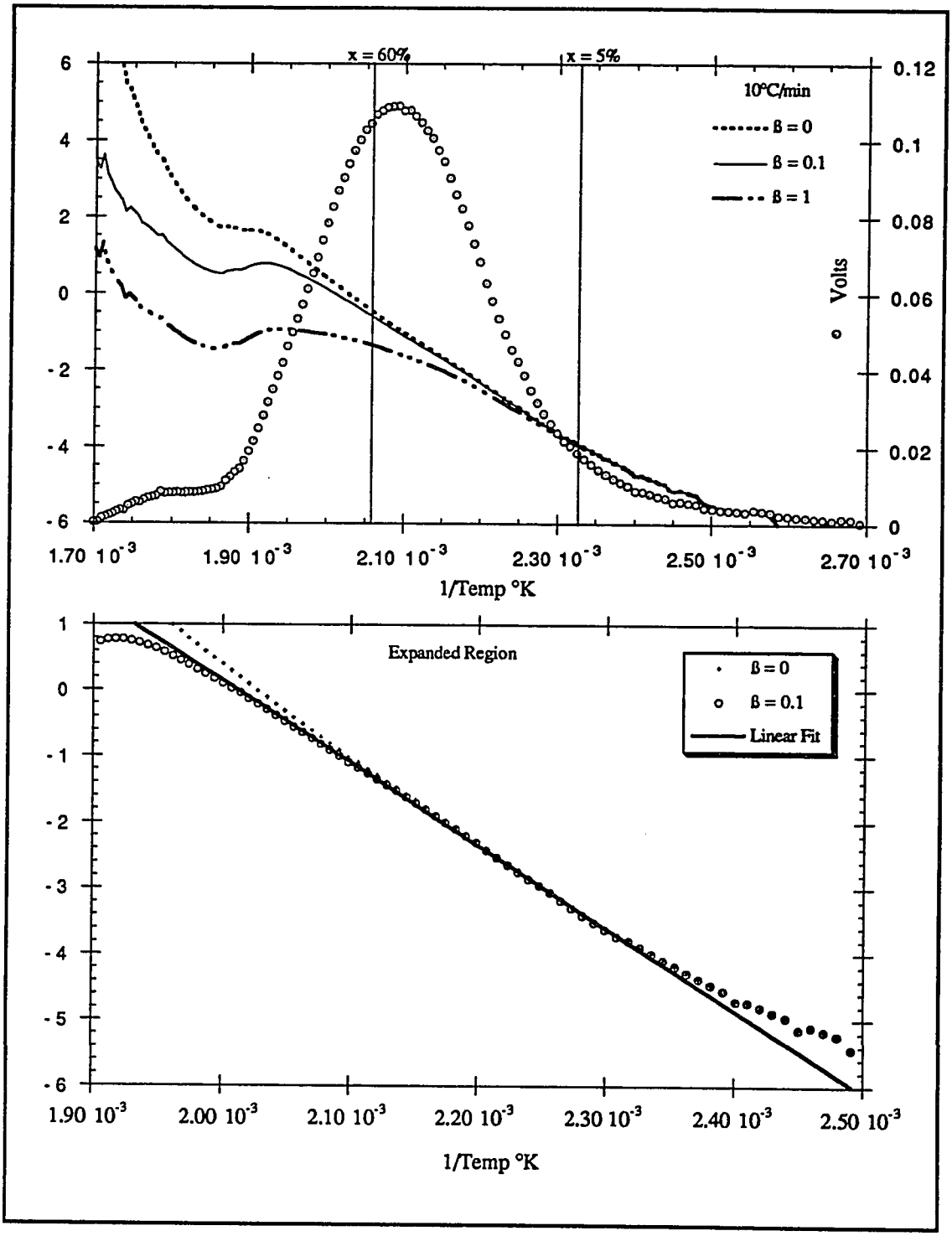

Figure 27: Arrhenius plot (log of the rate constant vs. reciprocal temperature) with an overlay of the dynamic DSC scan for the cyclotrimerization of AroCy L10 liquid dicyanate monomer at a scan rate of 10°C/min.

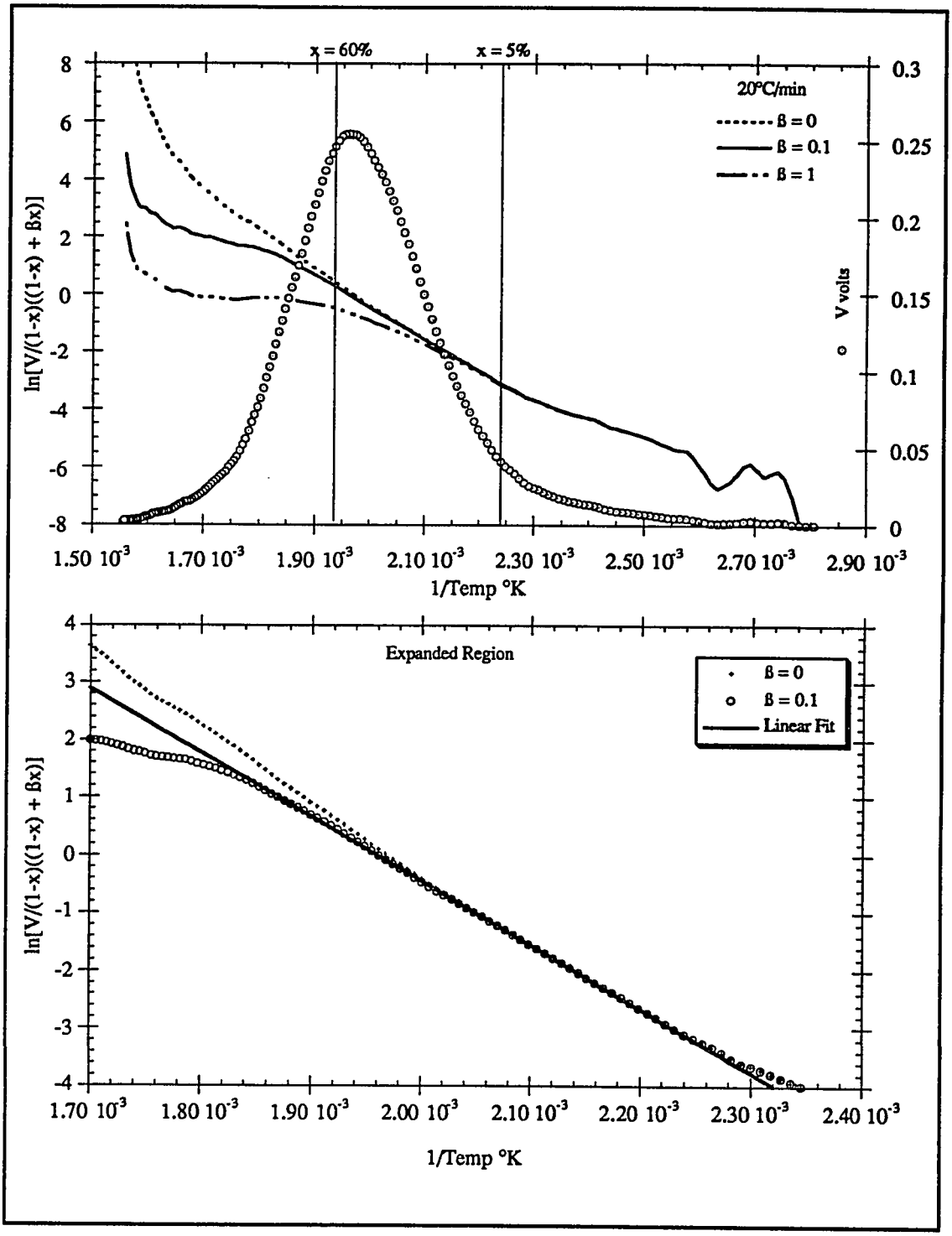

Figure 28: Arrhenius plot (log rate constant vs. reciprocal temperature) with an overlay of the dynamic DSC scan for the cyclotrimerization of AroCy L10 liquid dicyanate monomer at a scan rate of 20°C/min.

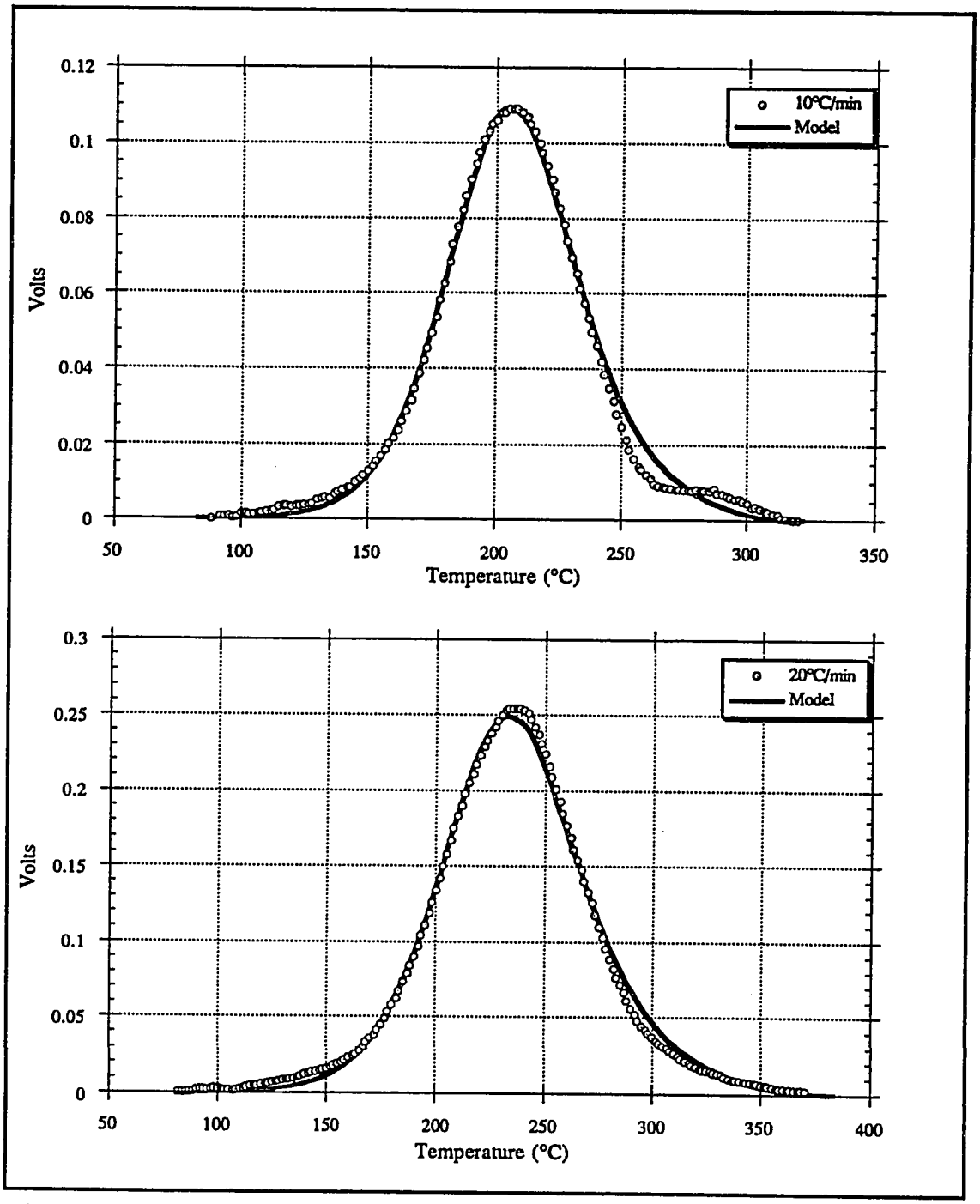

Figure 29: Comparison of predicted and actual dynamic DSC trace for AroCy L10 dicyanate resin cyclotrimerization with 1 mol % triethylamine. 10°C/min scan rate case: ß = 0.1, lnA = 21.41, E/R = 12500. 20°C/min scan rate case: ß = 0.1, lnA = 17.68, E/R = 11100.

As the reaction approaches the 100% conversion point it was also observed that the diffusion limited regime that causes the rate to drop off. Also note that the deviation is greatest for the slower scan rate. The lower scan rate shifts the peak exotherm temperature downward and so the bulk of the reaction also occurs at a lower temperature. Hence, the tendency for the reaction to become diffusion rate limited is increased. At higher scan rates the reaction temperature stays sufficiently above the glass transition temperature for more of the reaction. We can see this effect as the development of a shoulder on the high conversion (high temperature) side of the reaction in the 10°C/min case. At a scan rate of 5°C/min this effect was even more pronounced.

Cyanate/Anhydride coreaction. The lower reaction temperatures for this case permitted the use of the CPCy monofunctional cyanate with minimal volatilization. The CPCy can react at both ends of the difunctional PMDA without any chain growth so the viscosity of the reaction mixture should remain reasonably low. We prefer to use PMDA when possible instead of a monofunctional model, such as phthalic anhydride, because the PMDA structure and reactivity are unique with both anhydride rings attached to the same aromatic ring.

Tests were run at stoichiometric concentrations of anhydride to cyanate and with a 2 to 1 excess of anhydride. Isothermal DSC runs were made with these two compositions to examine differences. The isothermal runs were done with the cell and blank pan preheated to the reaction temperature before the sample pan was introduced. The scan was started as quickly as the cell could be closed (~ 10 seconds). This procedure produced a reaction trace that included most of the heatup portion of the curve as observed in Fig. 30. For simple n'th order kinetics the maximum rate is at the start of the reaction. Assuming this reaction is indeed simple n'th order, we conclude that the cell takes roughly 40 seconds to equilibrate. Much of the reaction occurs in the first 2 min at 160°C so undoubtedly some significant curing takes place prior to reaching the isothermal cure temperature and so the isothermal approach was judged to be unacceptable.

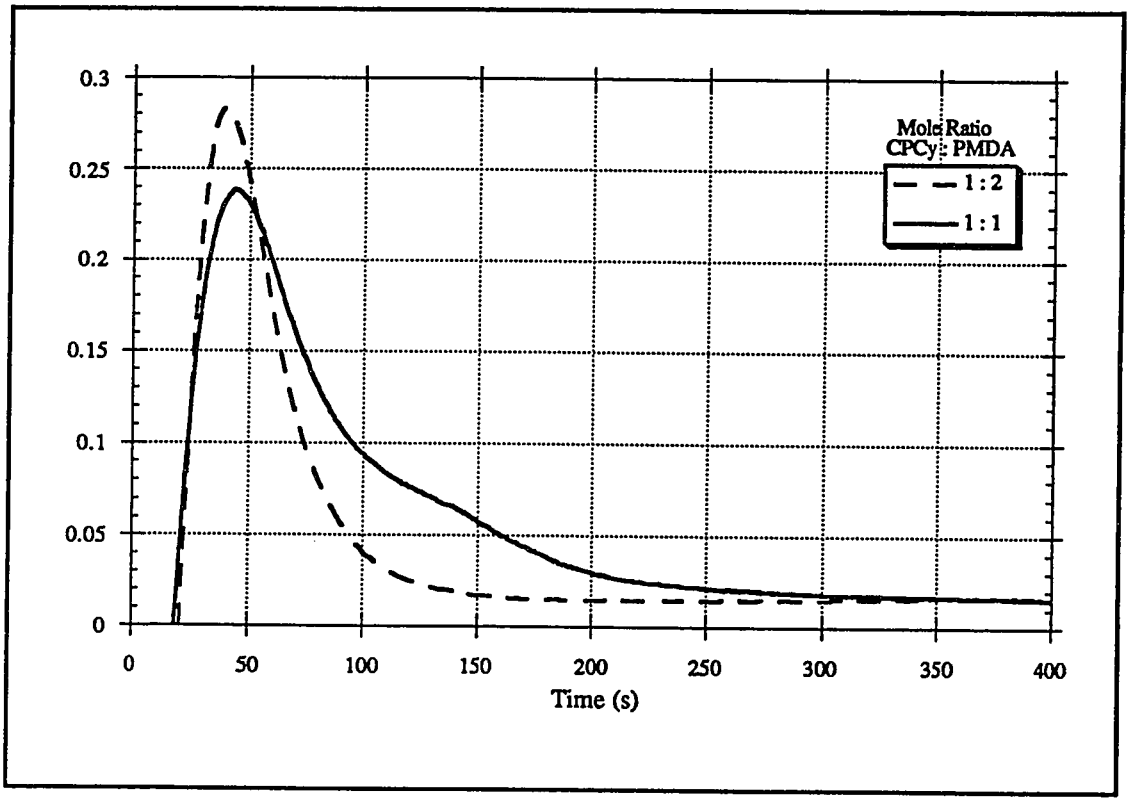

Figure 30: Isothermal DSC trace at 160 °C for the cyanate/anhydride coreaction.

Grigat [44] reports that the cyclotrimerization side reaction is not observed when the reaction temperature is maintained below about 200°C. FT-IR peaks associated with the triazine structure were however, observed in the separated products from the imidocarbamate synthesis at 180 °C. The isothermal curing at 160°C with a stoichiometric mixture of cyanate and epoxy also revealed the overlapping secondary reaction peak around 100 to 200 seconds that we assume is the competing cyclotrimerization reaction based on our earlier observation were it formed at measurable levels below 200 °C.

The reaction was heated at a rate of 10 to 20 °C/min under a magnifying glass. PMDA has a high melting point (286°C) and is not soluble in the cyanate mixture at room temperature. Blending the components was done using an agate mortar and pestle to ensure well dispersed and finely divided particles. The reaction mixture solidified by 180°C, but remained cloudy and largely unchanged in appearance until about 250°C, when the onset of melting was first observed. By about 280°C the mixture had completely melted. No crystallization was observed upon cooling. Dynamic DSC tests

reveal this endothermic peak near 250°C as indicated in Fig. 31. This peak is found well after the bulk of the reaction, suggesting that it could be either melting of the imidocarbamate product or the residual anhydride reactant. The melting endotherm disappears after the first scan.

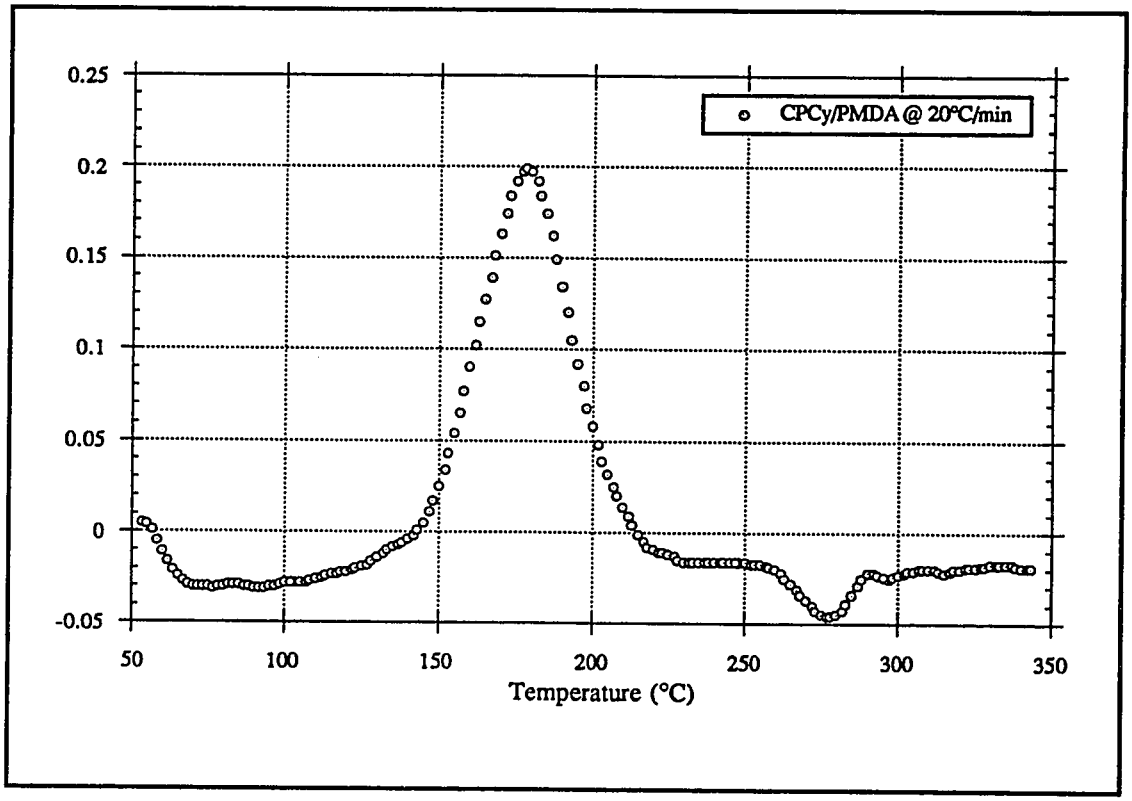

Figure 31: DSC scan at 20°C/min for a stoichiometric cyanate/anhydride (CPCy/PMDA) mixture with 1 mol % triethylamine catalyst.

Excess anhydride was used in one case to reduce the tendency for cyanate to homopolymerize. A simple second order rate expression fit the experimental data very well over much of the curing range for the 2:1 anhydride to cyanate molar ratio case, but not for the stoichiometric ratio of 1:1 (i.e. 1CPCy : 0.5PMDA). When the DSC scan rate was increased from 10 to 20°C/min the second order fit improved. The increased scan speed would produce a higher average reaction temperature that might reduce diffusional limitations without significantly increasing the cyclotrimerization side reaction. A better fit over the entire cure range at either scan rate was achieved however, by changing to a simplified autocatalytic reaction model of the form:

$$dx/dt = k_1(1-x)[1 + ß(1-x)x] \quad (19)$$

where; x = fractional conversion, and
$k_1 = Aexp(-E/RT)$
ß = proportionality constant (k_2/k_1)

This kinetic expression also implies that the rate constants for both terms in the model can be related by a single constant. In other words, it is assumed their apparent activation energies are equal (- 90 kJ/mol), and so the ratio is independent of temperature. In reality, the proportionality constant (β) varied significantly with the DSC ramp rate (i.e. 10 vs. 20°C/min), which suggests that it is only useful over a fairly narrow temperature range. Figure 32 presents a comparison of the dynamic DSC trace with the predicted trace using the Eq. 19 model and the fitting parameters shown in the figure caption. The

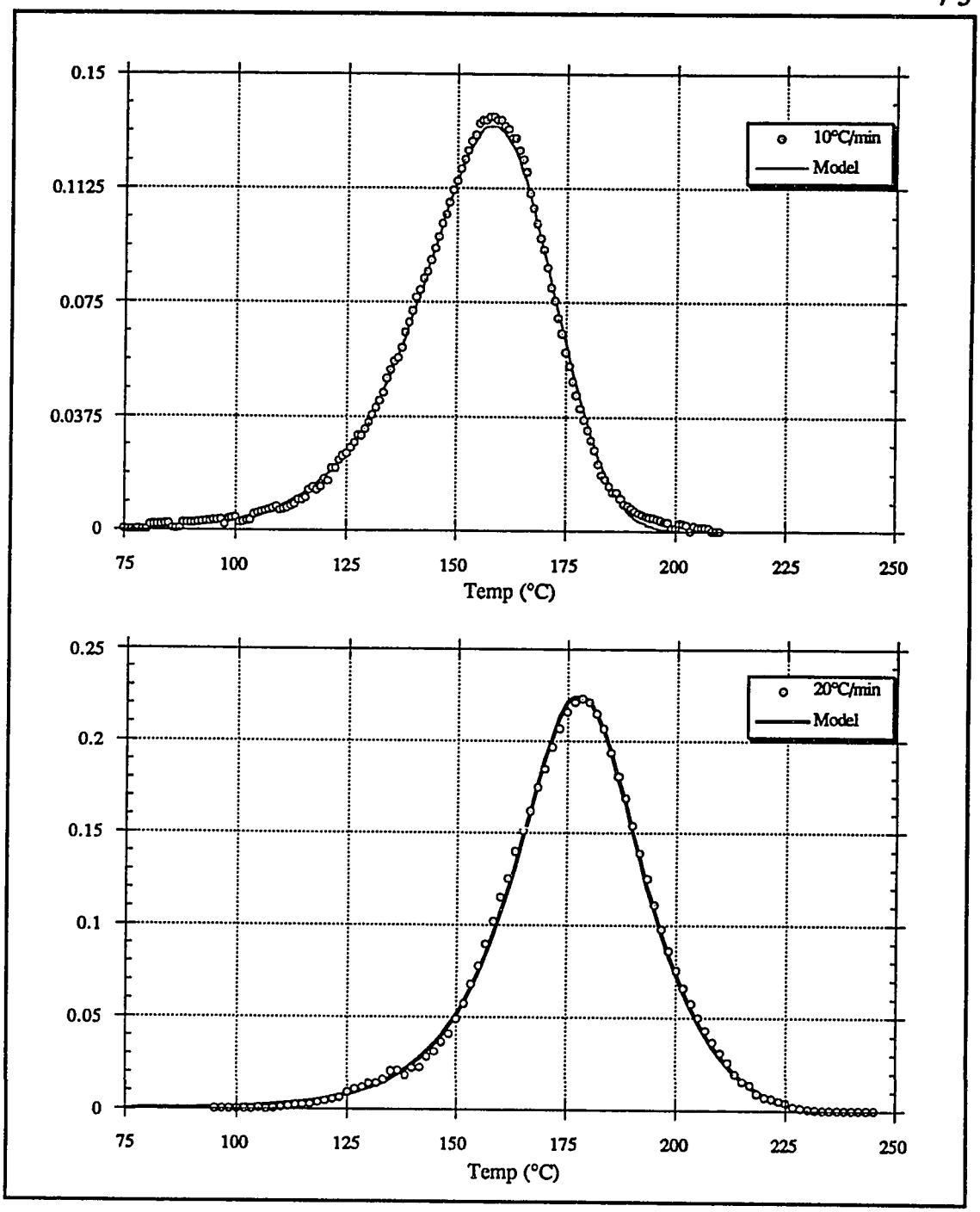

Figure 32: Comparison of predicted and actual dynamic DSC trace for a stoichiometric cyanate/anhydride (CPCy/PMDA) mixture with 1 mol % triethylamine catalyst. Case1: 10°C/min, ß = 1, lnA = 22.39, E/R = 11700. Case2: 20°C/min, ß = 5, lnA = 19.99, E/R = 11200.

A much better model could presumably be written with two independent rate constants. The additional testing required to develop such a model was judged to be unnecessary at this point. Since the model parameters were determined in the temperature range of interest (125°C to 200°C), the estimate for the two rate constants at a fixed temperature should be adequate for this study. Further studies of this reaction are warranted, but for the present analysis it is sufficient to simply bracket the range of the kinetic parameters.

Epoxy/anhydride esterification reaction. The literature is full of studies that describe this reaction. In the presence of a tertiary amine catalyst the secondary homopolymerization reaction is nearly nonexistent and so we have only to concern ourselves with the single esterification reaction. Even with monofunctional monomers this reaction produces large linear polyesters. A high degree of crosslinking will occur when at least one of the monomers is difunctional. PMDA was selected so the conditions would be similar to the preceding reaction between PMDA and cyanates and for the chemistry reasons given there.

Pyromellitic dianhydride (PMDA) was reacted with mono-epoxide PGE in a stoichiometric molar ratio of 2:1 (i.e. 2 mole PGE : 1 mole PMDA) and with a two times excess of anhydride groups (i.e. 1 mole PGE : 1 mole PMDA) . Typical dynamic scans are presented in Fig. 33. The baseline scan shown in one of the DSC traces is also typical and was collected during the second heating of the same sample. It is evident from this lower scan that curing was incomplete at the time the reaction was stopped near 350°C. The PMDA dissolution in the epoxy monomer is clearly observed prior to the reaction. Significant branching is also evident from the two exothermic peaks; particularly in the case with the stoichiometric 2:1 mixture. These two peaks are indicative of a diffusion controlled reaction; particularly with the broad, non uniform shape of the second peak. Such branching is expected with a difunctional anhydride. The smaller secondary and more uniform primary peak that is observed when excess anhydride groups are used is consistent with this explanation.

The reaction was also observed under a magnifying glass at a heating rate of approximately 20°C. Melting was detected near 70°C and gelling about 170°C; also consistent with the DSC data.

For the case of a 1:1 PGE/PMDA ratio (i.e. 2X excess anhydride) we find a good fit for a second order model up to around 65 -70% conversion as seen in the bottom curve of Fig. 34. The actual kinetic parameters were however, based on the data from 1 to 50% conversion and included the combined area of both reaction peaks in the calculation of conversion. Dynamic scans with a stoichiometric 2:1 PGE/PMDA ratio were not as well behaved. Both first and second order curves could be fit about equally well depending upon the range of data considered. For example, the top curve of Fig. 34 shows the quality of a linear fit to both the second and third order cases. The region from 1-50% conversion fits best with a third order curve while selecting the region from 5-50% is a better fit with a 2nd order.

We also note that the linear region does not extend much beyond 50% in the 2:1 PGE/PMDA molar mixtures. This suggests an earlier onset of gelling. In other words, the degree of branching and crosslinking is higher than when an excess of anhydride exists. This is to be expected since only one end of the anhydride ring will be reacted in some cases when there is an excess. The DSC runs that were made with excess anhydride are assumed to provide more reliable data. A summary of the kinetic parameters from selected DSC runs is provided in Table 4.

Table 4. Measured kinetic parameters for the amine catalyzed reaction between PGE epoxy and PMDA acid anhydride using dynamic DSC data and a simple kinetic model of the form: $dx/dt = k(1 - x)(C_{A0}/C_{E0} - x)$; with x = fractional conversion, $k = Aexp(-E/RT)$, C_{A0} & C_{E0} = initial concentration of the anhydride and epoxy groups respectively.

Sample ID	ramp rate (°C/min)	C_{A0}/C_{E0}	ln A (s^{-1})	E/R (°K)
DSC3B1a	10	2	19.6	10300
DSC3B1c	10	2	20.6	10500
DSC3B1i	20	1	16.4	9140
DSC3B1j	10	1	18.3	9830

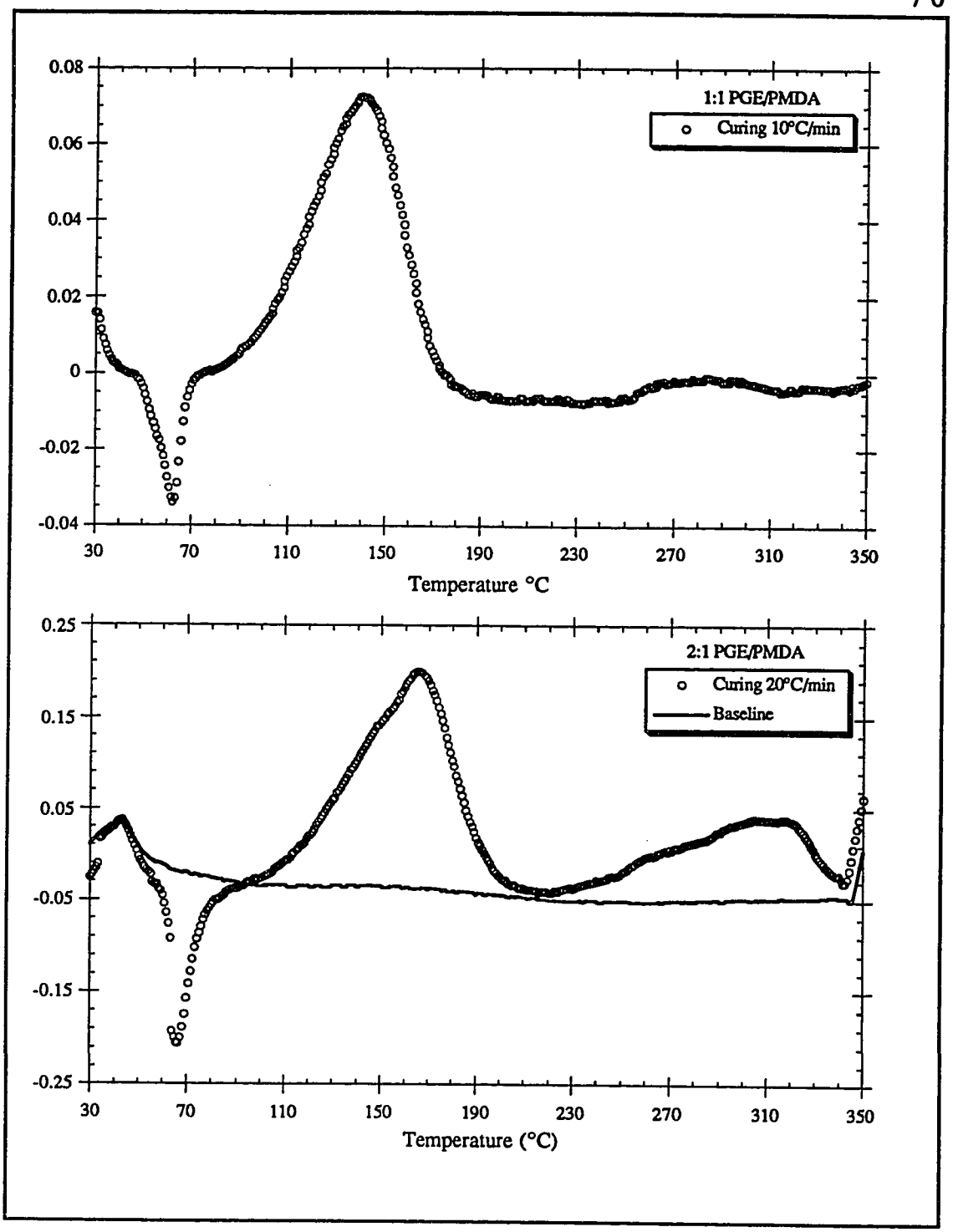

Figure 33: DSC scans at 10°C/min and 20°C/min for two epoxy/dianhydride (PGE/PMDA) reaction mixtures with triethylamine (TEA) catalyst.

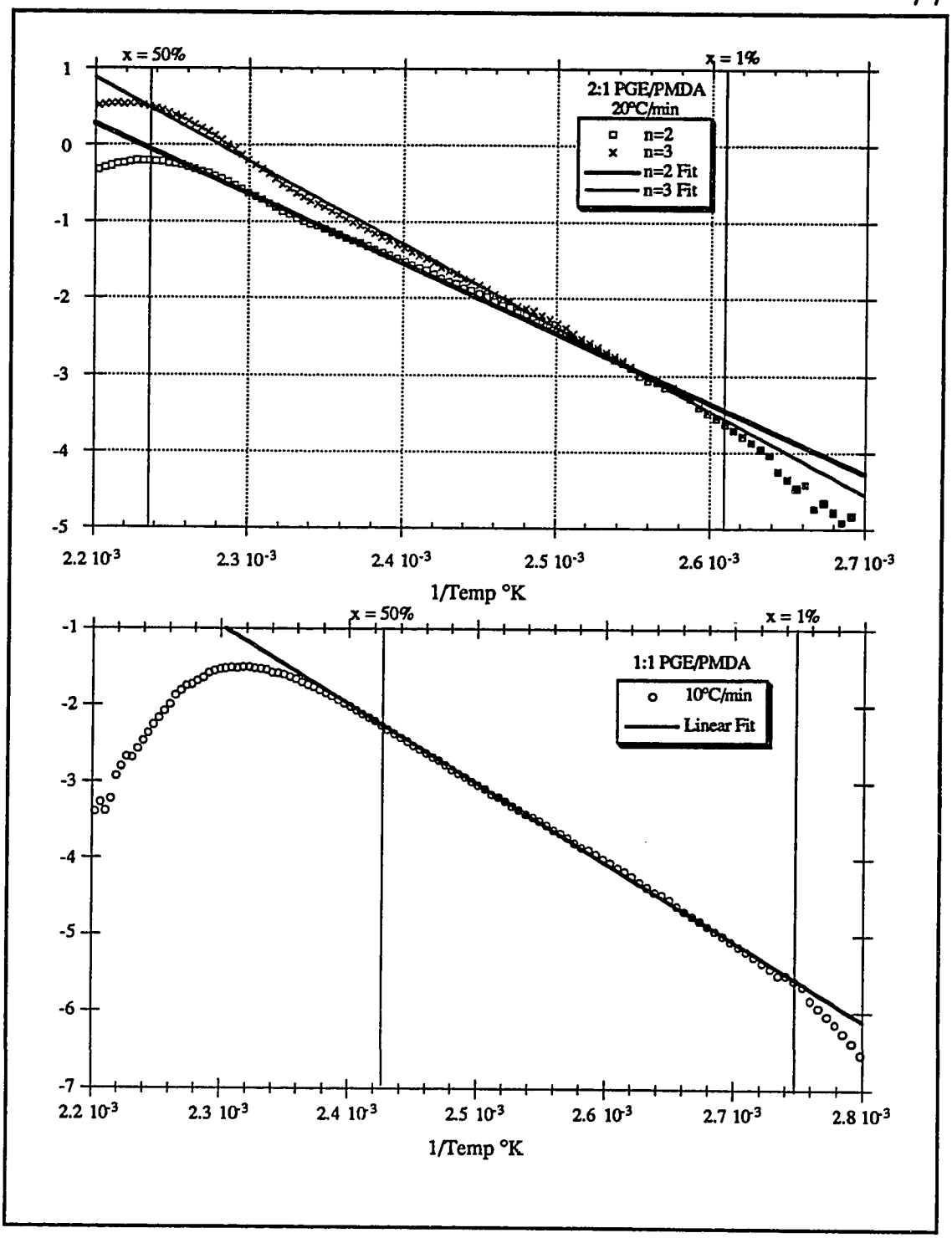

Figure 34: Arrhenius plot (log of the rate constant vs. reciprocal temperature) for the amine catalyzed polyesterification reaction between phenyl glycidyl ether (PGE) and pyromellitic dianhydride (PMDA) using dynamic DSC data.

Figure 35 presents typical isothermal DSC traces for the two anhydride levels. The higher reaction rate is apparent for the excess anhydride, 1:1 mixture as we would expect from the rate expression. There was no evidence of a significant secondary polyetherification reaction peak in either of the traces. The dynamic scan that was run after 10 min of reaction at 160°C produced only a single residual reaction peak near 270 °C.

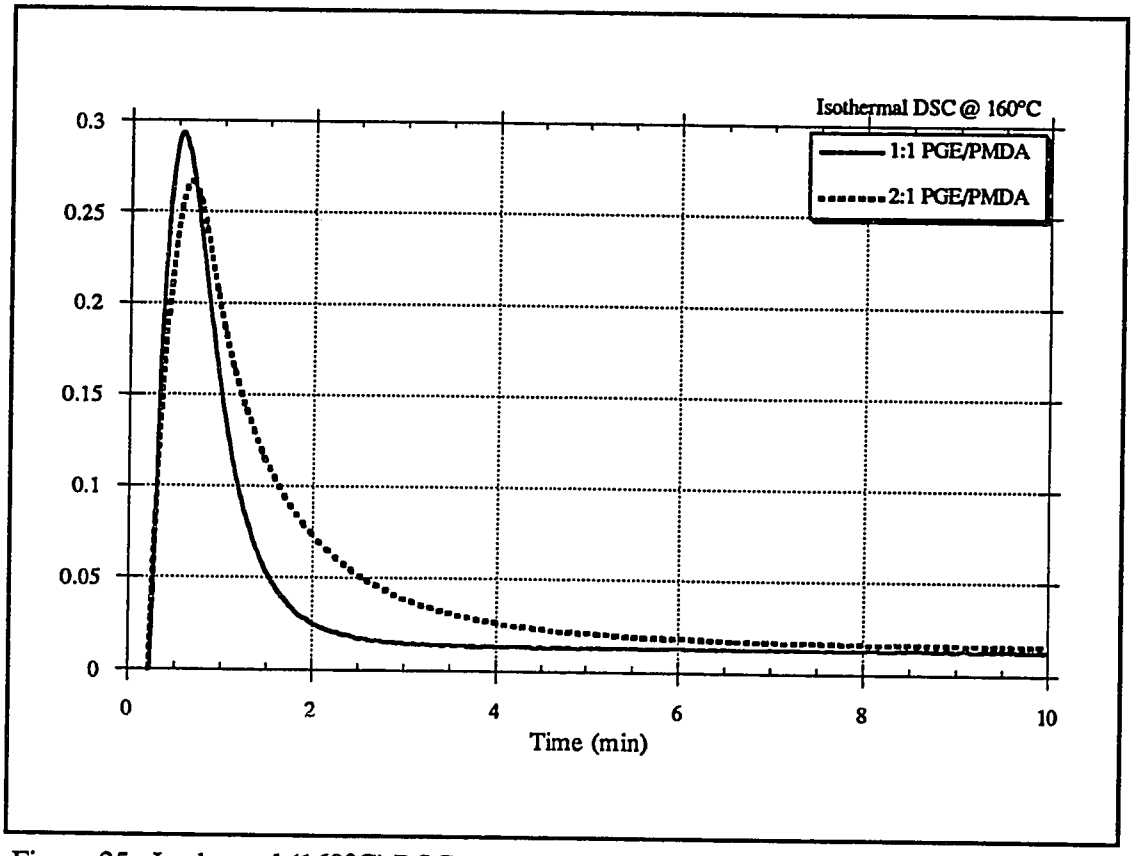

Figure 35: Isothermal (160°C) DSC trace of the amine catalyzed reaction between PGE epoxy and PMDA acid anhydride for a stoichiometric (2:1) mixture, and a (1:1) mixture containing excess anhydride.

Imidocarbamate/Epoxy reaction. The synthesized imidocarbamate N-(4-cumylphenoxycarbonyl)phthalimide (CPCP) was reacted with DGEBA epoxy both with and without triethylamine (TEA) catalyst. A typical DSC scan for the case with TEA is shown in Fig. 36. The stoichiometry of the catalyzed reaction remains unclear, however there is evidence suggesting a secondary reaction involving the formation of a separate

organic carbonate species. The batch stoichiometry may contribute to this secondary reaction so a large excess of epoxy was used in this set of experiments. Melting of the imidocarbamate crystals appears in the DSC to slightly overlap with the reaction exothermic peak. A high temperature shoulder is also noted in many of the runs. Visual observation of the reaction mixture using a magnifying glass showed that the melt remained quite fluid well beyond the bulk reaction peak. Therefore, this shoulder is thought to be a secondary reaction rather than a continuation of the main peak as a result of diffusion limited kinetics. Significant residual epoxy remained in the cured samples that contained excess epoxy in their initial mixtures. Amine-catalyzed epoxy homopolymerization may have contributed to this high temperature shoulder, although generally this latter reaction would not be significant at these temperatures for high purity DGEBA.

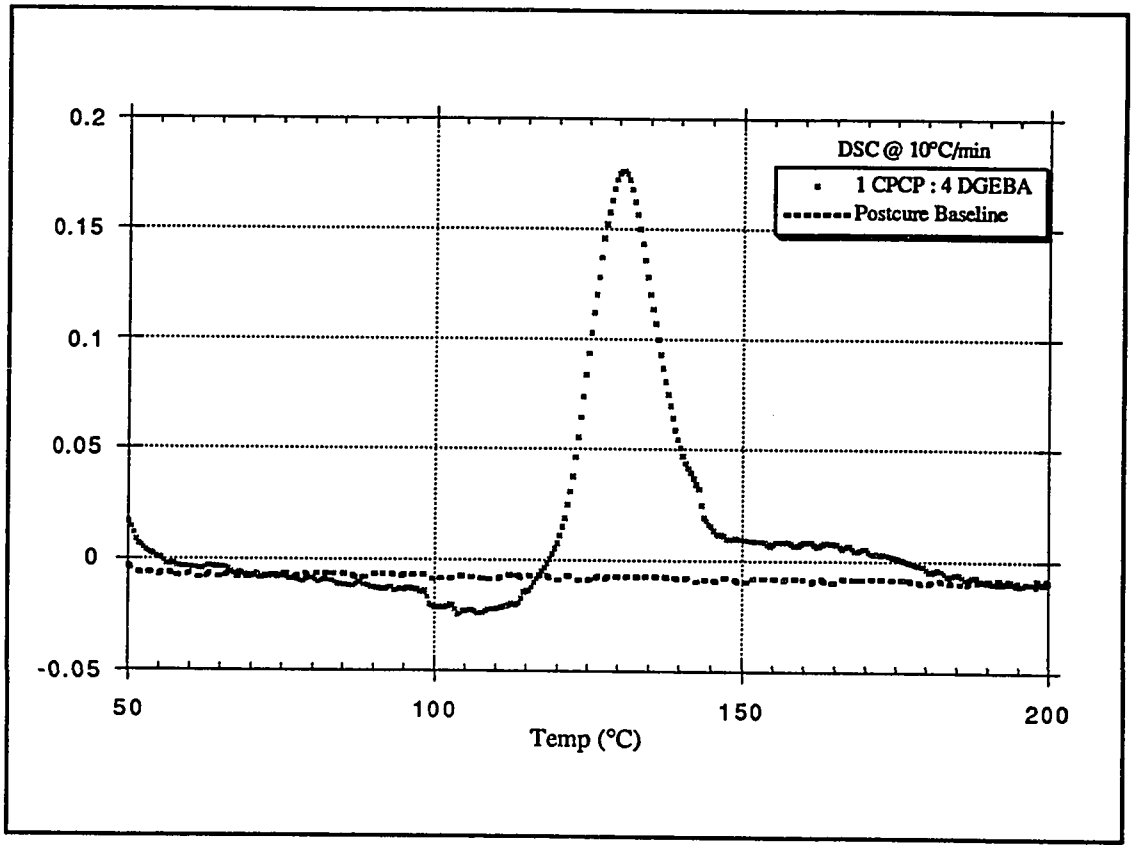

Figure 36: Typical dynamic DSC trace at 10°C/min for the amine catalyzed reaction between CPCP imidocarbamate and DGEBA epoxy resin for a 1 : 4 molar mixture.

The dynamic DSC runs with a 4 times excess of epoxy gave inconclusive kinetic modeling results. An acceptable fit for a simple kinetic model was obtained with a second order dependence on the imidocarbamate. Adding either a first or second order dependence on the epoxy provided about equally acceptable results compared with the zero order. Stoichiometric 1:1 mixtures could be approximated with a fourth order model, suggesting that a second order in both reactants would be the most appropriate choice. Apparently, a pseudo second order reaction occurs with a large excess in epoxy reactant.

Comparisons of FT-IR spectral changes and heats of reaction by DSC were made to examine the reaction stoichiometry. The change in peak height for the 915 cm^{-1} and the 970 cm^{-1} epoxy ring showed less than 1 mole epoxy for each 1 mole of imidocarbamate consumed. The FT-IR data showed poor reproducibility however; but the result was always less than 1 mole. Further evidence that the reaction involves only one or less mole of epoxy per mole of imidocarbamate is provided by the specific heat of reaction (ΔH_{rxt}) measurements from the DSC. The heat of reaction was shown to be consistent and independent of the epoxy level for samples with 1, 2 and 4 times excess epoxy. In all three cases the ΔH_{rxt} = 83-85 J/g·mole of imidocarbamate reactant.

4.4.3 Glass Transition Temperature Measurements

Curing schedules for advanced epoxy resin formulations often involves a lower temperature gel forming step followed by post curing above the glass transition temperature to develop the ultimate thermal an mechanical properties. Glass transition temperature Tg measurements were used to examine two cure sequences. Samples were cured at either 160°C or 195°C for nominally 5 days in Pyrex test tubes. With the aid of liquid nitrogen freezing the polymer was mechanically fractured and separated from the glass pieces. A finely ground powder was produced for use in FT-IR analysis and Tg measurements.

The differential scanning calorimeter was used in post curing and to measure the Tg. On the first DSC scan a 10 - 20 mg size sample was slowly heated to 300°C with a nitrogen blanket and then quickly quenched using a cell cooling attachment at 0°C. This high temperature post curing step was assumed to complete the crosslinking reaction and ensured a uniform thermal history for making Tg measurements. The Tg measurement

was made on the second ramp at 20 °C per minute using the onset of the baseline deflection for the value of Tg.

The Tg data showed measurable differences with both the resin composition and the cure schedule (Fig. 37). In general, a higher Tg correlated with an increase in either the cyanate or anhydride levels as expected, but not without a few anomalies. The Tg decreased with the initial anhydride addition for the 1:1 molar epoxy/cyanate ratio mixture but not the 3:1 mixture. The latter mix showed a substantial increase with the initial anhydride addition. The changes in Tg were generally small between the two cure temperatures compared with other effects, and perhaps not statistically significant since only two samples were used in most cases. On the other hand, the 195°C cure was higher in all but one case, indicating that the observed difference is probably real. The 3:1 epoxy to cyanate case with 20 phr offers another unique situation. Cure temperature in this one case had a much more significant effect. Chemical structural differences will be examined more fully in the subsequent sections in order to provide some explanation for these effects.

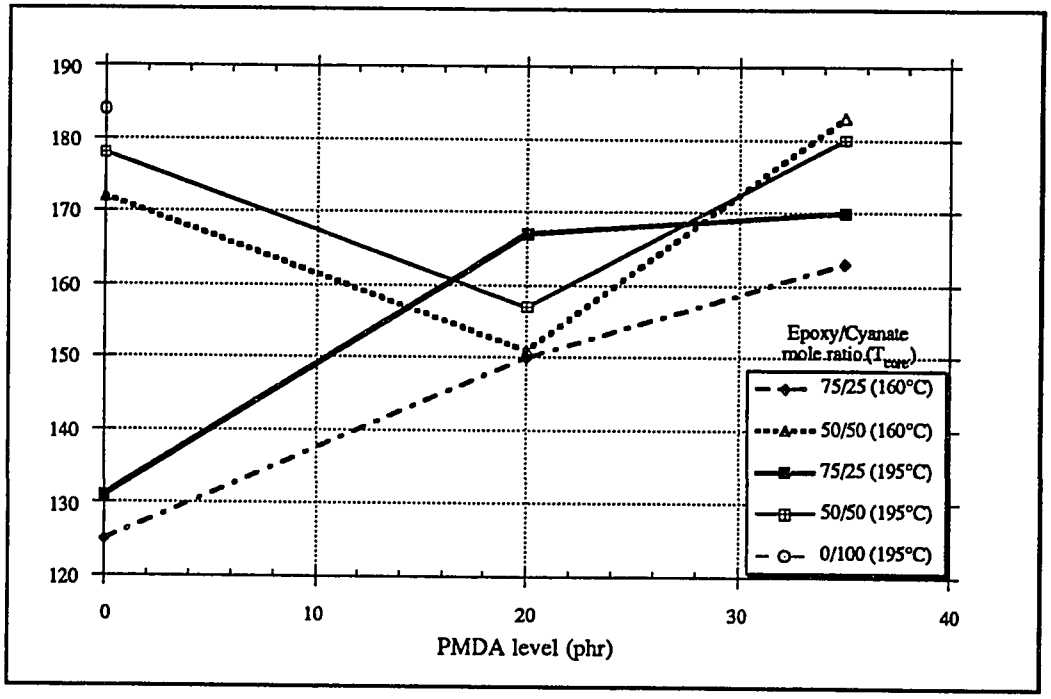

Figure 37: Effect of resin composition and cure schedule on the glass transition temperature (Tg) for a mixture of DGEBA epoxy resin, BEDCy dicyanate resin, and PMDA acid anhydride (in parts per hundred weight resin).

4.4.4 Polymerization Modeling Comparisons

Model compound studies combined with the DSC curing kinetics have confirmed the general outline for the reaction pathways and provided an estimate of the relative rates for each competing reaction. Referring to Fig. 9, reaction (6) appears to be much faster than all others, while reactions (2) and (3) are about the same order of magnitude and still significantly faster than the cyclotrimerization reaction (1). Reaction (2) shows autocatalytic behavior while reaction (3) fits simple 2'nd order kinetics. The cyanate trimerization reaction (1) can also be approximated with a second order kinetic model, but its rate constant is roughly two orders of magnitude lower than the other first level reactions and will clearly play only a secondary role whenever anhydride is available for reaction. With these preliminary observations we begin to see that the anhydride concentration may play the most crucial role in determining the network formation. If the anhydride concentration is sufficiently high the reaction should proceed almost entirely via pathways B and C, consuming all the cyanate and epoxy and preventing any reaction via pathway A. Lower levels of anhydride will of course, allow products from pathway A to be formed to various degrees.

The DSC experiments provided estimates of the Arrhenius parameters for the major reactions which can be used to predict the rate constants as a function of temperature. Their activation energies are sufficiently different that over the temperature range of interest (e.g. 150 to 250°C) there is a significant change in the ratio of rate constants as observed in Fig. 38. For example, at about 130°C the rate constant for the imidocarbamate/epoxy reaction begins to dominate. Below this value we note that the esterification reaction (3) is favored. The DSC data also suggests that the epoxy/anhydride reaction will initially be favored over the cyanate/anhydride reaction. This latter reaction was observed to follow autocatalytic behavior however, and so its overall rate will change with the degree of conversion in a way that is different than the competing epoxy/anhydride reaction. This effect can be seen in Fig. 39 where the relative rates of these two reactions are plotted against degree of conversion for two temperatures (100°C and 200°C). The increased reaction temperature causes the point where the curves cross to be shifted.

The relative rates presented in Fig 39 were calculated for a stoichiometric mixture of cyanate, epoxy, and anhydride using the simple 2'nd order kinetic model for the

epoxy/anhydride reaction and the autocatalytic models of Eqs. 18 & 19 for the cyanate cyclotrimerization and cyanate/anhydride reactions respectively. These rate equations were solved numerically and the initial cyanate cyclotrimerization rate was used as the normalizing factor. The imidocarbamate/epoxy reaction was not included in this analysis.

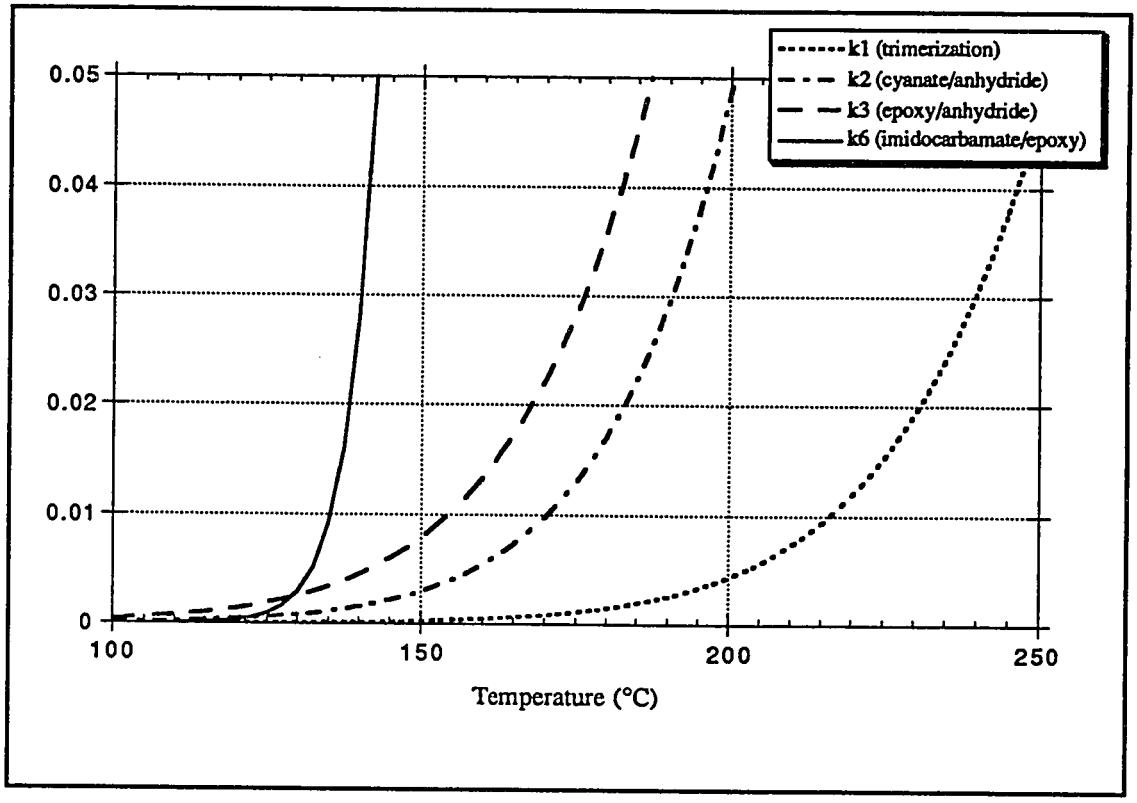

Figure 38: Predicted rate constants as a function of temperature for the major polymerization reactions based on the parameter fitting of DSC data.

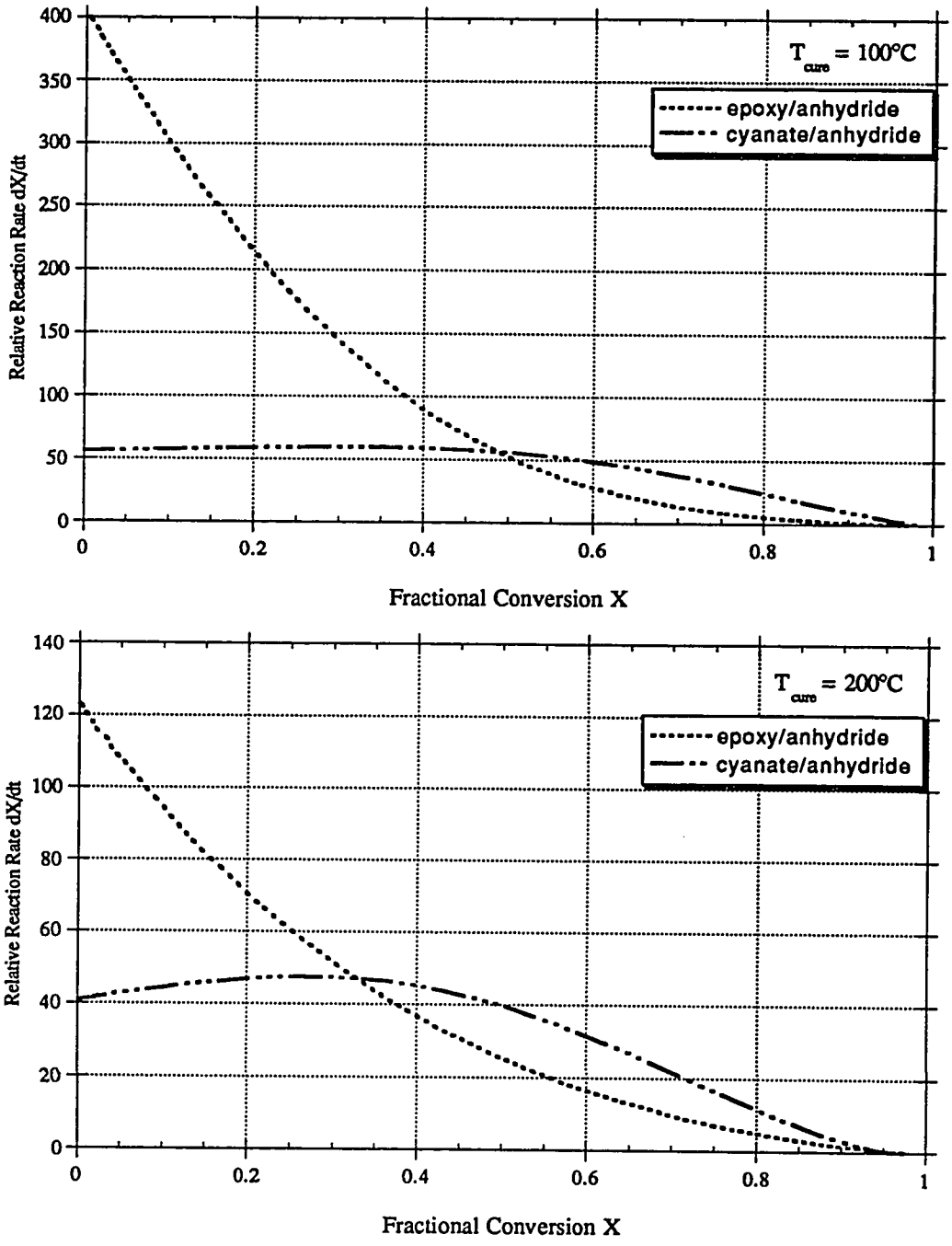

Figure 39: Relative reaction rate (dx/dt) as a function of fractional conversion and temperature for the two primary competing reactions involving acid anhydride.

More quantitative predictions can be made by numerically solving the system of coupled ordinary differential equations (ODE) for the complete system of individual reactions. The reactions in pathway A are adopted from the work of Bauer and Bauer. The rate constants used in their work were estimated from experimental data for a similar cyanate/epoxy system. The temperature range studied by Bauer and Bauer was limited to between 160 and 190°C. Furthermore, the rate constants were reported in terms of constant relative values; i.e. with the cyclotrimerization reaction as unity and independent of temperature. Presumably these authors observed a minor effect with temperature, at least in terms of its affect on the final product composition. Considering how reaction pathways B and C appear to dominate the curing, any minor differences in the relative rates of the secondary reactions in pathway A are not likely crucial.

FT-IR transmission analysis for the three mixtures without anhydride are presented in Fig. 40. The 1:1 cyanate to epoxy molar ratio mixture is shown for both the 160°C and the 195°C cure temperature case. In the latter case we note a large decrease in the cyanurate peaks at 1370 cm^{-1} and 1560 cm^{-1}, followed by an increase in the isocyanurate 1700 cm^{-1} peak and a decrease in the 1760 cm^{-1} oxazolidinone. The second peak appearing near 1740 cm^{-1} is assumed to be an isomer of oxazolidinone or oxazoline which normally is masked by a much stronger 1760 cm^{-1} band.

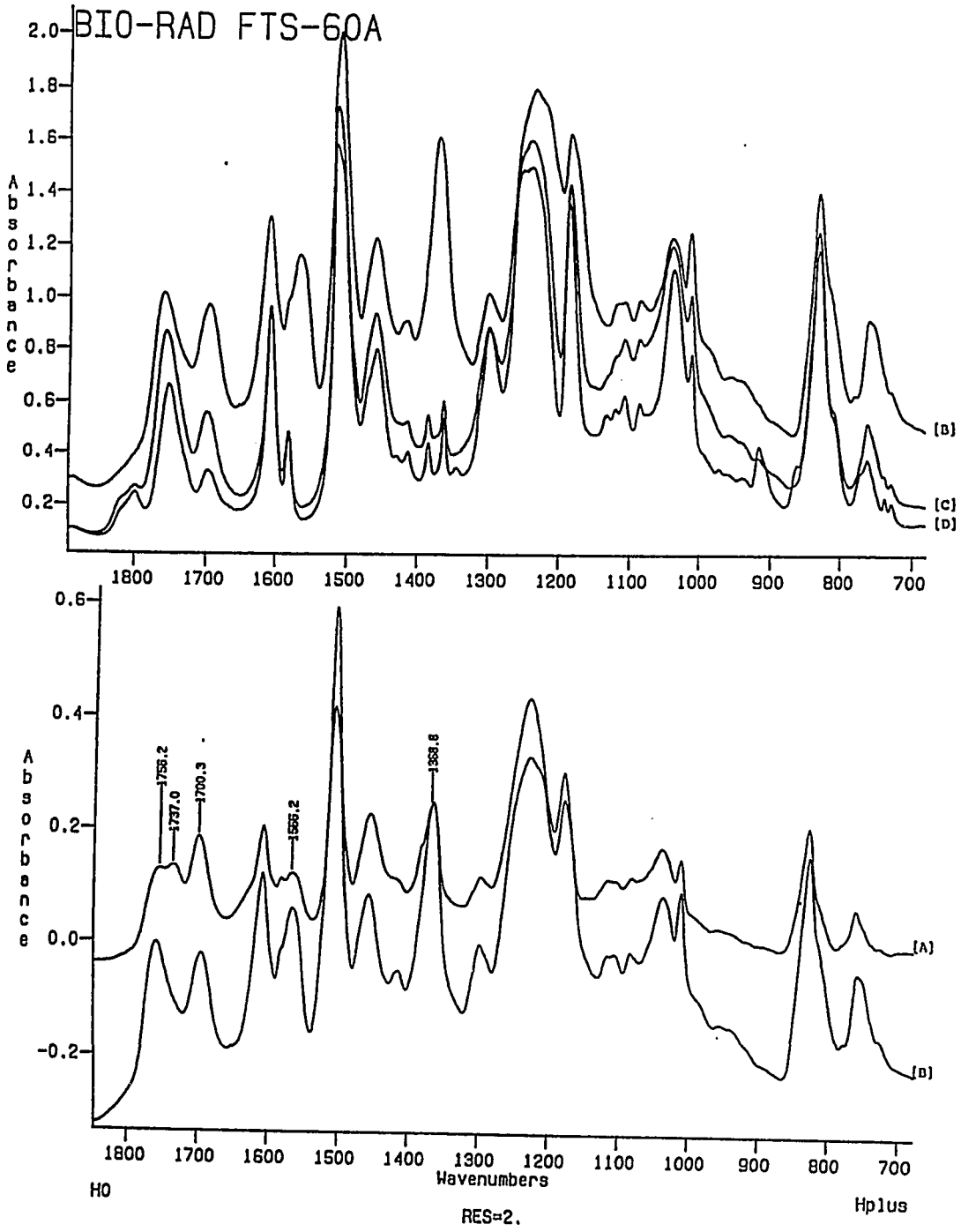

Figure 40: FT-IR spectral features for the dicyanate/epoxy coreaction in the presence of triethylamine. [A] 50/50 cyanate/epoxy mole ratio (T_{cure}=195°C); [B] 50/50 ratio (160°C); [C] 25/75 ratio (160°C); [D] 15/85 ratio (160°C);

Comparison of the spectrum for the three compositions cured at 160°C reveals a shift from two roughly equal peaks at a 1:1 molar ratio to a dominant 1760 cm^{-1} peak for the high epoxy case. The cyanurate peaks seem to nearly, if not completely disappear between the 1:1 and 1:3 molar cases and a small side band develops around 1800 cm^{-1}. This side band has not been identified.

According to the reaction scheme proposed by Bauer and Bauer, a 1:2 molar ratio is the stoichiometric requirement for complete reaction of all cyanurate to oxazolidinone in the absence of any secondary epoxy consuming reactions. When the phenol abstraction step is included, and assumed to go to completion, the stoichiometric ratio is increased to 1:3. Reaction of isocyanurate to oxazolidinone appears to continue some beyond the 1:3 cyanate/epoxy ratio as evidenced in the relative peak heights between the 1:3 and 1:5.7 cases. This may in fact be the result of some additional competing epoxy homopolymerization reactions, or possibly a large excess of epoxy is required before the reaction will go to completion in a reasonable length of time. Close examination of the FT-IR spectra reveals a small amount of residual epoxy which seems to support the second hypothesis.

For a cyanate/epoxy ratio of 1:5.7 (0.3:1.7) we observe a substantial unreacted epoxy level in the finished product. Peak absorbance ratioing indicates that roughly 50 to 60% of the epoxy reacted, or not too much different than the stoichiometric 1:3 amount. These observations lend further support for the general reaction scheme proposed by Bauer and Bauer, including the existence of a significant secondary epoxy-phenol polymerization reaction. The high level of residual epoxy in the 1:5.7 ratio sample further suggests that the principal secondary epoxy reaction is limited by the generation of phenols. This evidence does not however, preclude the possibility of amine catalyzed homopolymerization reactions which might also be prematurely terminated by some loss of the catalyst.

Polymerization simulations were run using a modified version of the Bauer and Bauer model. According to the their model the trimerization reaction can be adequately represented by:

$$dC/dt = -3k_1[C][OH] \qquad (20)$$

with an initial hydroxyl concentration $[OH_0] = 0.01$. Premature termination of the reaction occurs under these initial conditions because the trace hydroxyl is quickly consumed in the epoxy-hydroxyl side reaction. The proposed rate expression that follows allows trace hydroxyl groups such as moisture or alcohols to catalyze the cyclotrimerization without initiating the competing epoxy polymerization's. The phenols generated during the cyanate-epoxy coreaction are included in the second term on the RHS.

$$dC/dt = -3k_1[C]([OH]_0 + [OH]) \tag{21}$$

The model developed by Bauer and Bauer was modified with this rate expression and solved numerically using the LSODAR routine. Two minor stoichiometric corrections in their differential equations were also made. The relative levels of isocyanurate and oxazolidinone presented in Fig. 41 for the 1:1 molar case are appropriate for comparison to the experimental data. Bauer and Bauer assumed the extinction coefficients for these two carbonyl stretching bands were identical in order to estimate the relative rate constants for their model. Identical extinction coefficients means that two peaks with the same absorbance are at the same concentration level. Continuing with this assumption, the experimental data does not demonstrate complete conversion of the isocyanurate to oxazolidinone as required by the model for the 3:1 (0.5:1.5) stoichiometric epoxy level. Furthermore, the relative ratio of isocyanurate to oxazolidinone in the less than stoichiometric case of a 1:1 mixture does not agree even qualitatively for the 160°C cure. An increase in the cure temperature to 195°C improves the qualitative fit with the model for this latter case. Replacing the cyclotrimerization rate expression with the autocatalytic one that fit the DSC data will not significantly alter this final result.

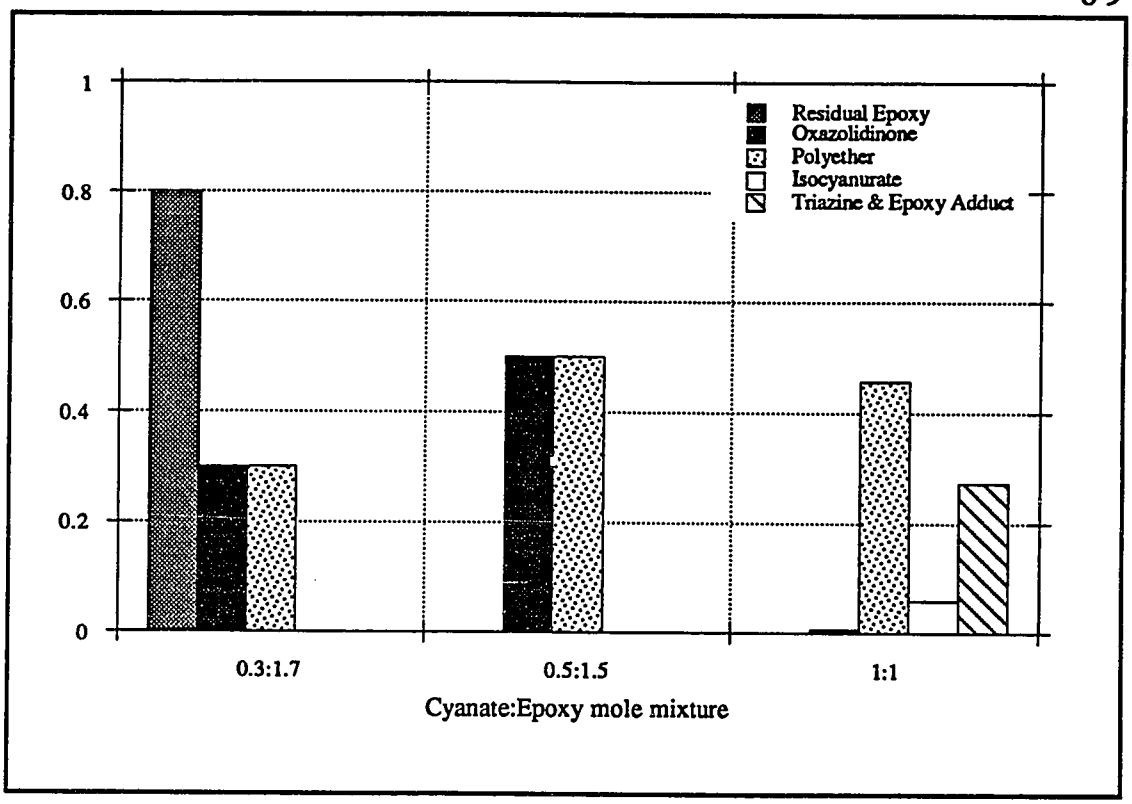

Figure 41: Predicted product composition as a function of the initial cyanate/epoxy level for a two component coreactive mixture using the kinetic model of Bauer and Bauer.

A minor change in the oxazolidinone rate constant might improve the data fit for the 1:1 mixture, but will not address the more fundamental problem of incomplete conversion to oxazolidinone that occurs even when a large excess of epoxy is used. The simple bimolecular reaction model proposed by Bauer and Bauer for the formation of oxazolidinone from isocyanurate and epoxy is a logical starting point for improving the fit of the model. It appears this part of their model was selected on the basis of simplicity and convenience rather than experimental data. Furthermore, this step in the reaction is the only one that involves both species of concern.

Relative rate constants derived from the DSC experiments predict that the reactions involving anhydride will occur at several orders of magnitude faster than the cyanate cyclotrimerization reaction, which is already almost two orders of magnitude faster than the second step in reaction pathway A. Under conditions where the anhydride effectively depletes either of the other two reactants, the epoxy or the cyanate, pathway A reactions

become insignificant and so does this part of the model. Therefore, the general mechanism proposed by Bauer and Bauer was assumed to provide an adequate description of the pathway A reactions for our purposes, and so was adopted with only relatively minor changes to the cyclotrimerization term. The rate of cyclotrimerization, R_1 was assumed to also include an autocatalytic term of the form:

$$R_1 = k_1([C]^2(1 + [OH]/[OH]_0) + a[C][T]) \quad (22)$$

This second order autocatalytic form was indicated by the DSC studies. The rational for changing the form of the hydroxyl term presumes that the catalytic effects of $[OH]_0$ are included in the original determination of k_1 from calorimetric data. Hence, only the relative increase in the hydroxyl level during curing needs to be included. Relative rate constants for the remaining reactions were assumed to remain unchanged for convenience; particularly since our interest is in the compositional range from 25 to 50 mole % cyanate and 20 to 35 phr PMDA levels where secondary pathway A reactions may be small compared with the other products.

Rate expressions for the three reactions outlined in pathways B and C for the cyanate-anhydride and the epoxy-anhydride reactions are combined with the modified kinetic expressions of Bauer and Bauer for the pathway A reactions to form the complete tricomponent model. The hypothesized kinetic scheme for this complete set of curing reactions is presented in Fig. 42.

(1) $3\,C \longrightarrow T$	$r_1 = k_1 ([C]^2 (1 + [OH]/[OH]_0) + a\,[C]\,[T])$
(2) $T + 3\,E \longrightarrow TE + 3\,PO$	$r_2 = k_2\,[T]\,[E]$
(3) $PO \longrightarrow OH$	$r_3 = k_3\,[C]\,[PO]$
(4) $E + OH \longrightarrow EOH$	$r_4 = k_4\,[E]\,[OH]$
(5) $E + A \longrightarrow 2\,S$	$r_5 = k_5\,[E]\,[A]$
(6) $C + A \longrightarrow I$	$r_6 = k_6 (([C]\,[A])^{0.5} + ß\,[C]\,[A]\,[I])$
(7) $I + E \longrightarrow Q$	$r_7 = k_7\,[I]^2\,[E]^2$
(8) $TE \longrightarrow IC$	$r_8 = k_8\,[E]\,[TE]\,f^3$
(9) $IC + 3\,E \longrightarrow 3\,OX$	$r_9 = k_9\,[E]\,[IC]$
(10) $EOH + E \longrightarrow EO + EOH$	$r_{10} = k_{10}\,[EOH]\,[E]\,[OH]$

Figure 42: Proposed kinetic scheme for overall reaction. Cyanate ester [C]; *s*-Triazine [T]; Epoxy [E]; Oxazolidinone [OX]; Phenyl ether [PO]; Phenol [OH]; Polyethers [EOH] & [EO]; Anhydride [A]; Polyester [S]; Imidocarbamate [I]; unknown Polyimide/carbonate adduct [Q]; Isocyanurate [IC]; Epoxy modified triazine [TE]. a & ß are constants and f = [TE]/([T] + [TE]).

The proposed model uses a simplified version of Bauer and Bauer's kinetic scheme (see Fig. 14) where the various isomeric products are assumed to be indistinguishable at least in terms of their kinetic behavior. In addition, a specific term to represent the formation of an extractable phenyl ether group (PO) has been added to step 2 for simplicity. The release of this phenol (Fig. 14e) and its subsequent reaction with epoxides (Fig. 14f) are represented by steps 3 and 4. Polyether forming reactions have been observed by several researchers during the curing of epoxy/dicyanate mixtures; although some hypothesize a

mechanism involving catalysis by the triazine [16,48] rather than direct reactions with phenols. Finally, step 10 has been added for the phenol catalyzed homopolymerization reaction between the epoxy group and the secondary hydroxyl formed in step 4.

A mass balance for the Fig. 42 reactions results in fourteen ordinary differential equations of the form:

$$d[C]/dt = R_C = -3r_1 - r_6 \quad (23)$$

$$d[T]/dt = R_T = r_1 - r_2 \quad (24)$$

$$d[E]/dt = R_E = -3r_2 - 3r_9 - r_4 - r_5 - r_7 - r_{10} = -3r_2 - R_{OX} - R_{EOH} - {}^1/_2R_S - R_Q - r_{10} \quad (25)$$

$$d[OX]/dt = R_{OX} = 3r_9 \quad (26)$$

$$d[PO]/dt = R_{PO} = 3r_2 - r_3 \quad (27)$$

$$d[OH]/dt = R_{OH} = r_3 - r_4 = r_3 - R_{EOH} \quad (28)$$

$$d[EOH]/dt = R_{EOH} = r_4 \quad (29)$$

$$d[A]/dt = R_A = -r_5 - r_6 = - {}^1/_2R_S - r_6 \quad (30)$$

$$d[S]/dt = R_S = 2\, r_5 \quad (31)$$

$$d[I]/dt = R_I = r_6 - r_7 = r_6 - R_Q \quad (32)$$

$$d[Q]/dt = R_Q = r_7 \quad (33)$$

$$d[TE]/dt = R_{TE} = r_2 - r_8 \quad (34)$$

$$d[IC]/dt = R_{IC} = r_8 - r_9 = r_8 - {}^1/_3\, R_{OX} \quad (35)$$

$$d[EO]/dt = R_{EO} = r_{10} \quad (36)$$

A comparison between the model and the experimental data can be made at various stages of curing. Samples of the reactants were removed from the oil bath and quickly quenched to stop the curing process during two of the experiments. These samples were subsequently analyzed using transmission FT-IR on either neat films for samples that were still soluble in chloroform and KBr pellets for all others. The peak heights were measured relative to a local baseline correction and normalization using an average of the 2970 cm^{-1} C-H stretching band and the 1607 cm^{-1} aromatic ring band.

Figure 43 presents the normalized peak heights for the three reactants as a function of time and at two different cyanate/epoxy ratios. A comparison with the kinetic model of Fig. 42 is also shown. In this case the rate constants were estimated using the DSC data. The rate constant for the step 10 epoxy homopolymerization was assumed to be negligible relative to the esterification reaction of step 5. The predicted concentration profiles show a dramatically different behavior. The general trend observed in both sets of experimental data indicates that the consumption of anhydride is followed closely by the cyanate disappearance with the epoxy trailing. The model predicts, based on the DSC data, that the amine catalyzed epoxy/anhydride esterification reaction should be a major pathway for this polymer system, however it is clear from the run data that this is not the case. Perhaps the catalyst is consumed or irreversibly bound in the competing imidocarbamate formation.

A closer examination reveals a good correlation between the shape of the predicted anhydride profile and the actual experimental profile for the cyanate resin. Thus, the experimental data suggests that imidocarbamate formation dominates this reaction system and that the epoxy reacts mostly with either the imidocarbamate or itself rather than the anhydride. A much better fit of the experimental data can be achieved by dramatically reducing the rate constant for the epoxy/anhydride esterification reaction.

A systematic trial and error approach was used to arrive at a more reasonable estimate of the relative rate constants. The cyanate/epoxy coreactions appears to play a secondary role in the range of resin mixtures we studied and so their rate constants were fixed at the values provided by Bauer and Bauer. A nonzero rate constant for the epoxy homopolymerization reaction (Fig. 42, step 10) was used since without it, a large unreacted fraction of epoxy resin remained in all simulations with the 1:3 cyanate/epoxy

mixture which did not agree with the experimental data. The relative rate constant for this latter reaction was selected to match the epoxy concentration profile.

Figures 44 - 46 shows the comparison with experimental data for the revised rate constants at two different levels of cyanate/epoxy mixtures. Reasonable qualitative agreement for the cyanate group is achieved with these changes, but in both cases the anhydride concentration profiles appear to follow significantly different kinetics. The experimental data suggests that the anhydride reaction has a more pronounced induction period.

Sensitivity studies were done where the ratio of rate constants for the various steps in the overall reaction were varied independently over several orders of magnitude. Fitting of the anhydride concentration profiles could not be improved with out significantly effecting the quality of fit for the cyanate and epoxy reactants.

Figures 47 and 48 illustrate the FT-IR spectral changes associated with the addition of anhydride at levels of 20 and 35 phr and the effects of cure temperature. For the 1:1 mixture the two cyanurate peaks nearly disappear, if not entirely, with the first addition of anhydride. The isocyanurate peak at 1780 cm^{-1} is still evident in the 20 phr case however, so reaction pathway A can not be ignored completely. We also observe the beginnings of imidocarbamate formation at 1770 cm^{-1}, which continues to develop for the 35 phr level. Note that the 1815 cm^{-1} imidocarbamate peak is now visible and the isocyanurate seems to be gone by the 35 phr level. Both anhydride levels show very small amounts of residual epoxy. The samples cured at 195°C show small reductions in the imidocarbamate peaks with a corresponding increase in the 1725 cm^{-1} peak as well as some increases in peaks near 1200 cm^{-1} where polyether stretching is seen. Increases are also observed in the 1385 cm^{-1} band which we attribute to the polyimide group.

The isocyanurate peak is not evident in the 3:1 mixtures with anhydride. If any oxazolidinone is present the concentration is low enough that it is also hidden by the larger peak at 1725 cm^{-1}. This main peak shifts to a higher wavenumber and becomes broader in shape with the anhydride increase from 20 to 35 phr. Several overlapping peaks in this region may account for the general shape of this dominant peak but the main reason for the wavenumber shift is the increased percentage of ester groups. The polyester carbonyl band is observed at around 1730 cm^{-1} while the largest polyimide peak

falls closer 1720 cm^{-1}. Polyester C-O stretching around 1100 cm^{-1} is observed to coincide with the carbonyl peak shift. With the 35 phr level we observe some residual imidocarbamate in the product In both cases we observe a small amount of residual epoxy. For these cases the low cure temperature may have produced incomplete curing as diffusional limitations restricted molecular mobility above the gel point. An increase in the cure temperature to 195°C eliminated the residual epoxy peak and the imidocarbamate peak in the 35 phr case. Secondary epoxy homopolymerization reactions may also have occurred with the elevated temperature cure.

A further decrease in the cyanate level to a ratio of 1:5.7 shifts the carbonyl peak towards the characteristic ester peak at 1740 cm^{-1} and the ester C-O peaks in the region between 1085 cm^{-1} and 1130 cm^{-1} become pronounced. A small amount of residual anhydride and epoxy are also observed in the sample cured at 160°C. Both of these residual reactant peaks nearly disappear with the 195°C cure schedule.

The model simulations were used to predict the polymers composition for the range of resin compositions studied. Comparison with the FT-IR spectral features for these resin mixtures offers encouragement that the model is qualitatively reasonable in many cases. However, the measurable cyanurate level predicted in one case does not agree with the experimental data, nor does the high residual epoxy level predicted for two of the cases if the epoxy homopolymerization reaction is excluded. The cyanurate level can be easily handled through adjustments in the existing rate constants. The large difference in the epoxy residual is additional evidence that the epoxy homopolymerization reactions are not negligible, but alternatively the problem might be due to an error in the epoxy/imidocarbamate reaction description. There remains some unresolved questions about the carbonate species we detected under certain conditions which lends credence to this latter explanation.

The carbonyl stretching region of the FT-IR spectra can be effectively used in making qualitative comparisons with model simulations. Unfortunately this region of the spectrum consists of multiple overlapping peaks so quantitative estimates are not very reliable. Figure 49 presents the predicted composition for the best fit case. The major ester constituent in two of the cases (15/85/35 and 25/75/35) is consistent with the 1739 cm^{-1} position of the carbonyl and the enhanced peaks around 1100 cm^{-1} in both of their FT-IR spectrum. Lowering the anhydride level to 20 phr for the 1:3 (25/75)

cyanate/epoxy mixture caused a more than twofold reduction in the ester level with only a relatively small decrease in the imide peak. A subsequent shift in the carbonyl peak to the lower value of 1728 cm^{-1} is consistent with this trend. The 1:1 cyanate/epoxy mixture has an even more sharply defined imide carbonyl peak at 1728 cm^{-1} that correlates well with the strong imide concentration predicted by the model simulations. The small imidocarbamate shoulders that are only observed in the samples with a 1:1 cyanate/epoxy mixture are also predicted by the model, although the predicted levels may be a little too low for the observed strength of these peaks. The 2% level of isocyanurate in the 1:1 mixture with 20 phr anhydride also agrees qualitatively with the 1695 cm^{-1} shoulder we observe in the actual spectrum. So does the disappearance of this shoulder when the anhydride is increased to 35 phr.

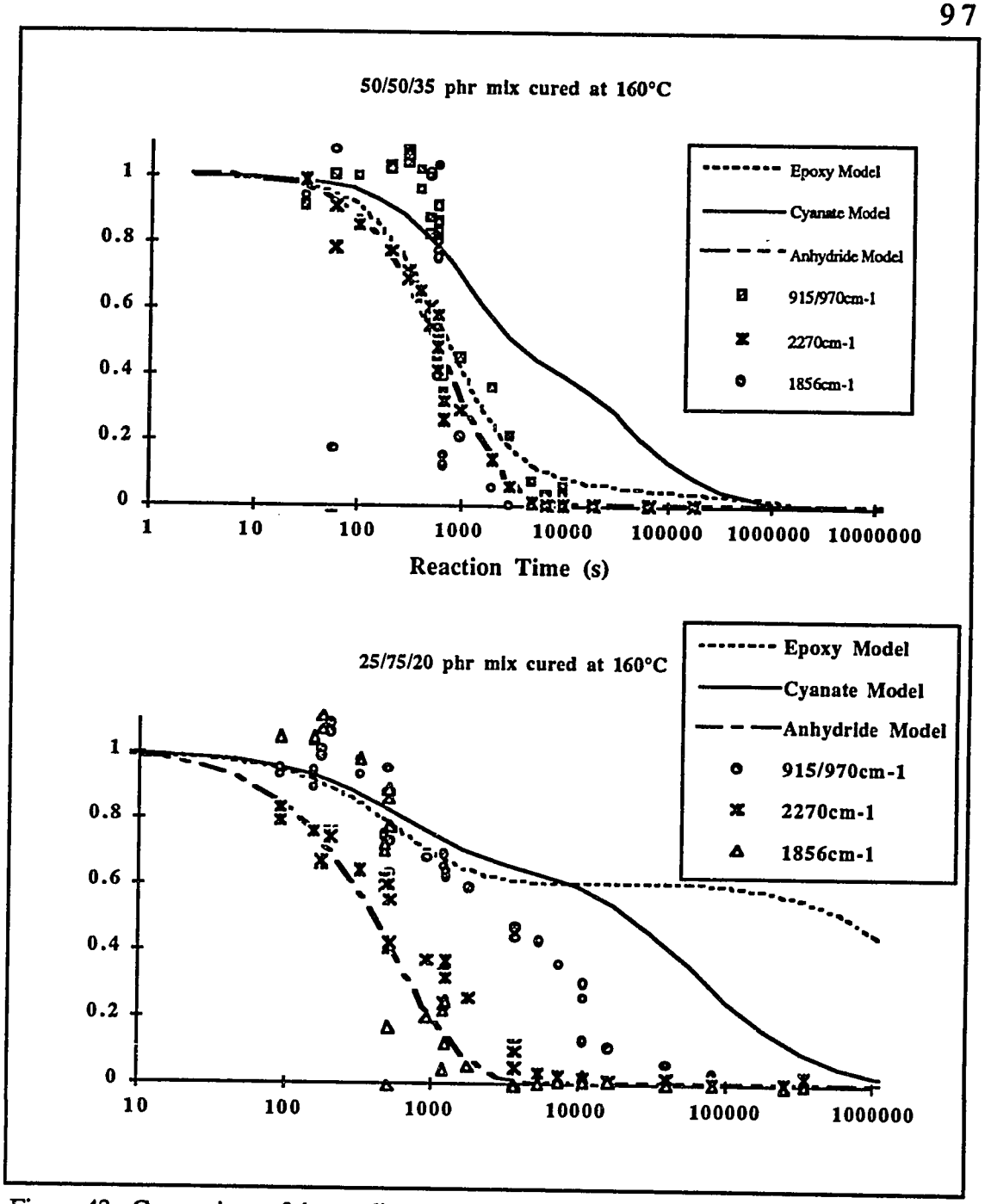

Figure 43: Comparison of the predicted concentration profiles with the experimental profiles from normalized FT-IR peak heights for the cyanate, epoxy, and anhydride reactants. Predicted profiles based on the DSC derived rate parameters of: $k_1 = 1$; $k_2 = 0.05$; $k_3 = 5$; $k_4 = 10$; $k_5 = 62.5$; $k_6 = 25$; $k_7 = 10^4$; $k_8 = 1$; $k_9 = 0.01$; $k_{10} = 0.0$

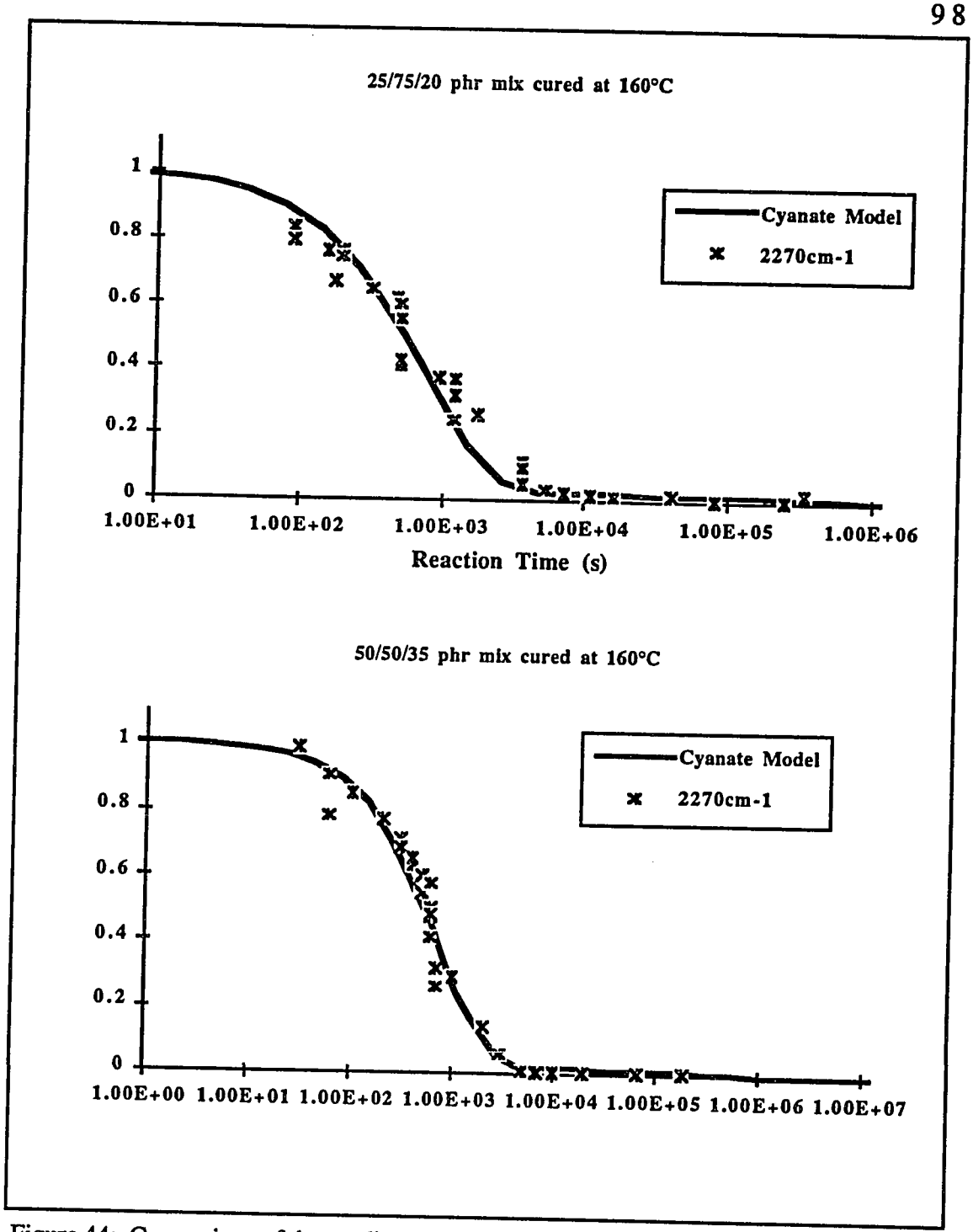

Figure 44: Comparison of the predicted vs. experimental concentration profiles from FT-IR peak height data for the cyanate reactant. Revised rate parameters: $k_1 = 1$; $k_2 = 0.05$; $k_3 = 5$; $k_4 = 10$; $k_5 = 2.5$; $k_6 = 10$; $k_7 = 10^4$; $k_8 = 1$; $k_9 = 0.01$; $k_{10} = 0.5$

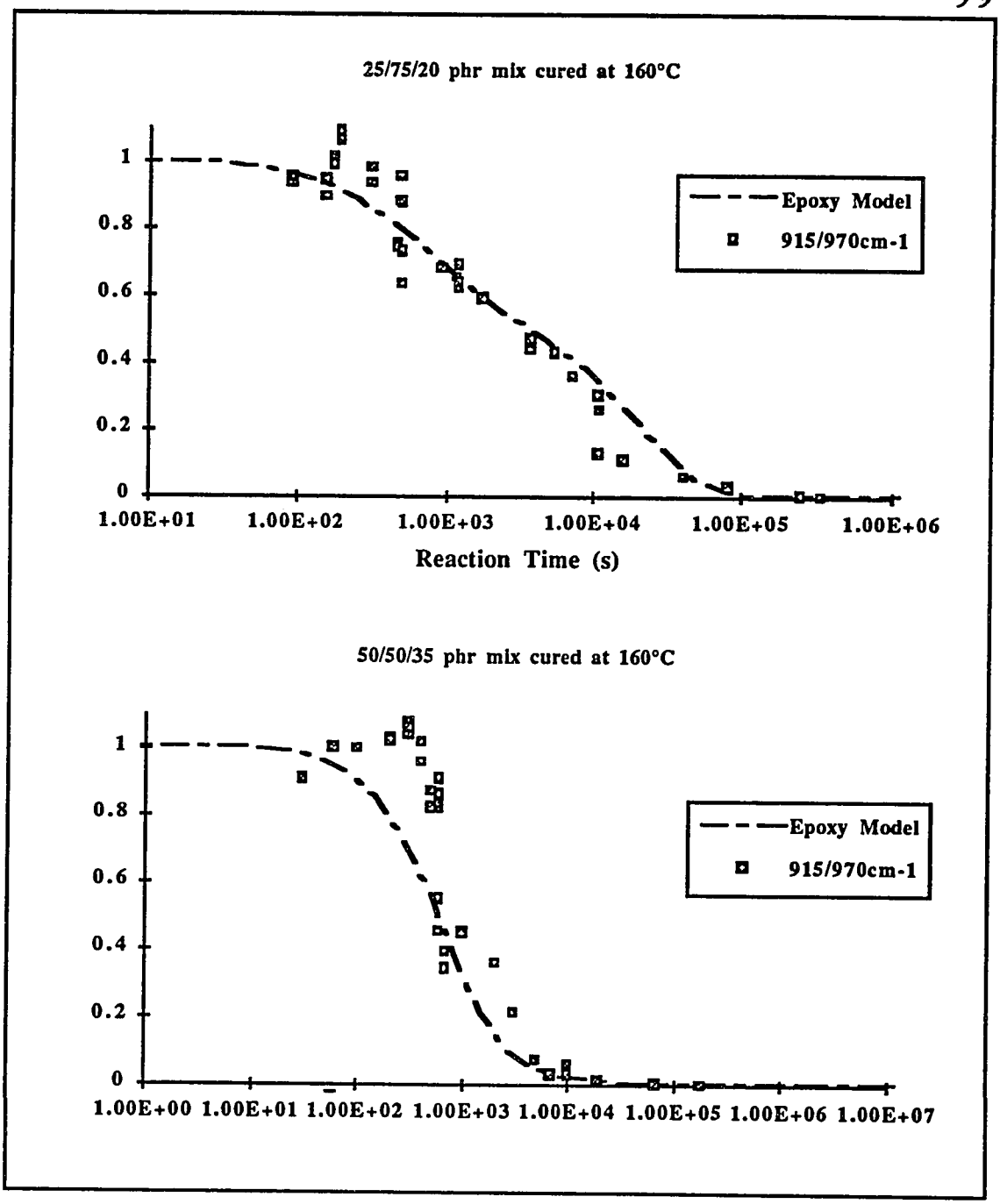

Figure 45: Model vs. experimental concentration profiles for the epoxy reactant.

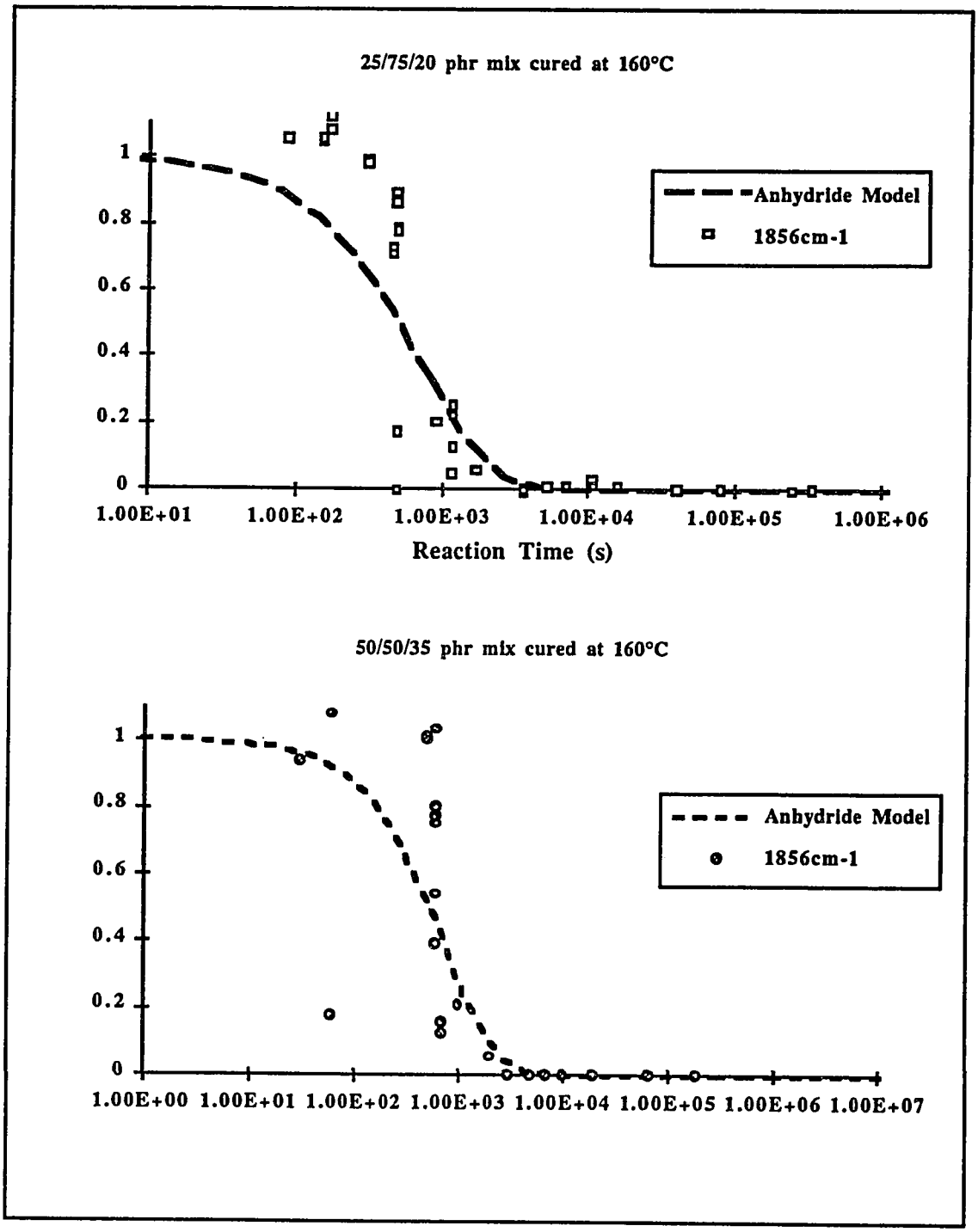

Figure 46: Model vs. experimental concentration profiles for the anhydride reactant.

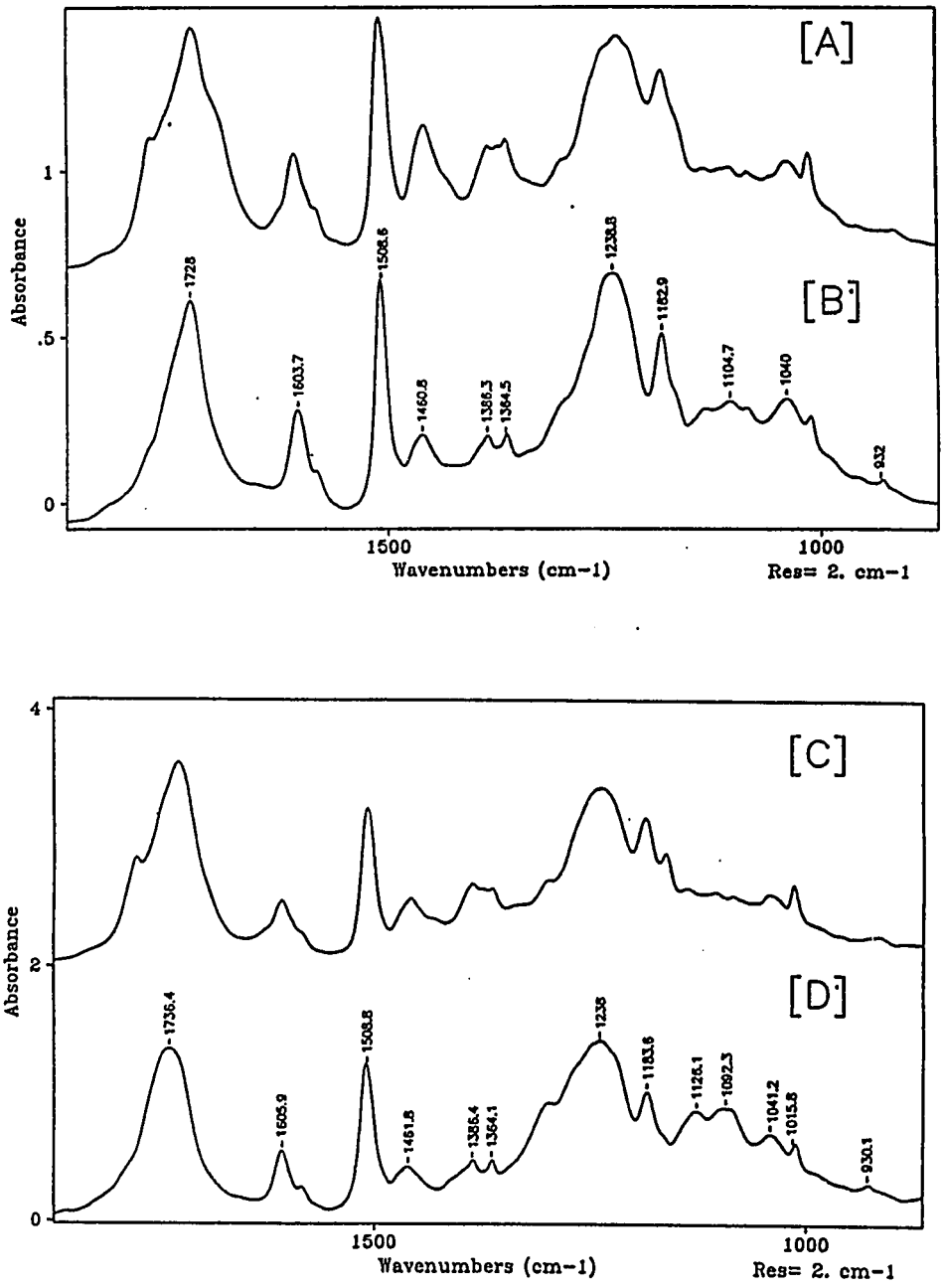

Figure 47: Effects of resin composition on the FT-IR spectral features of the crosslinked polymers. Cyanate and epoxy resin levels are reported in mole % with the anhydride in parts per hundred weight resin (phr). [A] 50/50/20 cyanate/epoxy/anhydride (T_{cure}=195°C); [B] 25/75/20 (195°C); [C] 50/50/35 (195°C); D] 15/85/35 (195°C).

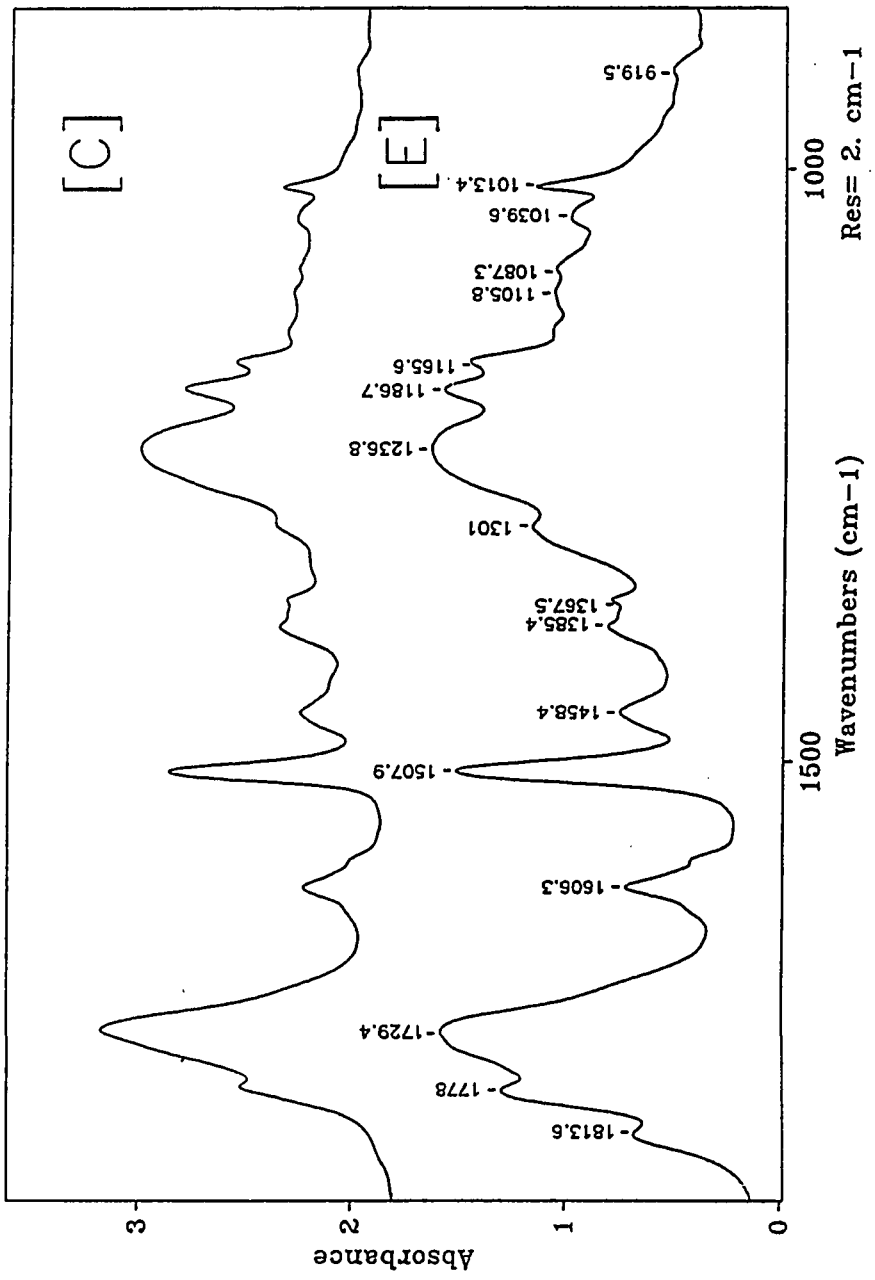

Figure 48: Effect of cure temperature on the FT-IR spectral features of the crosslinked polymer for an equimolar mixture of cyanate and epoxy resin with 35 phr anhydride. [C] T_{cure}=195°C; [E] T_{cure}=160°C.

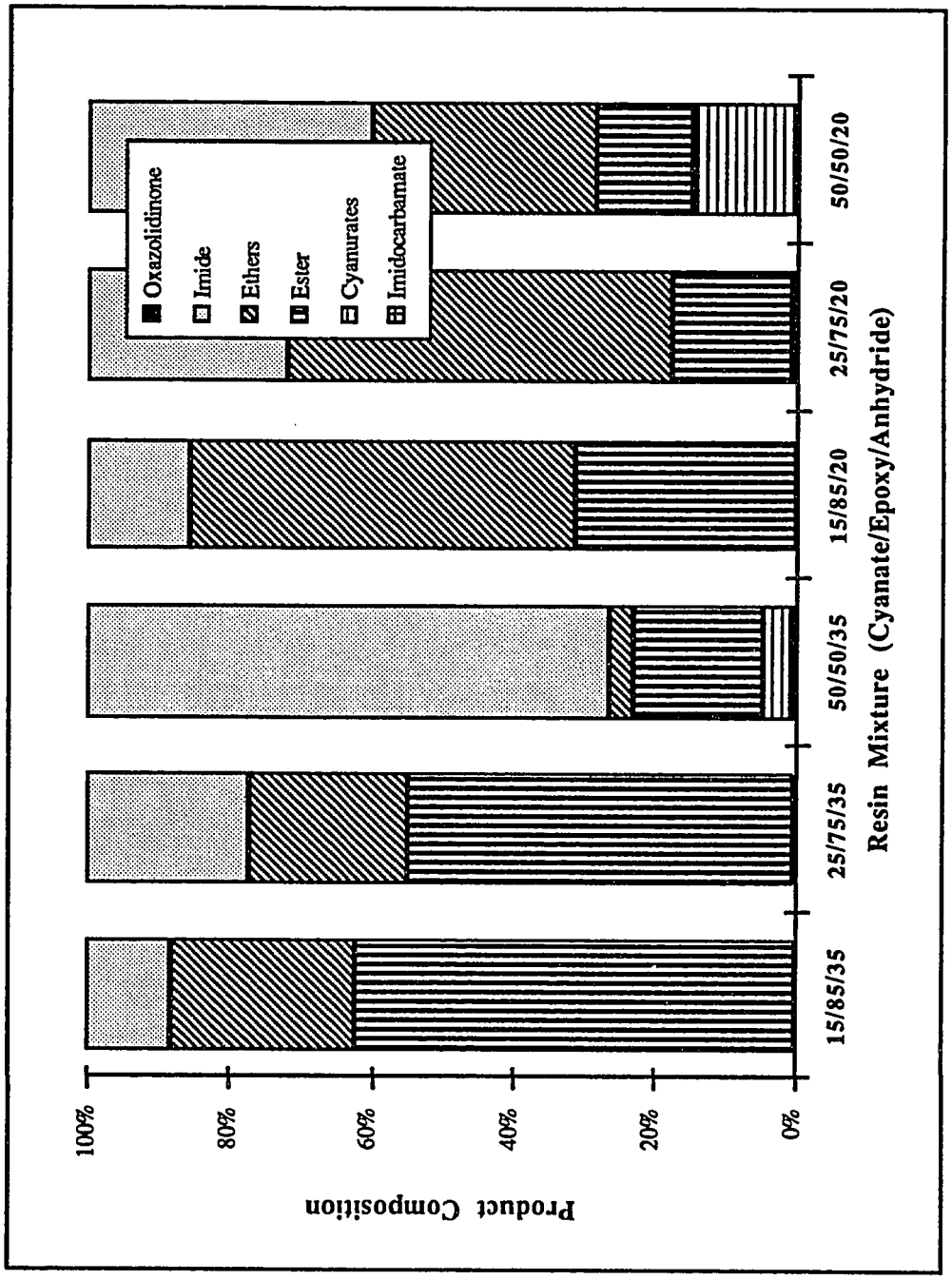

Figure 49: Predicted yields of various product groups for selected resin compositions

4.5 Phase II Summary and Conclusions.

A new polymer adhesive made of low molecular weight monomers that form into an interconnecting system of thermoplastic and thermosetting segments was developed for Nomex honeycomb core manufacturing. Instead of using solvent evaporation to achieve the intermediate tack conditions, we developed a two step curing approach with a stable B-stage prepolymer as the intermediate. The buildup of this complex polymer network from a three-way reactive mixture of epoxy, cyanate and carboxylic acid anhydride monomers was characterized with FT-IR and DSC techniques. Three major competing reaction pathways were identified:

A) cyanate trimerization followed by epoxy copolymerization,
B) cyanate/anhydride polymerization to form imidocarbamate structures, which further reacts with the epoxy resins, and
C) epoxy/anhydride esterification.

Kinetic parameters for these principal reactions were estimated from dynamic DSC tests and used in formulating an overall kinetic model. Comparisons between the model and experimental data suggests that the epoxy esterification reaction (pathway C) is largely over predicted by the independent DSC tests. Model simulations gave results that were qualitatively consistent with experimentally derived concentration profiles for some of the reactants after the epoxy esterification rate constant was sufficiently reduced. However, the experimental data for disappearance of the anhydride reactant seems to suggest that some steps in the reaction are not adequately described by the proposed model. Comparison with product yields was limited to qualitative observations because of significant overlap for many of the peaks in the FT-IR spectrum.

Polymer processing specifications for the particular honeycomb adhesive application defined a limited compositional envelope of interest. The optimal anhydride level happens to roughly coincide with an amount equal to the cyanate. Under these conditions reaction pathway B was shown to be predominant; to the extent that very little if any trimerization product was observed during the polymerization while anhydride was present. In the absence of anhydride the cyanate co-reacted with the epoxy resin to produce two distinct FT-IR peaks (1695 and 1760 cm^{-1}) in the carbonyl stretching region; with the 1760 cm^{-1} peak favored at a low cyanate to epoxy ratio. These peaks

were assigned to the isocyanurate and oxazolidinone structures respectively. A small secondary side peak at 1800 also develops in conjunction with the increasing 1760 cm^{-1} peak as the cyanate level is reduced below a 1:1 molar ratio with the epoxy. Under selected conditions the 1760 cm^{-1} peak split into two overlapping peaks (1740 and 1760 cm^{-1}). Both the 1740 cm^{-1} and the 1800 cm^{-1} peaks are assumed to originate from oxazoline or oxazolidinone related isomers.

Cure temperature does not appear to be a useful means of selectively controlling the polymer network. Curing rates were examined at 160°C and 195°C. Differences in the FT-IR spectrum of the products were small at best and suggest only minor changes in the yields of various products. Two factors contribute to this behavior. The apparent activation energies between the principal competing reactions are not dramatically different (± 10% according to the DSC data) and the rate of reaction pathway B is sufficiently dominant that it remains so even though the cyanate trimerization reaction (pathway A) is more temperature sensitive. The overall rate of the reaction is increased by about an order of magnitude for this 35°C temperature difference. This observed increase is more or less consistent with predictions from activation energies that were determined independently.

While spectral changes were not appreciably different between the two cure temperatures, measurable glass transition temperature Tg differences were detected. These differences tended to be small but consistently lower values were measured for the 160°C temperature case even after a 1-hour at 250°C post cure that attempted to complete the reaction and ensure uniform thermal history. The Tg measurably improved with the increase in anhydride concentration for the 1:3 cyanate to epoxy mixture but not for the 1:1 mixture. Increased crosslinking density as linear oxazolidinone and polyethers are replaced by branched imide and polyester groups is the explanation given for the improved thermal behavior with the 1:3 mixture. In the case of the 1:1 resin blend a sharp decrease is observed in Tg with the initial addition of anhydride from 0 to 20 phr levels. Further increases in the anhydride produced a recovery back to near the original Tg levels. The higher initial cyanate with the 1:1 mix results in measurable levels of the thermally stable polycyanurate groups when no anhydride is added. Consequently, the initial addition of anhydride competes for the cyanate and prevents polycyanurate formation. Still higher levels produce more of the branched imides and polyesters.

The glass transition measurements seem to confirm that the preferred polymer network is one with high levels of polycyanurate and polyesters. This could be achieved if the cyanate-anhydride were suppressed and the epoxy-anhydride reaction amplified so that both the cyanate was free to form cyanurate structures and the epoxy was unable to fully react the cyanurates to oxazolidinones. Alternative catalysts may provide the required selectivity.

The imidocarbamate reaction could be reasonably well fitted over the entire cure range with a simplified autocatalytic reaction model of the form:

$$dx/dt = k(1-x)[1 + a(1-x)x]$$

where; x = fractional conversion, and
$k = A\exp(-E/RT)$
a = proportionality constant

The form of this equation implies that the rate constants for the two terms in the model can simply be related over a limited temperature range by a constant. In other words, we have assumed their apparent activation energies are equal (- 90 kJ/mol). For these studies the temperature range was nominally 50°C. The measured variation in proportionality constants that were observed for the two different DSC ramp rates (i.e. 10 vs. 20°C/min) implies that some refinements are warranted if rate constants much beyond the narrow temperature range of study are to be calculated. The obvious starting point would be to assume the activation energies are not approximately equal. However, for isothermal curing the value of k is generally a constant (i.e. $k \neq f(x)$) and was measured in the temperature region of interest for this study (125°C to 200°C) so the proposed model is reasonable.

In the presence of a tertiary amine the imidocarbamate readily reacts with epoxy groups to form imides. Kinetic investigations of this reaction found the rate constant to be strongly temperature dependent (apparent activation energy - 300 kJ/mol) with a second order dependence on both reactants. Under certain conditions separate organic carbonate species also appeared to form. The conditions for forming these carbonates has not been successfully defined and only trace amounts of material have been isolated to date. Much additional study is needed to define this reaction better.

The polymerization of cyanate resins in the presence of a tertiary amine, reaction pathway A, were examined. DSC dynamic scans showed a significantly modified exothermic peak shape which was flatter, broader and shifted by as much as 60°C below the uncatalyzed resin peak. The amine catalyst had been purified by fractional distillation shortly before use but was not checked for purity level. FT-IR analysis revealed the characteristic cyanurate peaks and disappearance of the cyanate bands. The DSC data for the 1 mol% amine case fit a simplified autocatalytic kinetic model with a single activation energy of the form:

$$dx/dt = k(1-x)[(1-x) + ax]$$

Both first and second order autocatalytic models have been proposed by others for similar cyanate systems without catalysts. In one case the activation energy of the auto-catalyzed rate constant was determined to be 3 times larger than the start-up rate constant (134 vs. 44 kJ/mol) and in the other case it was 1.5 times smaller (~52 vs. 78 kJ/mol). The former study also measured an activation energy of 95 kJ/mol using a single overall reaction to describe the kinetics. This value compares well with the 90 kJ/mol value we measured for the above equation.

Diffusion-controlled reactions kinetics were observed above about 60% conversion for the cyanate trimerization reaction. The decrease in the reaction rate that accompanied this onset was more pronounced at low heating rates and resulted in the development of a secondary reaction shoulder on the high temperature side of the exothermic DSC peak. This shoulder was not obvious in the 20°C/min scan rate case but the experimental data still indicated a slightly slowed reaction rate compared with the model near the end of the cure.

5 REFERENCES

1. G. G Allan and R. A. Brouns, *INDA J.N.R.*, **3**(4), 38 (1991).
2. M. R. Wertheimer and H. P. Schreiber, *J. Appl. Polym. Sci.*, **26**, 2087 (1981).
3. T. S. Keller, A. S. Hoffman, B. D. Ratner and B. J. McElroy, in "Physiochemical Aspects of Polymer Surfaces", Vol. 2, K.L. Mittal, ed., Plenum Press, New York, NY, 1983, pp. 861-79.
4. A. S. Hoffman, T. S. Keller, A. Miyake, B. D. Ratner and B. J. McElroy, in "Proc. of PACHEC '83: The Third Pacific Chemical Engineering Congress" Vol. II, Seoul, Korea, May 8-11, 1983, C. Kim and S.-K. Ihm, eds., The Korean Institute of Chemical Engineers, Seoul, Korea, 1983, pp. 54-63.
5. L. S. Penn, F. A. Bystry and H. J. Marchionni, *Polym. Compos.*, **4**(1), 26 (1983).
6. R. E. Allred, E. W. Merrill and D. K. Roylance, in "Molecular Characterization of Composite Interfaces", H. Ishida and G. Kumar, eds., Plenum Press, New York, NY, 1985, pp. 333-75.
7. A. Garton and J. H. Daly, *Polym. Compos.*, **6**(4), 195 (1985).
8. Y. Wu and G. C. Tesoro, *J. Appl. Polym. Sci.*, **31**, 1041 (1986).
9. M. Takayanagi, S. Ueta, W.-Y. Lei and K. Koga, *Polymer J.* ,**19**(5), 467 (1987).
10. L. S. Penn, G. C. Tesoro and H. X. Zhou, *Polym. Compos.*, **9**(3), 184 (1988).
11. R. C. T. Chou, J. Y. C. Tsai and L. S. Penn, in "Advanced Materials: The Challenge for the Next Decade", 35th International SAMPE Symposium and Exhibition, Anaheim, CA., April 2-5, 1990, G. Janicki, V. Bailey and H. Schjelderup, eds., SAMPE International, Covina, CA, 1990, pp. 214-225.
12. J. Corden, in "Engineered Materials Handbook" Vol. 1, ASM International Handbook Committee, eds., ASM International, Metals Park, OH, 1987, pp. 721-28.
13. A. Marshall, in "Handbook of Composites", G. Lubin, ed., Van Nostrand Reinhold Co., New York, NY, 1982, pp. 557-601.
14. "Adhesives in use with Nomex Aramid Paper and Pressboard", Technical Brief, 11/22/88, Fibers Department, E. I. du Pont de Nemours & Co., Inc., Wilmington, DE.
15. D. A. Shimp, F. A. Hudock and S. J. Ising, in "Materials – Pathway to the Future", 33th International SAMPE Symposium and Exhibition, Anaheim, CA., March 7-10, 1988, G. Carrillo, E. D. Newell, W. D. Brown and P. Phelan, eds., SAMPE International, Covina, CA., 1988, pp. 754-66.
16. M. Bauer and J. Bauer, *Makromol. Chem., Macromol. Symp.*, **30**, 1 (1989).

17. D. A. Shimp, J. R. Christenson and S. J. Ising, "AroCy® Cyanate Ester Resins–Chemistry, Properties and Applications", Rhône-Poulenc Inc. Technical Brochure, Rhône-Poulenc Inc., Louisville, KY, January 1990.

18. R. B. Graver, in "High Performance Polymers: Their Origin and Development", R. B. Seymour and G. S. Kirshenbaum, eds., Elsevier Science Publishing Co., Inc., New York, NY, 1986, pp. 309-16.

19. D. H. Wertz and D. C. Prevorsek, *Plast. Eng.*, **40** (4), 31 (1984).

20. E. M. Woo, B. Fukai and J. C. Seferis, in "Proc American Society for Composites: 3rd Technical Conference", Seattle, WA, Sept. 25-29, 1988, Technomic Pub. Co., Inc., Lancaster, PA, 1988, pp. 192-201.

21. D. A. Shimp, in "Advanced Materials Technology '87", 32th International SAMPE Symposium and Exhibition, Covina, CA., April 6-9, 1987, R. Carson, M. Burg, K. J. Kjoller and F. J. Riel, eds., SAMPE International, Covina, CA, 1987, pp. 1063-72.

22. R. E. Hefner, Jr., "Advanced Epoxy Resins Containing Triazine or both Triazine and Oxazoline Groups" US Patent 4,506,063, March 19, 1985.

23. "Properties of Nomex Aramid Filament Yarns", Technical Bulletin NX-17, December 1981, E. I. du Pont de Nemours & Co., Inc., Wilmington, DE.

24. R. Kubens, H. Schultheis, R. Wolf, E. Grigat, H.-D. Schminke and R. Putter, "Resins Based on Aromatic Cyanic Acid Esters and Polyepoxide Compounds" US Patent 3,562,214, February 9, 1971.

25. J. Bauer and M. Bauer, *Acta Polymerica,* **39**(10), 548 (1988).

26. J. Bauer and M. Bauer, *Acta Polymerica*, **41**(10), 535 (1990).

27. J. Bauer and M. Bauer, *J. Macromol. Sci., Chem.*, **A27**(1), 97 (1990).

28. J. T. Gotro, B. K. Appelt and K. I. Papathomas, *Polym. Compos.*, **8**(1), 39 (1987).

29. J. T. Gotro and B. K. Appelt, *IBM J. Res. Dev.*, **32**(5), 616 (1988).

30. R. E. Hefner, Jr., "Hydroxy Aromatic Oligomers Containing Triazine and Oxazoline Groups and Epoxy Resins Prepared Therefrom" US Patent 4,487,915, December 11, 1984.

31. R. E. Hefner, Jr., "Vinyl Ester Resins Containing Triazine or both Triazine and Oxazoline Groups" US Patent 4,515,934, May 7, 1985.

32. R. E. Hefner, Jr. and M. N. White, "Polyurethanes Containing Triazine or both Triazine and Oxazoline, Triazine and Imino Carbamate or Triazine and Other N-heterocyclic Groups" US Patent 4,487,915, October 13, 1987.

33. J. A. Brydson, in "Plastics Materials", 5th ed., Butterworths, London,UK, 1989, pp. 697-728.
34. "Encyclopedia of Polymer Science and Engineering", Vol. 6, H. F. Mark, N. M. Bikales, C. G. Overberger and G. Menges, eds., John Wiley & Sons, New York, NY, 1986, pp. 322-382.
35. S. Paul, in "Comprehensive Polymer Science" Vol. 6, G. Allen and J. C. Bevington, eds., Pergamon Press, Oxford, UK, 1989, pp. 179-92.
36. H. Lee and K. Neville, "Handbook of Epoxy Resins" McGraw-Hill, Inc., New York, NY, 1967, Chap. 5.
37. "Epoxy Resins: Chemistry and Technology", C. A. May and Y. Tanaka, eds., Marcel Dekker, Inc., New York, NY, 1973.
38. B. S. Gorton, *J. Appl. Polymer Sci.*, **8**, 1287 (1964).
39. T. F. Mika, in "Epoxy Resins: Chemistry and Technology", C. A. May and Y. Tanaka, eds., Marcel Dekker, Inc., New York, NY, 1973, pp. 239-325.
40. S. Paul, in "Surface Coatings: Science and Technology" John Wiley & Sons Ltd., Chichester, UK, 1985, pp. 217-47.
41. R. F. Fisher, *J. Polym. Sci.*, **44**, 149 (1960).
42. L. Matejka, J. Lövy, S. Pokorny, K. Bouchal, and K. Dusek, *J. Polym. Sci. Polym. Chem. Ed.*, **21**, 2873 (1983).
43. E. Grigat and R. Pütter, *Angew Chem. internat. Edit.*, **6**, 206 (1967).
44. E. Grigat, *Angew. Chem.*, **82**, 81 (1970); *Angew. Chem. internat. Edit.*, **9**(1), 68 (1970).
45. V. A. Pankratov, A. A. Maiorova, V. V. Korshak and S. V. Vinogradova, *Vysokomol. Soyed.*, **A17**(10), 2189 (1975); *Polym. Sci. USSR (Engl. Transl.)*, **17**(9), 2525 (1975).
46. D. A. Shimp and W. M. Craig, Jr., in "Tomorrow's Materials: Today", 34th International SAMPE Symposium and Exhibition, Reno, NV, May 8-11, 1989, G. A. Zakrzewski, D. Mazenko, S. T. Peters and C. D. Dean, eds., SAMPE International, Covina, CA., 1989, pp. 1336-46.
47. B. Steinmann, *J. Appl. Polym. Sci.*, **37**, 1753 (1989).
48. D. A. Shimp, J. R. Christenson and S. J. Ising, in " Proc. of the SPI - Epoxy Resin Formulators Division Conference", Hollywood, FL., April 30 - May 2, 1990.
49. P. Penczek and W. Kaminska, *Adv. Polym. Sci.*, **97**, 41 (1990).
50. S. Ayano, *Chem. Econ. & Eng. Rev.*, **10**(3), 25 (1978).

51. J. A. Feldman and S. J. Huang, in "Cross-Linked Polymers - Chemistry, Properties, and Applications", R. A. Dickie, S. S. Labana, and R. S. Bauer, eds., ACS 367, American Chemical Society, Washington, DC, 1988, pp. 245-68.
52. L. S. Tan, E. J. Soloski and F. E. Arnold, in "Cross-Linked Polymers - Chemistry, Properties, and Applications", R. A. Dickie, S. S. Labana, and R. S. Bauer, eds., ACS 367, American Chemical Society, Washington, DC, 1988, pp. 349-65.
53. F. W. Lee, M. A. Boyle, P. Lefebvre and J.-P. Botman, in "Advanced Materials: The Challenge for the Next Decade", 35th International SAMPE Symposium and Exhibition, Anaheim, CA., April 2-5, 1990, G. Janicki, V. Bailey and H. Schjelderup, eds.,
SAMPE International, Covina, CA., 1990, pp. 162-74.
54. D. A. Shimp and S. J. Ising, in "Advanced Materials: The Challenge for the Next Decade", 35th International SAMPE Symposium and Exhibition, Anaheim, CA., April 2-5, 1990, G. Janicki, V. Bailey and H. Schjelderup, eds.,
SAMPE International, Covina, CA., 1990, pp. 1045-1056.
55. P. C. Yang, D. M. Pickelman, and E. P. Woo, in "Advanced Materials: The Challenge for the Next Decade", 35th International SAMPE Symposium and Exhibition, Anaheim, CA., April 2-5, 1990, G. Janicki, V. Bailey and H. Schjelderup, eds.,
SAMPE International, Covina, CA., 1990, pp. 1131-42.
56. M. Bauer, J. Bauer and G. Kühn, *Acta Polymerica*, **37**(11/12), 715 (1986).
57. S. L. Simon and J. K. Gillham, *J. Appl. Polym. Sci.*, **47**(3), 461 (1993).
58. S. Zeng, K. Ahn, J. C. Seferis, J. M. Kenny and L. Nicolais,
Polym. Compos., **13**, 191 (1992).
59. A. K. Bonetskaya, V. V. Ivanov, M. A. Kravchenko, V. A. Pankratov, Ts. M. Frenkel', V. V. Korshak and S. V. Vinogradova, *Vysokomol. Soyed.*, **A22**(4), 766 (1980); *Polym. Sci. USSR (Engl. Transl.)*, **22**(4), 845 (1980).
60. R. F. Cozzens, P Walter and A. W. Snow, *J. Appl. Polym. Sci.*, **34**, 601 (1987).
61. D. A. Shimp, "Metal carboxylate/alkylphenol curing catalyst for polycyanate esters of polyhydric phenols" U.S. Patent 4,604,452, August 5, 1986.
62. D. A. Shimp, "Metal acetylacetonate/alkylphenol curing catalyst for polycyanate esters of polyhydric phenols" U.S. Patent 4,785,075, November 15, 1988.
63. M. Fedtke, in "Frontiers of Macromolecular Science", T. Saegusa, T. Higashimura, A. Abe, eds., Blackwell Scientific Publications, Oxford, UK, 1989, pp. 149-54.

64. A. Vazquez, D. Bentaleb, and R. J. J. Williams, *J. Appl. Polym. Sci.*, **43**, 967 (1991).

65. M. Fedtke and F. Domaratius, *Polym. Bull. (Berlin)*, **15**, 13 (1986).

66. M. Shimbo, T. Nakaya, and T. Takahama, *J. Polym. Sci., Part B: Polym. Phys.*, **24**, 1931 (1986).

67. Y. Tanaka and H. Kakiuchi, *J. Macromol. Chem.*, **1**, 307 (1966).

68. C. Sellitti, J. L. Koenig and H. Ishida, *J. Polym. Sci., Part B: Polym. Phys.*, **28**, 1121 (1990).

69. M. K. Antoon and J. L. Koenig, *J. Polym. Sci., Polym. Chem. Ed.*, **19**, 549 (1981).

70. G. C. Stevens, *J. Appl. Polym. Sci.*, **26**, 4259 (1981).

71. J. Luston and F. Vass, *Adv. Polym. Sci.*, **56**, 91 (1984).

72. E. M. Woo and J. C. Seferis, *J. Appl. Polym. Sci.*, **40**(7-8), 1237 (1990).

73. M. Bauer, W. Tänzer, H. Much and R. Ruhmann *Acta Polymerica*, **40**(5), 335 (1989).

74. M. Bauer, J. Bauer, R. Ruhmann and G. Kühn, *Acta Polymerica*, **40**(6), 397 (1989).

75. V. V. Korshak *et al.*, *Izv. Akad. Nauk SSSR, Ser. Khim.*, **10**, 2369 (1983); *Bull. Acad. Sci. USSR, Div. Chem. Sci. (Engl. Transl.)*, **32**(10), 2135 (1983).

76. V. V. Korshak *et al.*, *Izv. Akad. Nauk SSSR, Ser. Khim.*, **7**, 1645 (1981); *Bull. Acad. Sci. USSR, Div. Chem. Sci. (Engl. Transl.)*, **30**(7), 1335 (1981).

77. D. Martin, *Chem. Ber.*, **97**(9), 2689 (1964).

78. C. A. Pryde, *J. Polym. Sci., Part A: Polym. Chem.*, **27**, 711 (1989).

79. P. R. Griffiths and J. A. de Haseth, in "Chemical Analysis" Vol. 83, P. J. Elving and J. D. Winefordner eds., John Wiley & Sons, New York, NY, 1986, pp.338-68.

80. R. Bruce Prime, in "Thermal Characterization of Polymeric Materials", Edith A. Turi, (ed.), Academic Press, New York, USA, 1981, pp. 435-563.

81. I. Yilgör, E. Yilgör, A. K. Banthia, G. L. Wilkes and J. E. McGrath, *Polymer Bulletin*, **4**, 323 (1981).

82. H. Lee and K. Neville, "Handbook of Epoxy Resins", McGraw-Hill, Inc., New York, NY, 1967, Chap. 12.

83. "Vogel's Textbook of Practical Organic Chemistry", 4th ed., 1978, pp. 267-68.

84. M. Bertrán, A. Mantecón, and V Cádiz, *Angew. Makromol. Chem.*, **168**, 81 (1989).

85. G. L. Hagnauer, B. B. LaLiberte and D. A. Dunn, in "Epoxy Resin Chemistry II", R. S. Bauer, ed., ACS 221, American Chemical Society, Washington D.C., 1983, pp. 229-44.
86. M. Bauer, J. Bauer and B. Garske, *Acta Polymerica,* **37**(10), 604 (1986).
87. Livermore Solver for Ordinary Differential Equations, with Automatic Method Switching for Stiff and Nonstiff Problems, and with Root-Finding (LSODAR, March 30, 1987 version), Linda R. Petzold and Alan C. Hindmarsh, Lawrence Livermore National Laboratory, Livermore, CA 94550.
88. A. C. Hindmarsh, "ODEPACK, a Systematized Collection of ODE Solvers", in Scientific Computing, R. S. Stepleman *et al.*, (eds.), North-Holland, Amsterdam, 1983, pp. 55-64.
89. L. R. Petzold, "Automatic Selection of Methods for Solving Stiff and Nonstiff Systems of Ordinary Differential Equations, *Siam J. Sci. Stat. Comput.*, **4**, 136 (1983).
90. K. L. Hiebert and L. F. Shampine, "Implicitly Defined Output Points for Solutions of ODE-s", Sandia report SAND80-0180, February, 1980.

Vita.

Richard Allan Brouns was born in Richland, Washington on February 15, 1956, to Richard John and Katherine Nyla Brouns. After receiving his high school diploma in 1974 from Tacoma Community College, Tacoma, Washington, he attended the University of Washington where he received a Bachelor of Science Degree in Chemical Engineering in June, 1978. For the next ten years Mr. Brouns was employed by Battelle Pacific Northwest Laboratory in Richland, Washington, where he worked on the research and development of processes for treating hazardous chemical and nuclear wastes. From September 1988 through March 1993 he attended graduate school at the University of Washington. His Doctor of Philosophy degree in Chemical Engineering was awarded on August, 1993.